Dissertation

submitted to the

Combined Faculties for the Natural Sciences and for Mathematics

of the Ruperto-Carola University of Heidelberg, Germany

for the degree of

Doctor of Natural Sciences

Presented by

Dipl. mol. med. Claudius Wagner

born in Filderstadt.

Oral Examination: 13th June, 2019

Role of matrix metalloproteinase-9 in cystic fibrosis lung disease and evaluation of therapeutic strategies

Referees: Prof. Dr. Stefan Wölfl
Prof. Dr. Marcus Mall

Table of contents

Abbreviations

A1AT	Alpha-1-antitrypsin
AB-PAS	Alcian blue periodic acid-Schiff
Actb	β-Actin gene
ASL	Airway surface liquid
BAL	Bronchoalveolar lavage
βENaC-Tg	Transgenic overexpression of β subunit of ENaC
C57BL/6	Inbred laboratory mouse strain
CatG	Cathepsin G
CBA	Cytometric bead array
CCSP	Club cell secretory protein
CD	Cluster of differentiation
CF	Cystic fibrosis
CFTR	Cystic fibrosis transmembrane conductance regulator
Chi3l1	Chitinase-3-like protein 1
Cl^-	Chloride anion
COPD	Chronic obstructive pulmonary disease
CXCL	CXC chemokine ligand
DAMP	Damage-associated molecular pattern
dd	Double distilled
ENaC	Epithelial sodium channel
ELISA	Enzyme-linked immunosorbent assay
FEV_1	Forced Expiratory Volume in 1 second
fMLP	Formyl-methionine-leucine-phenylalanine
Gob5	Chloride channel accessory 1 gene
GSH	Glutathione
GSSH	Oxidized glutathione
h	Human
HE	Hematoxylin eosin staining
IL	Interleukin
KC	Keratinocyte chemoattractant, mCXCL1
LIX	LPS induced CXC chemokine, mCXCL5
LPS	Lipopolysaccharide of gram-negative bacteria
m	Murine
MCC	Mucociliary clearance
MIP-2	Macrophage inflammatory protein 2, mCXCL2
MMP	Matrix metalloproteinase

Na^+	Sodium cation
NaCl	Sodium chloride
NE	Neutrophil elastase
PAMP	Pathogen-associated molecular pattern
PBS	Phosphate buffered saline
PCL	Periciliary liquid layer
PCR	Polymerase chain reaction
PR3	Proteinase 3
PRR	Pattern recognition receptor
RT	Reverse transcription
Scnn1b	Gene of the β-subunit of the epithelial sodium channel
SCN^-	Thiocyanate
Tg	Transgenic or transgene
TGF	Transforming growth factor
Th	T helper
TIMP	Tissue inhibitor of matrix metalloproteinases
TLR	Toll-like receptor
V	Vena
WT	Wild-type
Ym1	Gene of chitinase-like 3

List of figures

Abstract

Current hypotheses suggest that a disrupted antiprotease-protease balance results in structural tissue damage in cystic fibrosis (CF) lung disease. Clinical studies identified elevated neutrophil elastase (NE) levels as risk factor for the onset of structural lung damage in young CF patients. A recent study reported that levels of NE-activated matrix metalloproteinase (MMP)-9 correlated with the progression of bronchiectasis in CF patients. Studies in mice with lung-specific overexpression of the β subunit of the epithelial Na^+ channel (βENaC-Tg) confirmed a crucial contribution of NE activity to CF-like lung disease. However, *NE* deletion only partially reduced structural lung damage, i.e. emphysema, suggesting that additional factors contribute to tissue destruction in βENaC-Tg mice.

The present study investigates the pathogenic role of MMP-9 in βENaC-Tg mice. Similar to CF patients, MMP-9 protein levels were elevated in bronchoalveolar lavage (BAL) fluid of βENaC-Tg mice as detected by gelatin zymography. To determine the contribution of MMP-9 to the pathogenesis of βENaC-Tg mice, mortality, pulmonary inflammation, transcript levels of mucins, distal airspace enlargement and soluble MMP-9 activity in BAL fluid were studied in WT, *Mmp9*$^{-/-}$, βENaC-Tg and βENaC-Tg/*Mmp9*$^{-/-}$ mice. Additionally, measurement of lung function in NE or MMP-9 deficient βENaC-Tg mice enabled the comparison of the individual influence of the respective protease on lung tissue mechanics.

Inflammatory cytokines and neutrophil chemoattractants were elevated in βENaC-Tg mice and not altered in BAL fluid of βENaC-Tg/*Mmp9*$^{-/-}$ mice. In addition, pulmonary leukocyte infiltration, mucin expression and goblet cell metaplasia were not dependent on MMP-9 and elevated to similar levels in βENaC-Tg and βENaC-Tg/*Mmp9*$^{-/-}$ mice. Lung volume measurement and morphometric quantification of distal lung histology showed an increased emphysema severity in βENaC-Tg mice which was not reduced in βENaC-Tg/*Mmp9*$^{-/-}$ mice. Free soluble MMP-9 activity could not be detected in BAL fluid neither of βENaC-Tg mice nor of littermate controls. Increased concentrations of tissue inhibitor of matrix metalloproteinases (TIMP)-1 as main endogenous MMP-9 inhibitor indicate an intact antiprotease-protease balance in BAL fluid of βENaC-Tg mice. Lung function testing revealed no improvement of static compliance, inspiratory capacity or tissue elastance by *Mmp9* deletion in βENaC-Tg mice. The assessment of lung function displayed a significant amelioration of these parameters in βENaC-Tg/*NE*$^{-/-}$ compared to βENaC-Tg mice. According to these results, preclinical trials were performed targeting NE with the small molecule inhibitor sivelestat to test the effect on disease development

in newborn βENaC-Tg mice. Systemic sivelestat delivery by intraperitoneal injections reduced airway mucus obstruction but did not affect leukocyte infiltration or emphysema severity in two week-old βENaC-Tg mice compared to vehicle controls.

In summary, the analysis of MMP-9 deficient mice suggests that MMP-9 is not crucial factor in the pathogenesis of βENaC-Tg mice. This may be related to balanced antiprotease levels in the lungs of βENaC-Tg mice, which are frequently depleted in CF patients. Therefore, it is difficult to deduce from the current studies the pathogenic potential of MMP-9 in more severe stages of CF lung disease. In contrast to *Mmp9* deletion, NE deficiency improved lung function in βENaC-Tg mice. The preclinical trials with sivelestat showed that NE inhibition was insufficient to reproduce the results of NE deletion in βENaC-Tg mice. Thus, further treatment studies are needed using compounds with improved pharmacokinetic properties that enable effective NE inhibition in pulmonary tissue.

Zusammenfassung

Gegenwärtigen Hypothesen zufolge kann ein unausgeglichenes pulmonales Antiprotease-Protease Gleichgewicht strukturelle Gewebeschäden bei Patienten mit Mukoviszidose (CF) auslösen. In klinischen Studien wurde festgestellt, dass eine erhöhte Neutrophile Elastase (NE) Aktivität ein Risikofaktor darstellt für die Entstehung von strukturellen Lungenschäden bei jungen CF Patienten. In einer kürzlich veröffentlichten Studie wurde berichtet, dass die Konzentration von NE-aktivierter Matrix-Metalloproteinase (MMP)-9 mit dem Fortschreiten von Bronchiektasen bei CF-Patienten korrelierte. Studien an Mäusen mit lungenspezifischer Überexpression der β-Untereinheit des epithelialen Na^+-Kanals (βENaC-Tg) bestätigten einen entscheidenden Beitrag von NE Aktivität zur CF-ähnlichen Lungenerkrankung. *NE* Deletion reduzierte jedoch nur teilweise die strukturellen Lungenschäden, d.h. das Emphysem, was darauf hindeutet, dass zusätzliche Faktoren zur Gewebezerstörung in βENaC-Tg-Mäusen beitragen.

Die vorliegende Studie untersucht die pathogene Rolle von MMP-9 in βENaC-Tg-Mäusen. Ähnlich wie bei CF-Patienten wurden erhöhte MMP-9-Proteinspiegel in bronchoalveoläre Lavage (BAL)-Flüssigkeit von βENaC-Tg-Mäusen festgestellt. Um den Beitrag von MMP-9 zur Pathogenese von βENaC-Tg-Mäusen festzustellen, wurden Mortalität, pulmonale Entzündung, Transkriptspiegel von Mucinen, Schweregrad des Emphysems und lösliche MMP-9-Aktivität in BAL-Flüssigkeit von WT, *Mmp9*$^{-/-}$, βENaC-Tg und βENaC-Tg/*Mmp9*$^{-/-}$ Mäusen untersucht. Zusätzlich ermöglichte die Messung der Lungenfunktion in NE- oder MMP-9-defizienten βENaC-Tg-Mäusen den Vergleich des individuellen Einflusses der jeweiligen Protease auf mechanische Eigenschaften des Lungengewebes. Es wurden erhöhte Konzentrationen von Entzündungs-Cytokinen und Neutrophilen-Chemokine in βENaC-Tg-Mäusen gemessen, die in der BAL von βENaC-Tg/*Mmp9*$^{-/-}$ Mäusen nicht verändert waren. Darüber hinaus zeigten Leukozyteninfiltration, Mucinexpression und Becherzellmetaplasie keine Abhängigkeit von MMP-9 d.h. war unverändert in βENaC-Tg und βENaC-Tg/*Mmp9*$^{-/-}$ Mäusen. Die Messung des Lungenvolumens und Morphometrie der distalen Lungenhistologie zeigten bei βENaC-Tg-Mäusen einen höheren Schweregrad des Emphysems, der in βENaC-Tg/*Mmp9*$^{-/-}$ Mäusen nicht reduziert war. Darüber hinaus konnte keine freie lösliche MMP-9-Aktivität in der BAL-Flüssigkeit weder von βENaC-Tg-Mäusen noch Wurfgeschwistern nachgewiesen werden. Erhöhte Konzentrationen von „tissue inhibitor of matrixmetalloproteinases“ (TIMP)-1, als wichtigster endogener MMP-9-Inhibitor, deuten auf ein intaktes Antiprotease-Protease Gleichgewicht in der BAL Flüssigkeit von βENaC-Tg-Mäusen hin. Lungenfunktionsmessungen zeigten keine Verbesserung der statischen

Compliance, der inspiratorischen Kapazität oder der Gewebeelastizität durch *Mmp9* Deletion in βENaC-Tg-Mäusen. Die Untersuchung der Lungenfunktion in βENaC-Tg/*NE*$^{-/-}$ Mäusen zeigte eine signifikante Verbesserung dieser Parameter im Vergleich zu βENaC-Tg-Mäusen. Basierend auf diesen Ergebnissen wurden präklinische Studien mit dem niedermolekularen NE Inhibitor Sivelestat durchgeführt, mit dem Ziel den Effekt auf die Entwicklung des Krankheitsheitsgeschehen in neugeborenen βENaC-Tg-Mäusen zu untersuchen. Die systemische Abgabe von Sivelestat durch intraperitoneale Injektionen reduzierte die Atemwegsobstruktion durch Mukus, verminderte jedoch nicht die Infiltration durch Leukozyten oder den Schweregrad des Emphysems in zwei Wochen alten βENaC-Tg-Mäusen im Vergleich zu Kontrolltieren.

Zusammenfassend lässt die Analyse von MMP-9-defizienten Mäusen darauf schließen, dass MMP-9 kein entscheidender Faktor in der Pathogenese von βENaC-Tg-Mäusen ist. Dies kann mit den austarierten Antiprotease-Spiegeln in den Lungen von βENaC-Tg-Mäusen zusammenhängen, die bei CF Patienten häufig verringert sind. Daher ist es schwierig, aus den aktuellen Studien das pathogene Potenzial von MMP-9 in schwereren Stadien der CF Lungenerkrankung abzuleiten. Im Gegensatz zur *Mmp9*-Deletion verbesserte das Fehlen von NE die Lungenfunktion in βENaC-Tg-Mäusen. Die präklinischen Studien mit Sivelestat zeigten, dass die erzielte NE-Hemmung unzureichend war und die Ergebnisse der *NE*-Deletion in βENaC-Tg-Mäusen nicht reproduziert werden konnten. Daher sind weitere Behandlungsstudien erforderlich, bei denen Verbindungen mit verbesserten pharmakokinetischen Eigenschaften verwendet werden, die eine wirksame NE-Hemmung im Lungengewebe ermöglichen.

1 Introduction

1.1 Cystic fibrosis

Cystic fibrosis (CF) is a disease with autosomal recessive inheritance caused by more than 2000 documented mutations in the cystic fibrosis transmembrane conductance regulator (CFTR) Cl^- ion channel [27, 68, 133]. In populations with European descent around 4 % of all individuals carry a mutated allele causing a prevalence of 1 : 2,500 and a total of ~70,000 CF patients worldwide [27, 90].

1.1.1 Early pathophysiology of cystic fibrosis lung disease

Loss of CFTR functions lead to the production of altered secretions in all exocrine glands. Among them, pulmonary airway epithelia are severely affected and the resulting chronic lung disease causes > 80 % of the CF-associated mortality [112]. CFTR is highly expressed in submucosal glands and also in airway epithelium by ionocytes, ciliated, club and goblet cells [65, 103]. CFTR is permeable for a wide range of anions, but physiologically relevant is the conductivity for Cl^-, HCO_3^- , glutathione (GSH), I^- and SCN^- ions [83]. Airway epithelia permit a paracellular water transport to a decreasing degree in proximal direction of the conducting airways. Airway epithelia are covered by a ~ 10 µm thick airway surface liquid (ASL) layer which can be further divided in the periciliary layer (PCL) and the mucus layer [16]. Normal mucus is transported cranially from lower airways propelled by coordinated ciliary beating within the PCL of airway epithelial cells or by cough. Both ways enables the clearance of cellular debris, pathogens and other irritants from the lungs [38, 179].

The exact pathogenesis of CF lung disease is unknown. According to current hypothesis, the ASL height is particularly dependent on the conductance of the epithelial Na^+ channel (ENaC) and CFTR [38, 129]. Functional CFTR inhibits ENaC and thereby critically determining ASL height. CFTR mutation abrogates Cl^- secretion in airway epithelia and promotes ENaC-mediated Na^+ hyperabsorption. Because ion transport is coupled with water flow, ASL remains isotonic but is depleted in CF airways [91, 93].

Mucus normally consists of 97 % water and 3 % solids which are composed of ions, mucins in particular MUC5B and MUC5AC, non-mucin proteins, lipids and cellular debris [38]. In CF, airway mucus solids rise to >8 % largely due to volume depletion, elevated concentrations of MUC5B, MUC5AC and additionally presences of intracellular components in particular actin and DNA [38]. It has been proposed that the solute concentration rises in consequence of ASL liquid depletion until the osmotic pressure of

thickened visco-elastic mucus gels exceeds the osmotic pressure in the PCL which leads to a reduction of the PCL high and compression of cilia [16]. Consequently, impaired mucociliary clearance (MCC) results in chronic airway mucus obstruction [38]. Further, MCC is ineffective in removal of irritants from the lungs and mucus obstruction might cause hypoxic cell necrosis in airway epithelia [43]. In addition, CFTR dysfunction may directly affect hypoxic vasoconstriction thereby further aggravating lung perfusion-ventilation mismatch and increasing systemic hypoxemia [146]. Necrotic cells may release intracellular pro-inflammatory cytokines, e.g. interleukin (IL)-1α [43]. In addition, intracellular proteins and nucleotides may signal as damage-associated molecular pattern (DAMPs), e.g. heat shock proteins, and trigger a sterile inflammation by stimulation of pattern recognition receptors (PRRs), e.g. toll-like receptor 4 (TLR4), on epithelial cells or macrophages [20]. Hypoxia, IL-1α and TLR mediated NF-κB activation induces the expression of MUC5AC and metaplasia to goblet cells i.e. mucin secreting cells derived from club cells [76, 174]. In contrast, MUC5B shows a constitutive expression and only a limited upregulation during inflammation [38]. In summary, the induced mucin hypersecretion by inflammatory stimuli aggravates airway mucus obstruction in CF lung disease [91].

1.1.2 Signs and symptoms at later stages of CF lung disease

During the course of CF, lungs often become colonized by bacteria leading to chronic infection with intermittent exacerbations. Glycans of airway mucins may provide the substrate for some bacterial strains and hypoxia favors the growth of facultative anaerobic bacteria e.g. Pseudomonas (P.) aeruginosa [173]. Bacterial infection leads to the release of pathogen-associated molecular patterns (PAMPs) e.g. lipopolysaccharides (LPS) and chemoattractants e.g. formyl-Met-Leu-Phe (fMLF or also termed fMLP). In combination with an impaired MCC, this is thought to amplify the recruitment and activation of large numbers of leukocytes.

Chronic inflammation, airway mucus obstruction, infection and exposure of epithelia to persistently activated leukocytes is thought to cause epithelial damage, aberrant tissue remodeling and destruction of extracellular matrix (ECM) [127, 159]. In CF patients, structural lung damage is present as widening of small bronchi, termed bronchiectasis [127]. A destruction of alveolar walls summarized as emphysema has been observed in older CF patients [144, 169]. These progressive and irreversible structural changes of tissue architecture may affect lung function.

Lung function measurement of CF patients typically show an impaired expiratory airflow which is related to airway obstruction and/or a compromised elastic lung recoil [127]. The forced expiratory volume in one second (FEV_1) is used to detect the changes in

expiratory airflow and is often expressed as % of predicted values (FEV_1%). Reference values are calculated based on ethnic group, gender, height and age [55]. The lung volume change over a defined applied pressure difference is expressed as lung compliance and reflects the ability of a lung to expand or stretch. Typically, the compliance is highly elevated in emphysematous lungs and reduced in pulmonary fibrosis. In general, during a breathing cycle pressure and lung volume changes show a hysteresis during inspiration and expiration. Despite a matter of ongoing research, the energy dissipation responsible for hysteresis is thought to be related to a gradual opening of closed e.g. atelectatic alveoli during unfolding of alveolar tissue [37]. Atelectasis can arise from airway mucus obstruction [120]. In addition, changes in surface tension during inspiration are discussed as cause for hysteresis. In conclusion, force is needed during inspiration which is not recovered during deflation [37].

CF patients show a progressive decline in lung function as indicated by diminishing values for FEV_1% predicted in lung function measurements. This decline starts early and accelerates with late childhood and may lead to respiratory failure [73, 112]. Ultimately, this necessitates lung transplantation in severe cases of CF and rendering lung disease the major determinant for the reduced life expectancy of approximately 37 years [112].

1.2 Role of neutrophilic inflammation in CF lung disease

In CF lung disease, the dominant leukocytes are neutrophils. Neutrophil counts in sputum correlate inversely with FEV_1 decline in CF patients [136]. This indicates an important role of neutrophils in the progression of CF lung disease. However, disease-promoting mechanisms of neutrophils remain elusive. Neutrophils accumulate by a combination of an increased life span, a potentiated influx and also by a reduced clearance via MCC, cough or efferocytosis by alveolar macrophages [95, 107]. The increased influx is related to an increased generation of chemoattractant (see below) and life span of neutrophils was shown to be increased in response to exposure to bacterial products or to various cytokines which delays apoptosis [23, 95].

1.2.1 Recruitment of neutrophils into the lungs and involved chemokines

Although PRRs are also present on epithelial cells, tissue resident alveolar macrophages are considered to have a key role in the early inflammatory response as sentinel cells and by secretion of cytokines e.g. tumor necrosis factor α (TNF-α) and chemokines e.g. CXC chemoattractants to initiate an inflammatory response [154, 168]. In addition, IL-1 receptor signaling may induce inflammatory chemokine expression [111].

CXC chemokines are diverse between species including humans and mice. In humans, CXCL8 or interleukin 8 (IL-8) is considered to be the major chemokine for neutrophils

[29]. In mice, two functional IL-8 homologues keratinocyte-derived chemoattractant (KC) (also named mCXCL1), macrophage inflammatory protein 2 (MIP-2) (also named mCXCL2) and additionally LPS-induced CXC chemokine (LIX, also named CXCL5) and murine specific lungkine (also named mCXCL15) mediate neutrophil recruitment into the inflamed respiratory tract [29, 100]. During inflammation KC and MIP-2 are primarily secreted by macrophages [28]. In contrast, lungkine is expressed by bronchial epithelial cells and major sources for LIX are platelets in the blood and during inflammation alveolar type II cells in lung parenchyma [100].

Lungs differ from all other organs in terms of the site of infiltration. Neutrophils transmigrate mainly at pulmonary capillaries and not at post-capillary venules [34, 130]. Transmigration takes places preferentially at cell-cell borders where gaps are present or formed between intercellular junctions and the basement membrane is discontinuous.

1.2.2 Neutrophil granule composition and role in infection

CF patients suffer from recurrent bacterial infection and persistent colonization with opportunistic pathogens [127]. Granules are essential for the function of neutrophils to limit bacterial infections [25]. Four types of granules have been classified and are sequentially formed during neutrophil maturation: first, primary or azurophil granules are formed which contain neutrophil elastase (NE), proteinase 3 (PR3), cathepsin G (CatG) and neutrophil serine protease-4 (NSP4) [74, 119]. NE, PR3 and CatG are specifically expressed in neutrophils and stored as active enzymes. Secondary or specific granules contain the pro-form of collagenase pro-MMP-8. Pro-MMP-9 is present in a subfraction of specific granules and in particular in tertiary granules. Both granule types contain additionally $gp91^{phox}$ which is a critical subunit of the NADPH oxidase [25]. Of note, neutrophils express all proteases only during granulopoeisis in the bone marrow [9, 39]. Secretory vesicles as forth granule type contain various plasma proteins and represent a reservoir for membrane receptors for neutrophil adhesion and subsequent activation e.g. integrins CD11b-CD18, fMLP-receptor, $gp91^{phox}$ [9].

The 4 granule types differ in their tendency to undergo exocytosis and follow a hierarchy corresponding to the sequence of their generation during granulopoeisis [25]. For example, during chemotaxis all of the secretory vesicles are released while only a minor fraction of azurophil granules is secreted. Specific and tertiary granules show an intermediate exocytosis rate.

It is now accepted that a significant fraction of the secreted proteases remains bound to the surface of neutrophils apart from free soluble protease pool [122]. However, the function of the surface-bound protease activity in comparison to free soluble proteases remains unknown. NE binds the neutrophil surface via electrostatic interaction with

sulfated-proteoglycans while PR3 and MMP-9 interact with several transmembrane-receptors [74, 157].

The function of neutrophils as phagocytes is dependent on their granule content. Phagocytosis of bacteria triggers the fusion phagosomes with azurophil and in part also specific granules [25]. Bacteria are killed mainly by reactive oxygen species (ROS) generated by NADPH oxidase and also by proteases e.g. NE which cleaves bacterial membrane proteins [7, 164]. In addition, neutrophils are able to secrete their nuclear DNA in a process termed NETosis which represents an extracellular killing mechanism in particular for large, indigestible pathogens [11, 164]. During the formation of neutrophil extracellular traps (NETs) NE, PR3, CatG as well as MMP-9 are deposited together with nuclear DNA and other components e.g. histones [13]. Pathogens are trapped in NETs and killed by DNA itself and potentially by associated proteins, including CatG and NE [13, 54].

These bactericidal processes may also promote CF lung disease. ROS release and associated oxidative stress may cause a stiffening of the mucus gel by oxidizing mucins [177]. Additionally, DNA secretion during NETosis may alter mechanical properties of the mucus gel. The resulting changes in mucus rheology may impair MCC, favor chronic colonization with bacteria and worsen airway mucus obstruction [38].

1.3 Neutrophil-derived proteases as modulator of CF lung disease

Chronic pulmonary inflammation is thought to cause or aggravate pathophysiological epithelial and structural alterations. These include goblet cell metaplasia, mucin hypersecretion, enlargement of bronchi and distal airspaces, i.e. bronchiectasis and emphysema, eventually leading to impaired lung function [91–93, 118]. In CF airways, the cell covering ASL contains high concentration of NE, PR3, CatG, MMP-8 and MMP-9 [159]. These proteases may be secreted by neutrophils and are able to degrade a wide range of substrates either of microbial origin but also of different pulmonary tissues.

1.3.1 Role of NE in CF lung disease

Most ECM proteins are substrates but also several cytokines, opsonizing factors, ion channels and scavenger receptors are cleaved by neutrophil-derived proteases [29, 107, 159]. The prolonged exposure to proteolytic activity can lead to epithelial and tissue damage during chronic neutrophilic inflammation. In particular, extracellular NE activity was shown to promote several key pathogenic processes that are associated with CF lung disease including impairing MCC, stimulating airway remodeling and potentiating inflammation [159].

Under physiologic conditions, NE activity is limited by intracellular compartmentalization and if secreted in airspaces by the presence of the endogenous antiproteases such as elafin (in humans but not present in mice), secretory leukocyte protease inhibitor (SLPI) and α1-antitrypin (A1AT) [74]. Elafin and SLPI are secreted locally by leukocytes and epithelial cells while A1AT is produced by hepatocytes and reaches the lung via the blood circulation [170]. With progression of CF lung disease high numbers of neutrophils accumulate in the lung that release their granules content [88, 149]. Over time, this is thought to overwhelm the antiprotease shield that protects lung tissue from proteolytic damage [159].

A disrupted protease-antiprotease balance may cause a vicious cycle of tissue damage and further release of pro-inflammatory mediators. NE induces the expression of IL-8 in human airway epithelial cells. In mice, NE instillation increase KC levels in BAL fluid and stimulates the release of high-mobility group box 1 from macrophages which both act as neutrophil chemoattractants [52].

Although direct evidence is lacking several *in vitro* and *ex vivo* studies support the hypothesis that NE may alter epithelial function. NE was shown to cause cell detachment in primary airway epithelial cell cultures, decrease proliferation, induce apoptosis and impair wound closure even at low concentration as present in young CF patients [47, 159]. Furthermore, *in vitro* studies showed that NE triggers cell cycle arrest, induces goblet cell metaplasia, enhances MUC5AC expression and mucin secretion and reduces ciliary motility in bronchial epithelial cells [2, 159].

NE was shown to cleave and inactivate the ENaC inhibitor short palate, lung, and nasal epithelium clone 1 (SPLUNC1) [64]. Moreover, NE can also directly activate ENaC and degrade CFTR which all combined potentially aggravate airway obstruction and may impair epithelial regeneration in chronic inflammatory lung diseases [2, 74, 93].

Resolution of inflammation is impaired in CF patients which in part might be attributed to increased protease levels. For example, phagocytosis of apoptotic cells by macrophages prevents the release of intracellular pro-inflammatory DAMPs, stimulates anti-inflammatory cytokines and initiates resolution of inflammation [107, 158]. NE degrades the phosphatidylserine-receptor, thereby inhibits efferocytosis, provokes secondary necrosis which leads to a release of DNA, actin, proteases and promotes chronic inflammation [107, 159].

Structural lung damage in CF patients is observed early as bronchiectasis and in older patients as mild form of emphysema [144]. In CF airways, a significantly higher number of NE and MMP-9 positive cells have been detected in lamina propria of ectatic bronchial walls [178]. Furthermore, abnormal and fragmented elastin fibers have been reported in lungs of CF patients [14]. As mentioned, NE can cleave several subepithelial ECM

components including elastin [159] and elevated NE activity coincided with increased levels of urinary desmosine which is a proteolytic elastin degradation product. ECM degradation and remodeling is thought to lead to aberrant epithelial regeneration and thereby causing ectatic bronchi. Alterations in mechanical properties of lung tissue can be assessed clinically by lung function measurement of patients.

1.3.1.1 Correlation of NE levels with clinical parameters in CF lung disease

CF patients with identical CFTR mutations may experience a different rate in progressive decline in lung function. Various inflammatory sputum biomarkers were assessed to predict progressive reduction in lung function. Prospective studies in young patients identified protease activity, in particular of NE and MMP-9, as a predictive marker for disease progression [48, 136].

Increased levels of NE in bronchial secretions were identified as risk factor for the development of bronchiectasis and showed an association with deterioration of lung function in CF patients [136, 142]. This supports the hypothesis that NE has a crucial role in the pathogenesis of CF lung disease. In a recent study, NE activity in sputum supernatant and on surface of sputum neutrophils correlated best with FEV_1% or the functional residual capacity, respectively [33]. The latter estimates the volume that remains in the lungs after expiration and may indicate the presence of bronchiectasis in CF patients.

Elevated NE activity coincided with lower levels of its inhibitors. In particular, SLPI and concentrations of NE complexed with A1AT show a declining trend during disease progression in CF patients [136]. NE seems to have an important role in tilting the protease-antiprotease balance. It was shown to degrade SLPI and TIMP1, the major inhibitor of MMP-9 [157, 170]. Furthermore, NE may activate pro-MMP-9 while MMP-9 cleaves A1AT suggesting a synergistic and potentiating activity of both proteases [46, 85].

1.4 Matrix metalloproteinase 9: structure, cellular sources, biochemistry and role in inflammation

Several studies pointed out that MMP-9 is elevated in sputum or BAL fluid of CF patients [30, 48] and *in vitro* studies suggest an involvement in modulation of inflammation, wound healing and ECM remodeling [29, 115, 154, 157]. This suggests a contribution of MMP-9 in the pathogenic events of CF lung disease although a closer examination is lacking.

1.4.1 Activation, catalytic mechanism and substrate specificity are determined by distinct structural modules in MMP-9

In general, proteases are enzymes which irreversibly hydrolyze the peptide bond of their protein substrate. This process is in most cases highly specific and often has various regulatory functions with proteolysis often marking a switch in a cellular response e.g. in apoptosis induction or initiates signaling cascades, for example in blood coagulation. Proteases are subdivided into 5 different classes based on their hydrolytic mechanism: in cysteine, serine and threonine proteases the respective amino acid sidechain acts as nucleophile to attack the peptide bond while in aspartic and metalloproteases an activated H_2O serves directly as the reactive molecule [125]. Metalloproteases and serine protease are the two largest classes in mice and humans [113].

MMPs are a major subfamily of metalloprotease which all form a complex with Zn^{2+} ions. Three histidine residues in the sequence HEXXHXXGXXH bind one Zn^{2+} ion to form the active center while glutamate serves as a base during catalysis [152]. According to the current model of MMP proteolysis, the hydrolytic cycle of a peptide bond starts with polarizing a water molecule by Zn^{2+}. H_2O then protonates the glutamate residue in the active center and the remaining hydroxide ion reacts with the peptide´s carbonyl C-atom to form a carboxyl group. The bound proton by glutamate is transfer to the secondary amine in the peptide bond and thereby cleaving the protein by rearrangement of covalent bonds (Figure 1.1) [40, 147]. The pH optimum of MMP-9 has been determined at near neutral values of ~7.5 [109].

All MMPs, except for MMP-23, are translated into inactive pro-forms i.e. zymogens. The pro-peptide covers the substrate binding cleft and a cysteine in the conserved “cysteine switch sequence” coordinates via its thiol group with the zinc ion to prevent the entry of water to the active center [147]. Under physiological conditions, the pro-peptide of MMP-9 can be removed by trypsin and various other secreted MMPs e.g. MMP-2, 3 or 13. Additionally, plasmin, tissue kallikrein and neutrophil-derived serine proteases in particular NE and CatG were shown to cleavage-activate pro-MMP-9 [154, 157].

Pro-MMP-9 has a molecular weight of 92 kDa and the active form 82 kDa although intermediate sizes can be present and further truncated forms have been reported. Also oligomers with a size > 200 kDa and hetero-complexes with neutrophil-gelatinase associated lipocalin (NGAL) in the range of approximately 130 kDa have been reported [157]. In addition, the actual weight might differ between individual molecules due to differences in glycosylation (see below). *In vitro* several reagents, e.g. 4-aminophenyl mercuric acetate (APMA), have been used to activate pro-MMP9 which all disrupt the

interaction of pro-peptide´s cysteine with Zn^{2+}. Alternatively, renaturing unfolded pro-MMP-9 results in activation of the enzyme [156].

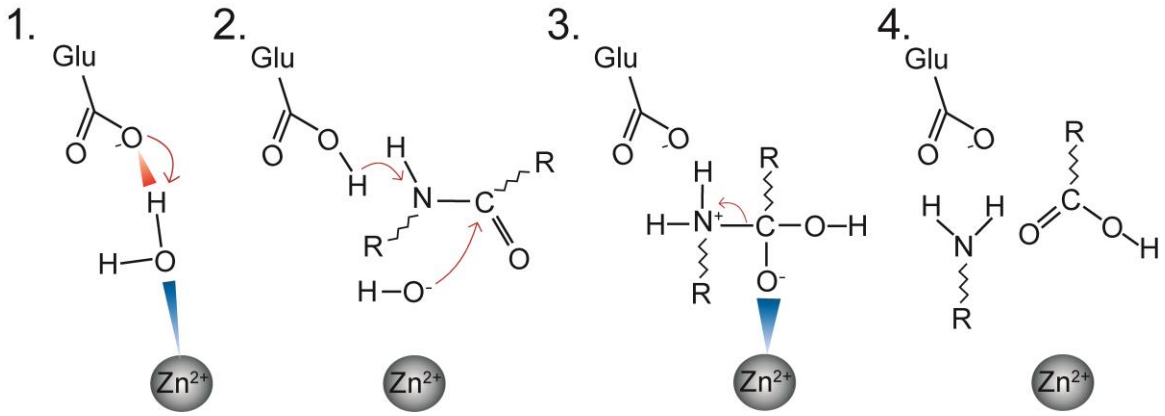

Figure 1.1: **Model of the catalytic mechanism of MMPs.** Initially, the zinc ion polarizes a water molecule (1.) which transfers a proton to glutamate in the active center. The scissile carbonyl bond is polarized by interaction with Zn^{2+}. The hydroxide anion (2.) attacks the carbonyl C atom while the bound H^+ is transferred to the scissile secondary amine in the peptide bond which results in a tetrahedral intermediate (3.). The peptide is cleaved by rearrangement of covalent bonds (4.) but stays bound to the enzyme. The product release is triggered by binding of a new water molecule and marks the rate limiting step in the proteolytic cycle (based on [40, 147]).

The substrate specificity of MMP-9 is mainly determined by its S1' pocket, by three fibronectin repeats that are inserted in the catalytic domain and by the C-terminal hemopexin domain which serves for binding of substrates (e.g. type IV collagen or fibronectin), of inhibitors and of cell surface receptors (e.g. integrins, CD44, Ku70/Ku80) [157][147]. A synonym for MMP-9 is gelatinase B, while gelatinase A refers to MMP-2, indicating their closely related structure and specificity.

1.4.2 Cellular sources and regulation of MMP-9 activity

In general, MMP-9 activity is regulated i) by transcription, ii) by zymogen activation and iii) by presence of endogenous inhibitors in particular TIMPs. The basal expression of *Mmp9*, in contrast to *Mmp2*, is very low in most cell types. *Mmp9* transcription is highly induced by physical or chemical stress, by growth factors (e.g. EGF and VEGF), by cytokines (e.g. IL-1, TNF-α), by hormones (e.g. vitamin D_3), by bacterial products (e.g. LPS) and by cell-matrix adhesion (e.g. in macrophages by integrin-fibronectin/collagen) [22, 154].

Various lung parenchymal and lung resident cell types may express MMP-9 upon induction. These include: fibroblasts, airway smooth muscle cells, endothelial cells,

bronchial epithelial cells, alveolar type II cells, alveolar macrophages, dendritic cells, monocytes, eosinophils, immature neutrophils and lymphocytes including T and B cells [110, 154, 157]. Neutrophil-derived MMP-9 is subject to an additional regulatory mechanism: the stimulation of granule secretion. Hypoxia as present locally in obstructive lung diseases was shown to upregulate neutrophil degranulation [61]. Of note, neutrophils are able to secret A1AT, while MMP-9 is released without simultaneous liberation of its main inhibitor TIMP1. Therefore, chronic neutrophilic lung disease likely show increased levels of unopposed MMP-9 activity.

In the blood the general protease inhibitor α2-macroglobulin restricts MMP activity. In other tissues, TIMPs limit MMP activity: TIMP1-4. Although all TIMPs inhibit MMP-9, TIMP1 has the highest affinity and additionally its expression is induced by similar stimuli as for *Mmp9* [22]. Consequently, most of those cells secreting MMP-9, simultaneously release TIMP1 which contributes to a protease-antiprotease balance in the affected tissue [22, 156]. TIMP1 inhibits MMP activity by tight binding to various sites of the protease. TIMP1 can complex the catalytic Zn^{2+} and occupy the substrate binding site but also associate with C-terminal domains of pro- and active MMP-9 [106, 154].

1.4.3 Role of MMP-9 in pulmonary inflammation and potential implications for CF lung disease

Traditionally, most research in the CF field focused on the role of NE while *in vivo* studies on other proteases remain limited. The functions of proteases are defined by their substrates which themselves are spatially and temporally organized within cells and tissues. *In vitro* studies may identify substrates while an *in vivo* evaluation of proteases is essential to determine their function in health and disease.

MMP-9 has been implicated in regulating cytokine and chemokine potency with different effects between murine and human homologues. Human MMP-9 cleaves IL-8 and thereby potentiates its chemotactic activity for neutrophils. In humans and mice, MMP-9 converts pro-IL-1β into its active form [94]. Murine MMP-9 cleaves and potentiates LIX while human MMP-9 has several cleavage sides on the human homologue CXCL5 (epithelial derived neutrophil activating protein-78, ENA-78) which leads to transient activation and subsequent inactivation [29, 155]. In addition, MMP-9 activity contributes to the generation of small peptides, PGP, by degrading collagen. These are termed matrikines and have chemotactic properties for neutrophils by binding to CXCR1 and 2 [45, 166]**.** MMP-9 may activate latent transforming growth factor (TGF)-β [175]. This might be of interest since polymorphism increasing TGF-β expression have been associated with more severe CF lung disease [27, 75]. TGF-β was shown to be a very

potent neutrophil chemoattractant and therefore might aggravate inflammation in CF lung disease [10].

The hypothesis that MMP-9 might assist in leukocyte infiltration may originate from its ability to degrade basement membrane type IV collagen. Nevertheless, an involvement of MMP-9 in leukocyte recruitment *in vivo* is still controversial [8, 32]. Also anti-inflammatory functions have been proposed e.g. limiting macrophage recruitment by cleaving intercellular adhesion molecule receptor integrin β2 (CD18) [153]. Of note, anti- and pro-inflammatory effects of MMP-9 seem to be context dependent even when studied in similar models [17, 99].

MMP-9 degrades various ECM proteins, e.g. fibronectin or laminin, and similar to all neutrophil serine proteases also digests elastin [115]. Increased NE or MMP-9 activity have been linked to an aberrant ECM remodeling and impaired regeneration of lung parenchyma in a model for ventilator-induced lung injury [58, 59]. Upon epithelial cell damage, MMP-7 and MMP-9 expression is detected in regenerating lung tissue [115]. MMP-9 is found in migrating basal cells and wound repair can be blocked with MMP-9-specific antibody treatment. The effect of MMP-9 on respiratory epithelial pathophysiology is less well studied. MMP-9 activated pro-IL-1β can induce MUC5B expression in airway epithelial cells [44, 157]. This suggests that increased MMP-9 activity might contribute to airway mucus obstruction in CF lung disease.

Nevertheless, the potential opposing effects of MMP-9 activity in modulating leukocyte chemotaxis, ECM degradation and wound repair illustrate that *in vivo* studies are needed to determine the role of MMP-9 in the pathogenesis of CF lung disease.

1.4.3.1 Correlation of MMP-9 levels with clinical parameters in CF lung disease

Several studies measured MMP-9 levels either in sputum or BAL fluid and related those to acute pulmonary exacerbations, bacterial colonization, lung function and disease severity in CF patients. Most studies focused on soluble MMP-9 protein levels. A study by Delacourt et al. reported that MMP-9 activity is elevated in CF patients with acute exacerbations compared to asthma patients and detected a correlation with type IV collagen degradation products in sputum supernatant [30]. MMP-9 levels were correlated with elevated neutrophil degranulation markers. In stable CF patients, MMP-9 activity showed an inverse correlation with lung function parameters (FEV1% and forced vital capacity %). No association of MMP-9 activity and pulmonary bacterial burden was determined [30]. Other studies detected elevated sputum MMP-9 levels either during exacerbations but also in CF patients with stable lung disease [63, 104]. A study by Sagel et al. showed an imbalance between MMP-9 and TIMP1 and found an inverse correlation with FEV_1% in CF patients with stable disease [135]. Of note, not all studies

reported a relation between MMP-9 levels and disease severity or progression in CF patients [46, 136]. In a prospective study over three years various inflammatory sputum biomarkers were measured including MMP-9, TIMP1, IL-1β, neutrophil counts and NE and associated with lung function changes in CF patients [136]. Only NE, total neutrophil counts and IL-1β showed a significant correlation with decline in FEV_1 in CF patients. MMP-9 concentration was elevated but not changed over the studied period.

Further studies in CF patients detected higher MMP-9 levels in BAL compared to controls [126]. MMP-9 correlated with higher lactoferrin concentrations which indicates that neutrophils were the main source of MMP-9 in the studied CF cohort. Recently, Garrat et al. reported that NE concentration, neutrophil counts and MMP-9 levels correlate with each other in BAL fluid of pre-school CF patients [48]. Moreover, higher abundance of MMP-9 in BAL fluid correlated with the progression of bronchiectasis in CF patients [48].

These correlative studies suggest that MMP-9 may promote CF lung disease. It is important to note that correlation of protease activity with clinical parameters may be of value to quantify the risk for patients or to predict clinical outcome. However, additional studies are needed to carefully determine the contribution of candidate proteases to pathologic signs in model organisms of CF lung disease.

1.5 βENaC-Tg mice as model for the study of CF lung disease

Mice deficient for CFTR do not show a lung phenotype resembling lung disease of CF patients [143]. Mice with lung specific overexpression of the β-subunit of ENaC were generated to mimic human CF lung disease [89]. In healthy airways, CFTR limits ENaC-mediated Na^+ absorption and crucially regulates ASL ion and volume homeostasis [91]. Lack of functional CFTR, e.g. by ΔF508 mutation, leads to ASL volume depletion and thickened airway mucus (see above).

1.5.1 βENaC-Tg mice phenocopy key characteristics of CF lung disease

The club cell secretory protein (CCSP) promotor driven overexpression of the βENaC-transgene (βENaC-Tg) in mice is sufficient to cause an increased club cell-mediated Na^+ absorption which results in a reduction of ASL volume, slows mucociliary clearance and initiates a spontaneous neutrophilic inflammation [89, 92]. βENaC-Tg mice suffer from airway mucus plugging which causes an increased neonatal mortality [66, 92].

The trigger of inflammation in the absence of bacterial infection in early CF lung disease remains unknown [69]. Studies in βENaC-Tg mice highlight hypoxic epithelial necrosis associated with airway mucus obstruction as potential mechanism to cause sterile inflammation [43, 86]. Increased pulmonary levels of cytosolic DAMPs, in particular IL-

1α, were similarly reported for neonatal βENaC-Tg mice and young CF patients [43, 102]. IL-1α-IL-1 receptor signaling induces subsequently pro-IL-1β expression [43, 80]. Pro-IL-1β is typically activated by inflammasome-associated caspase-1 [80]. The stimuli for inflammasome assembly are divers and include bacterial components. The resulting inflammatory response is predominantly carried by T-helper cell type 2 (Th2) signature cytokines e.g. IL-13 in βENaC-Tg mice. Alternative activated macrophages and epithelial cells secret high amounts of eotaxin, KC and MIP-2 which mediates the recruitment of eosinophils and neutrophils into the lungs of βENaC-Tg mice [89, 92].

In parallel, goblet cells increase in number and express high levels of mucins i.e. *Muc5ac, Muc5b* and *Muc4* [92]. The persistent inflammation leads to emphysema formation in distal lung parenchyma of βENaC-Tg mice. The structural tissue damage alters inspiratory capacity, lung compliance and other lung function parameters [92]. In summary, βENaC-Tg mice represent a phenotype which shows key characteristics of early CF lung disease i.e. ASL depletion, mucus obstruction and inflammation [179].

1.5.2 Characterization of NE activity and NE deletion in βENaC-Tg mice

βENaC-Tg mice have proven to be a valuable model for studying the pathogenic contribution of proteases to CF-like lung disease [49, 150, 162]. In a previous study, NE activity was detected only on the surface of neutrophils while soluble NE was completely inhibited in BAL supernatant of βENaC-Tg mice [49].

NE deficient βENaC-Tg mice display less pulmonary neutrophilia in the presence of elevated KC and MIP-2 levels [49]. Goblet cell metaplasia and mucin mRNA levels were substantially reduced while mucus obstruction was unchanged. This suggests that ENaC-mediated Na^+ absorption was sufficient to cause airway mucus plugs in the absence of mucin hypersecretion in βENaC-Tg/*NE*$^{-/-}$ mice. Further, *NE* deletion in βENaC-Tg mice did not compromise innate immune function since no exacerbation of bacterial infection was detected [49]. The *NE* knockout partially reduced emphysema formation. This observation indicates that additional mechanisms contribute to lung damage in βENaC-Tg mice and potentially to CF lung disease in humans.

1.6 Current status for treatment of CF lung disease with protease inhibitors

Currently, no protease inhibitor has been approved for the treatment of CF patients. Only few clinical trials have been performed with protease inhibitors in CF patients which all targeted NE [107, 123]. Inhalation of A1AT aerosol for 4 weeks reduced sputum neutrophil counts, NE activity and P. aeruginosa colony forming units but failed to improve lung function in CF patients [51].

In another trial, application of a small molecule NE inhibitor AZD9668 for 4 weeks reduced urinary desmosine levels and IL-6 levels but did not diminish sputum neutrophilia, improve lung function or other clinical outcomes in CF patients [36]. In summary, the available data for the treatment of CF lung disease with protease inhibitors is limited and conclusion about the therapeutic strategy or their potency cannot be drawn. Further studies in model organism are needed to carefully dissect the contribution of candidate proteases to pathologic alterations in order to evaluate critical targets in CF lung disease.

1.7 Aims of the thesis

The aim of this thesis was to evaluate the role of MMP-9 in the pathogenesis of βENaC-Tg mice and to target relevant proteases by small molecule inhibitors in preventive preclinical trials. Genetic deletion of *Mmp9* in βENaC-Tg mice and determination of key phenotypic characteristics enabled the inference on MMP-9-dependent alterations in mice with CF-like lung disease. The analysis included monitoring of survival, determination of pulmonary inflammatory response, assessment of airway mucus obstruction and quantification of emphysema severity in WT, *Mmp9*$^{-/-}$, βENaC-Tg and βENaC-Tg/*Mmp9*$^{-/-}$ mice.

First, MMP-9 protein levels were assessed in BAL fluid of WT, *Mmp9*$^{-/-}$, βENaC-Tg and βENaC-Tg/*Mmp9*$^{-/-}$ mice using gelatin zymography. A change in survival was inferred by comparing observed genotype frequencies in adult mice with those calculated by Mendel´s Laws. Furthermore, determining inflammatory cytokines, chemokines and leukocyte counts in BAL fluid enabled the detection of differences in inflammatory cytokine profile and pulmonary leukocyte infiltration in WT, *Mmp9*$^{-/-}$, βENaC-Tg and βENaC-Tg/*Mmp9*$^{-/-}$ mice. Assessment of expression of secreted airway mucins Muc5b and Muc5ac by qRT-PCR, together with morphometric analysis of mucus content in main bronchi in histologic sections enabled the evaluation of airway mucus obstruction. Additional analysis of goblet cell metaplasia in airway sections and quantification of goblet cell marker expression complemented the analysis by determination of airway epithelial alterations. Moreover, lung volume measurement and morphometric quantification of distal airspace enlargement in tissue sections were used to elucidate changes in emphysema severity in βENaC-Tg compared with βENaC-Tg/*Mmp9*$^{-/-}$ mice and littermate controls.

Lung function measurements were compared in NE and MMP-9 deficient βENaC-Tg mice to assess a potential overlap in the impact of NE and MMP-9 on lung tissue mechanics. Based on these findings, a treatment strategy was developed for a preventive therapy in newborn βENaC-Tg mice with small molecule protease inhibitors. Preclinical studies with the NE inhibitor sivelestat in neonatal βENaC-Tg mice and WT littermates were performed and evaluated by assessment of airway mucus obstruction, leukocyte counts in BAL fluid and distal airspace enlargement. Furthermore, different drug application routes were studied to assess the concept of systemic sivelestat treatment to reduce proteolytic lung damage in chronic neutrophilic pulmonary diseases.

2 Materials and Methods

2.1 Experimental animals

All mouse experiments were approved by the Regierungspräsidium Karlsruhe. *Mmp9*$^{-/-}$ (B6.FVB(Cg)-Mmp9tm1Tvu/J, Jackson laboratories, Bar Habour, ME, USA) [161], *NE*$^{-/-}$ (Jackson laboratories, Bar Habour, ME, USA) mice were intercrossed with βENaC-Tg mice [89] to generate WT, *Mmp9*$^{-/-}$, βENaC-Tg, βENaC-Tg/*Mmp9*$^{-/-}$ and *NE*$^{-/-}$, βENaC-Tg/*NE*$^{-/-}$ mice. NE deficient mice had been backcrossed for >12 generation and *Mmp9* deficient mice for at least 6 generation to a C57BL/6 genetic background. Mice were housed under specific pathogen-free conditions with free access to chow and water and 12h day/night cycle. The characterization of MMP-9 and NE deficient βENaC-Tg mice was performed in adult 6 to 8 week-old mice and preclinical trials in newborn mice WT and βENaC-Tg mice.

2.2 Genotyping

Tail biopsies were boiled at 95°C in 100 µl alkaline lysis reagent (25 mM NaOH, 0.2 mM EDTA, pH 12; Sigma Aldrich, Schnelldorf, Germany) for 40 min. Samples were put on ice for 2 min and 100 µl neutralizing reagent was added (40 mM Tris-HCl pH 5). The supernatants containing DNA were used for polymerase chain reaction (PCR) using Prima Amp 2x Hot start Red PCR mix (Steinbrenner, Wiesenbach, Germany).

Primers:

Common name	Gene	Description	Annealing temperature	Sequence
βENaC	*Scnn1b*	forward	56 °C	CTT CCA AGA GTT CAA CTA CCG
		reverse		TCT ACC AGC TCA GCC AGA GTG
Neutrophil elastase	*Elane*	forward	60 °C	GGA ACT TCG TCA TGT CAG CA
		WT reverse		TGC ACA GAG AAG GTC TGT CG
		KO reverse		TGG ATG TGG AAT GTG TGC GAG
Matrix metallo-proteinase 9, Gelatinase B	*Mmp9*	WT forward	60 °C	GTG GGA CCA TCA TAA CAT CAC A
		WT reverse		CTC GCG GCA AGT CTT CAG AGT A
		KO forward		CTG AAT GAA CTG CAG GAC GA
		KO reverse		ATA CTT TCT CGG CAG GAG CA

Genotype was confirmed by monitoring the band pattern of the PCR products after agarose gel electrophoresis.

2.3 Bronchoalveolar lavage and differential cell count

BAL of mouse lungs and differential cell count (DCC) were performed as previously described [92]. Mice were anaesthetized by intraperitoneal injection of ketamine (120 mg/kg body weight) (Bremer Pharma GmbH, Warburg, Germany) and xylazine (16 mg/kg) (cp-pharma, Burgdorf, Germany) and sacrificed by incision in the abdominal V. cava inferior. Diaphragm and thorax were resected and the left main bronchus was ligated to separate the left pulmonary lobe.

Bronchoalveolar lavage was performed with the four right pulmonary lobes. Through a tracheostoma a calculated volume (bodyweight (g) x 17.5 µl) of sterile phosphate buffered saline (PBS, Gibco, Thermo Fisher Scientific, Darmstadt, Germany) was applied. The adjustment of BAL volume was necessary to account for developmental differences in lung size and accurately reflects the total inspiratory capacity until adult hood is reached [77]. PBS was gently inserted and withdrawn three times using a 1 ml syringe. The recovered BAL fluid was centrifuged at 600 x g to pellet the containing mucus plugs and cells. Supernatant were frozen at -80 °C and BAL cell number was determined with a Neubauer chamber.

30,000 cells of the BAL pellet were centrifuged on a glass slide using a cytospin, dried and stained 3 min with May-Grünwald (1:1) (Merck, Darmstadt, Germany) and 7 min with Giemsa (1:10) (Merck, Darmstadt, Germany) solution for differential cell count. Cell types were identified according to their size, nuclear shape and staining properties. A total of 400 cells were counted to obtain the percentage of each cell type in the BAL fluid. Counts of each cell type per volume (cells/ml) were calculated with the total collected BAL volume and the determined total cell number in BAL fluid.

2.4 Gelatin zymography

Principle

Gel zymography can be used to monitor enzyme or inhibitors amounts in solution [71, 156]. The technique is mostly confined to assess protease levels but also other enzymes e.g. chitinases can be detected with a modified protocol [148]. Common principle is that enzyme activity converts a substrate, which is detected in a second step. In gelatin zymography denatured collagen is co-polymerized in a normal sodium dodecyl sulfate (SDS) containing polyacrylamide gel. After SDS polyacrylamide gel electrophoresis (PAGE) under non reducing conditions, the denaturing SDS is washed out which enables the gelatinases to refold to their native conformation and regain activity. Refolding is thought to lead to activation of the gelatinase pro-forms. By incubation at 37°C for several hours gelatin in the gel is degraded which can be detected in a second step by coomassie staining of the gel. In summary, the gelatinases are separated

according to their size during SDS page and pro- and active form appear as blank bands, where gelatin was digested, in the coomassie stained gel. Gelatin zymography has a sensitivity in the low pg range for active MMP-2 or MMP-9. Gel zymograms do not represent the actual enzyme activity in the sample as endogenous inhibitors are separated from their target protease during SDS PAGE.

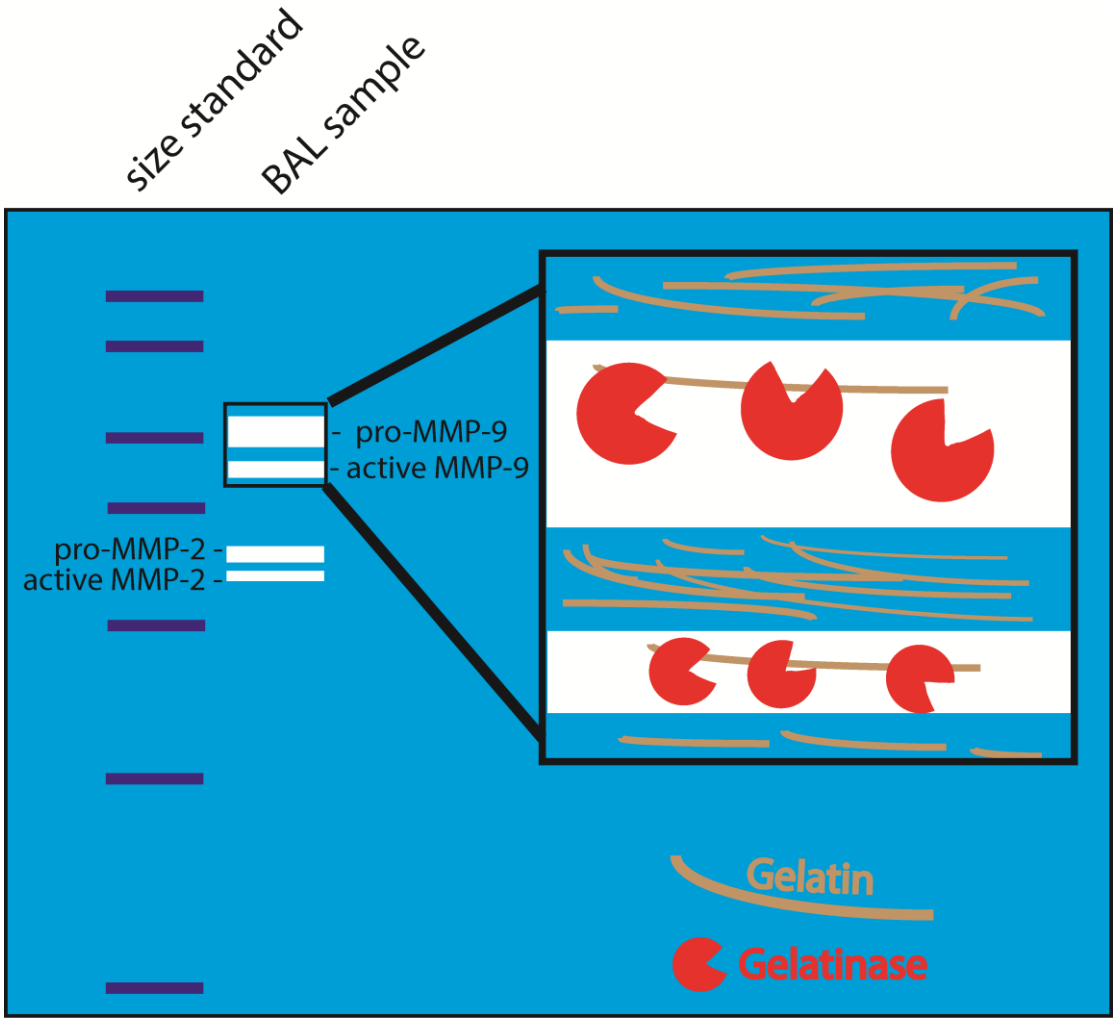

Figure 2.1: Principle of gelatin zymography. Schematic example of a coomassie stained gelatin zymography gel. The upper two white (not stained) bands in the lane of the BAL sample represent pro- and active MMP-9 and the lower pro- and active MMP-2. On molecular level (inset) pro-MMPs become activated after refolding and dislocation of their inhibitory pro-peptides. Activated pro- and active forms of MMPs digest incorporated gelatin within days of incubation at 37°C. In coomassie stained gels, spots of gelatinase activity become visible as clear bands.

Polyacrylamide-gelatin zymography:

Stacking gel:

Reagent	Concentration	Volume (µl)
ddH_2O		926.5
Tris-HCl pH 6.8	0.5 M	378
SDS	10 %	15
acrylamide-bisacrylamide	40 %	148.5
TEMED		3
APS	10 %	30
	Total volume:	1500 µl

Resolving gel 10% with 0.2 % gelatin:

Reagent	Concentration	Volume (µl)
ddH_2O		1859
Tris-HCl pH 8.8	1.5 M	666
SDS	10 %	40
acrylamide-bisacrylamide	40 %	1000
gelatin	2 %	400
TEMED		5
APS	10 %	30
	Total volume:	4000 µl

Bovine type B gelatin (Sigma Aldrich, Schnelldorf, Germany) was dissolved at 37-56°C in water and copolymerized at a concentration of 0.2 % in a 10 % polyacrylamide gel (0.75 mm thickness). As standard 2 ng/µl of recombinant murine pro-MMP-9 (R&D Systems, Minneapolis, MN, USA) were diluted in 90 µl TCNB buffer (Tris 50mM, $CaCl_2$ 10 mM, NaCl 150 mM, Brij35 0.05%, Sigma Aldrich, Schnelldorf, Germany) and activated with 10 µl 10 mM amino-phenyl mercuric acetate (APMA, final 1mM; Sigma Aldrich, Schnelldorf, Germany) for 2 h at 37°C. Activated MMP-9 or BAL samples were incubated > 10 min with 4 x Laemmli buffer (Biorad, Munich, Germany) without reducing agent at room temperature. SDS PAGE was performed at 140 V and 15 mA per gel for 3-4 hours at 4

°C. Subsequently, gels were rinsed with ddH_2O and incubated with renaturing buffer (2.5 % Triton X100; AppliChem, Darmstadt, Germany) twice for 0.5-1 h while rocking at RT. After rinsing the gels with ddH_2O and they were transferred into development buffer (Tris 50 mM pH 7.5, $CaCl_2$ 5 mM, $ZnCl_2$ 1 µM, 0.01 % NaN_3) for 30-45 min under gentle agitation. Gels were placed in fresh development buffer and incubated for 38-42 h at 37°C. For visualizing gelatin degradation, gels were rinsed with ddH_2O and stained with coomassie R250 solution (5 % (v/v) methanol, 10 % (v/v) acetate, 0.5 % (w/v) Coomassie R250; Carl Roth, Karlsruhe, Germany) for 1 h. Gels were destained with 40 % methanol and 10 % glacial acetate (Carl Roth, Karlsruhe, Germany) for 2 - 15 h at RT until bands of the protein size standard (Precision Plus Dual color standard, Biorad, Munich, Germany) and clear bands of gelatinase activity were visible.

2.5 Lung histology

Structural damage was assessed in hematoxylin eosin (HE) stained sections of distal lung tissue by stereological methods i.e. mean linear intercept and destructive index. For quantification of mucus obstruction and goblet cell metaplasia in the airways Alcian blue periodic acid Schiff (AB-PAS) stained sections of the left main bronchi were evaluated to determine the mucus volume density or goblet cell counts.

2.5.1 Fixation, Embedding and sectioning

The lavaged right lung was ligated under a constantly applied pressure of 25 cm column of 4 % paraformaldehyde (PFA, neutral buffered; Fischar, Saarbrücken, Germany). The left lung was ligated and not lavaged to preserve mucus plugs. Right and left ligated lungs were immersion fixed with neutral-buffered PFA at 4°C overnight. Lungs were washed in PBS three times each three minutes and non-lung tissue was removed. The inflated right lung was used for lung volume measurement (see below). For storage, lungs were kept at 4°C in 70 % ethanol (Carl Roth, Karlsruhe, Germany).

Lung lobes were separated and right lobes` hilus regions were cut to create an even plane for sectioning. Apical left lobe was removed to ensure orientation during embedding. All lobes were dehydrated in embedding cassettes (Sanowa, Leimen, Germany) by increasing ethanol concentration from 70 % to 2 x 96 % ethanol for 30 min, twice in 100 % ethanol for 45 min then followed by overnight incubation in 100 % xylene (Carl Roth, Karlsruhe, Germany). Embedding cassettes containing the lungs were placed in 55 °C warm dissolved paraffin and incubated under an applied vacuum for 2 h and 1 h at atmosphere pressure. The single left lobe or all four right lobes were placed in separate molds containing 1 mm solidified paraffin and subsequently filled with 65 °C paraffin (Paraplast, Carl Roth, Karlsruhe, Germany) using an embedding station (Leica

EG1150H, Leica Microsystems, Nussloch, Germany). Paraffin embedded lungs were left at 4°C for >16 h before sectioning.

Paraffin blocks were cut with a microtome (Leica Microsystems, Nussloch, Germany) in 5 µm sections for measurement of mucus obstruction and structural lung damage. To obtain single cell layer slices, 1.5 µm sections were prepared for goblet cell quantification.

2.5.2 Lung volume measurement

For the assessment of histological parameters the organ size is relevant. The volume displacement method [140] enables the detection of organ volume by submerging the lung in PBS and detecting the weight change of the container on a balance. Attached tissue and excess liquid is removed from the inflated, fixed right lung lobes. The right lung is submerged in PBS and kept in place with a thin wire without touching the container wall or bottom (Figure 2.2). The weight is recorded which is a direct estimate of the replaced volume by the lung.

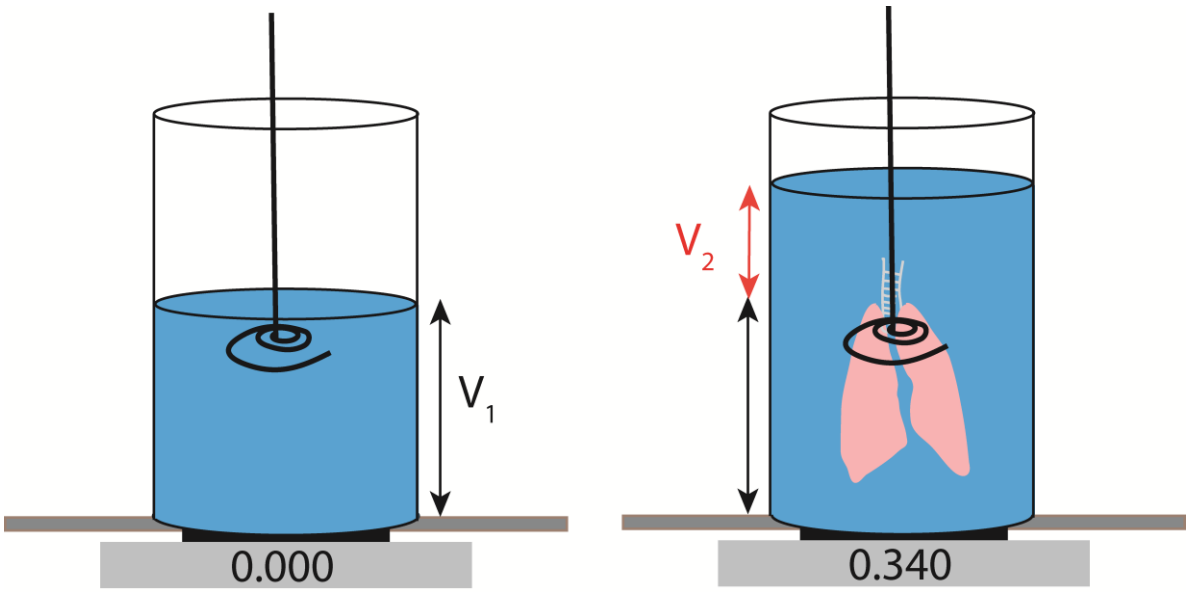

Figure 2.2: Experimental setup for lung volume measurement. A glass beaker is filled with PBS (V_1), placed on a balance and a wire is positioned in the container. The volume increases (V_2) with the submerged lung which is detected by an increased weight on the balance.

By using a wire for submerging the floating lung the difference in density of the lung and liquid is compensated by outside force. Therefore, the lung volume is calculated with the density of PBS (~1 g/cm^3) and the weight before and after submersion.

1) $\rho = V_1/m_1 = (V_1+V_2)/(m_1+m_2)$
2) $V_2 = \rho * m_2$

Thus, according to equation 2) is the lung volume (V_2) equal to the measured mass (m_2) multiplied with the density of PBS.

ρ = density
V_1 = volume before submerging the organ
V_2 = volume of the organ = volume of the displaced liquid
m_1, m_2 = mass of the liquid ($_1$) and displaced liquid ($_2$)

2.5.3 HE and AB-PAS staining

The sections were deparaffinized 2 x 10 minutes in xylene and rehydrated 2 x 5 minutes in 100 % ethanol, 2 x 2 minutes in 96 % ethanol, 2 min in 70 % ethanol and finally rinsed twice in ddH_2O. Right lung sections were stained with hematoxylin Gill's 3 (Sigma Aldrich, Schnelldorf, Germany) and eosin G (Carl Roth, Karlsruhe, Germany). Blue hematoxylin binds DNA while positively changes acidophilic structure, e.g. cytoplasm or collagen, interact with light red eosin dye. For AB-PAS staining, slides with section were rehydration and placed in Alcian Blue solution (Sigma Aldrich, Schnelldorf, Germany) for 30 minutes followed by 5 minutes in periodic acid (Sigma Aldrich, Schnelldorf, Germany) and 15 minutes Schiff´s reagent (Sigma Aldrich, Schnelldorf, Germany). Acidic saccharides, e.g. sulphated or sialic acid containing mucins, are stained by Alcian blue while neutral carbohydrates react with the subsequent PAS reagent and can be detected in magenta colour. As a result, neutral basement membrane proteoglycans are stained with magenta colour while airway luminal mucus and goblet cells contain both blue and magenta stained mucins.

2.5.4 Quantification of structural lung damage by measurement of mean linear intercepts and destructive indices

Images of HE stained lung sections were taken at 16x magnification with an inverted microscope (Olympus IX-71 microscope (Olympus, Hamburg, Germany) equipped with a camera (DP73; Olympus, Hamburg, Germany) and analyzed using Cell F imaging software (Olympus, Hamburg, Germany).

For mean linear intercept (MLI) measurement a total of 10 images per mouse were analyzed. On the photograph 4 parallel lines were placed with the same length as the image. The intersecting points of the line with alveolar walls were counted for two lines. The total counts of intersections were divided by the length of the two lines. Thereby, the

mean linear intersection distance or intercept was obtained. This parameter can be regarded as approximation of the mean size of a terminal respiratory structure i.e. alveolus and alveolar duct.

Destructive index (DI) is a measure of the apparent emphysema severity i.e. destruction of alveolar structure. A 45 µm x 40 µm grid of points is overlaid on an image of alveolar tissue. The points are classified as lying in a destructed or normal area. The criteria for determination of the region directly surrounding or adjacent to the point as destructed are a) at least two interruptions in alveolar walls or b) at least two isolated parenchyma islets or c) presence of emphysematous lesions within the area [134]. The DI is calculated as the ratio of the number of destructed point and total point counted (normal + destructed). For each animal a minimum of 300 points were evaluated.

2.5.5 Quantification of mucus obstruction by mucus volume density and goblet cell counts

Stereological methods are used to infer information on 3D structures from 2D measurements. A volume density is the ratio of the object volume e.g. mucus and to the volume of the whole structure e.g. airway [180]. Volume densities can be directly derived from histological sections by measurement of the area of the mucus covering surface in the section divided by the area of the whole airway. Harkema et al. established a slightly modified parameter called mucus volume density which is defined as [56]:

3) $V_S = V_V/S_V$.

Equation 3) can be converted to:

4) $V_S = A_M/A_A * V_A/S_A$.

V_S = mucus volume density

V_V = Volume of mucus/ volume of airway = volume density

S_V = airway covering surface area/volume of airway

A_M = area covered by mucus

A_A = area airway

V_A = Volume of the airway

S_A = surface area of the airway

The relationship between surface volume density S_V to boundary length B_A is given by:

5) $S_V = S_A/V_A = 4/\pi\ B_A/A_A$.

B_A = length of boundary of whole structure = length of airway basal lamina

Formula 4) and 5) can be transformed to [180]:

6) $V_S = A_M/B_A * \pi/4$.

The parameters in equation 6) can be obtained in 2D sections. The mucus volume density V_S has the unit: nl/mm^2. Airway mucus volume density was measured in AB-PAS stained sections of the left proximal main bronchi. Image analysis of airway section included manual subtraction of the airway surrounding structures, image conversion to gray scale and threshold setting. Mucus covering area, total basement membrane or apical epithelial lumen boundary length was used for calculation of mucus volume density with formula 6).

Goblet cells were counted in 1.5 µm AB-PAS stained airway sections and values were normalized to basement membrane length.

2.6 Cytokine measurement with enzyme linked immunosorbent assay and cytometric bead array

The murine chemokine KC (synonym: mCXCL1) and the cytokines IL-1α, IL-1β, IL-13 were measured in BAL supernatant using cytometric bead array (CBA) kits (BD Biosciences, Heidelberg, Germany) according to manufacturer´s instructions. The concentration of MIP-2 (synonym: mCXCL2) and LIX (synonym: mCXCL5) and murine TIMP-1 was determined in BAL supernatant by enzyme linked immunosorbent assay (ELISA) (R&D Systems, Minneapolis, MN, USA).

2.7 Semi-quantitative reverse transcription-PCR for gene expression studies

2.7.1 RNA extraction from mouse lung with Trizol

The left lung was transferred into 15 ml Falcon tube containing 1 ml of Trizol (Thermo Fisher Scientific, Darmstadt, Germany) and homogenized with a rotor-stator (IKA, Staufen, Germany). The sample was left for 20 minutes at room temperature for cell lysis. For phase separation 200 µl chloroform (Sigma Aldrich, Taufkirchen, Germany) were added and incubated for 3 minutes at room temperature. After centrifugation at 12,000 x g for 10 minutes at 4°C the upper aqueous phase was transferred in 1.5 ml test tubes (Eppendorf safe-lock tubes, Eppendorf, Hamburg, Germany). For total RNA precipitation 500 µl isopropanol (100%) was added, mixed and incubated for 10 minutes at room temperature. By centrifugation at 14,000 x g for 10 minutes at 4°C RNA was pelleted and subsequently washed with 75 % ethanol and air dried. The dry pellet was resuspended in RNAse-free water and the concentration and quality was measure in a photometer (DeNovix, DS-11 Spectrometer, DeNovix Inc, Wilmington, USA) according to Lambert-Beer´s law.

2.7.2 cDNA synthesis and quantitative reverse transcription-PCR

To clone a complementary (c)DNA copy of all RNA strands in the sample, random hexamer primers were used in reverse transcription mix. The reaction mix for cDNA synthesis was prepared as followed:

Reagent	Concentration	Volume (µl)
Hexamer primers	100 nM	2
dNTPs	10 mM	1
RNA	1 µg	x
Nuclease free H_2O		ad 13 ul

The mixture was heated in a PCR cycler (Veriti, Thermo Fisher Scientific, Darmstadt, Germany) to 65 °C for 5 min. Samples were cooled on ice for 2 minutes and a mixture was added containing 4 µl FS buffer, 1 µl dithiotreitol (DTT), 1 µl H_2O and 1 µl Superscript III RT (Invitrogen, Karlsruhe, Germany).

Quantitative reverse transcription (qRT)-PCR was performed on an Applied Biosystems 7500 Real Time PCR system (Applied Biosystems, Darmstadt, Germany) with TaqMan Universal PCR master mix and inventoried TaqMan gene expression assays were used for *Muc5ac* (Mm01276718_m1), *Muc5b* (Mm00466391_m1), chloride channel accessory 1 (*Gob5*) (Mm01320697_m1), matrix metalloproteinase 12 (*Mmp12*) (Mm00500554_m1), matrix metalloproteinase 8 (*Mmp8*) (Mm00439509_m1), matrix metalloproteinase 13 (*Mmp13*) (Mm00439491_m1), matrix metalloproteinase 2 (*Mmp2*) (Mm00439498_m1), chitinase-like 3 (*Ym1*) (Mm00657889_mH), secretory leukoprotease inhibitor (*Slpi*) (Mm00441530_g1), BPI fold containing family A, member 1 (*Splunc1*) (Mm00465064_m1) and β-actin (*Actb*) (Mm00607939_s1).

qRT-PCR mix:

Reagent	Volume (µl)
TaqMan master mix (2x)	10
Taqman assay	1
cDNA	1
H_2O	8

Cycler program:

Temperature	Duration	
50 °C	2 min	
95 °C	10 min	
95 °C	15 s	40 x
60 °C	1 min	

The amplification cycle of crossing a fixed threshold (C_T) for fluorescence intensity was determined for the target gene and relative copy number was calculated with the efficiencies of the PCR cycle according to Pfaffl et al. [121]. Values were normalized to *Actb* values of the sample and expressed for each genotype as fold-change relative to WT samples.

2.8 Western Blot

SDS PAGE was done using precast gels (Any kD Mini-PROTEAN TGX Precast Protein Gels, Biorad, München, Germany) in a Biorad electrophoresis system at 50 V for 10 minutes and separation for 1.5 -2 h with 15 mA per gel and 140 V. Gels were blotted on PVDF membranes (Trans-blot Turbo, Biorad, Germany) using a Trans-blot turbo transfer system (Biorad, München, Germany). Standard blotting settings were chosen with 7 minutes transfer duration. Membranes were incubated for 1 minute in washing buffer (20 mM Tris pH 7.5, 150 mM NaCl, 0.1 % Tween 20) and protein free spot on the membrane were saturated with blocking solution (5% bovine serum albumin (BSA, Sigma Aldrich, Schnelldorf, Germany) in washing buffer) for 1h at room temperature. Blots were washed three times for 3 minutes with washing buffer. Primary antibodies were diluted in 10 ml blocking buffer. Blots were incubated with the primary antibodies at 4°C overnight under agitation. Membranes were washed 2 x 3 minutes and 1 x 5 minutes with washing buffer. Horseradish-peroxidase coupled secondary antibodies directed against the host of the primary antibody were diluted in washing buffer and incubated with the blots for 1 h at room temperature. Excess antibody solution was washed off 2 x 5 minutes and 1 x 10 minutes with washing buffer. For detection equal volumes, e.g. 1-4 ml, of luminol and of hydrogen peroxide solution (Clarity Western ECL, Biorad, Germany) were mix and incubated in the dark with the blots for 4 minutes. Chemiluminescence was detected with a CCD camera typically for 1-3 minutes (ChemiDoc MP, Biorad, München, Germany).

Primary antibodies:

Murine antigen	Host	Dilution/Concentration	Vendor
SerpinA1 (A1AT)	rabbit	0.5 µg/ml; 1 : 1000	Boster Biological Technology

Secondary antibodies:

Antigen	Host	Dilution	Vendor
anti-rabbit	goat	1 : 20000	Sigma Aldrich

2.9 Detection of MMP-9 activity with DQ Gelatin

Gelatin zymography enables the qualitative detection and discrimination of different gelatinases according to their molecular weight. Complementary, a soluble fluorescein-conjugated gelatin reporter was used for the quantitative detection of gelatinase activity in BAL supernatant (DQ gelatin EnzCheck; Molecular Probes, Eugene, USA). Detection limit of the assay is specified as 7 ng/ml gelatinase concentration.

For activity measurement in a plate reader (EnSpire, Perkin Elmer, Waltham, USA) 40 µl BAL samples or diluted activated MMP-9 (see chapter “Gelatin zymography” 2.4) were mixed with 10 µl DQ-Gelatin (125 µg/ml) in black half area 96 well plates (Corning Inc., Acton, USA). Fluorescence was excited at 495 nm and emission was recorded at 515 nm wave length over a period of 1 h. Initial slopes of fluorescence intensity over time were calculated as a measure of gelatinase activity in BAL supernatant. In the evaluation of MMP-9 activity in BAL supernatant a final concentration of 0.02 ng/µl APMA-activated rmMMP-9 was used as positive control.

2.10 Lung function measurement in mice

Mice were anaesthetized by intraperitoneal injection of 80 mg/kg sodium pentobarbital (cp-pharma, Burgdorf, Germany). Via a cannula inserted into a tracheostoma, the mouse was connected to a small animal ventilation apparatus (flexiVent, SCIREQ, Montreal, Quebec, Canada.). Under continuous computer controlled mechanical ventilation, mice were paralyzed by an intraperitoneal injection of 1.6 mg/kg pancouronium bromide (Inresa Arzneimittel GmbH, Freiburg, Germany). For ventilation the following settings were chosen: tidal volume of 10 ml/kg body weight, 150 breaths/minute and positive end-expiratory pressure of 3 cm H_2O. Lung tissue mechanics were assessed by different maneuvers of various ventilation pressures or volumes performing 4 technical replicates for each lung function parameter.

The inspiratory capacity (IC) is defined as the maximal lung volume obtained with an applied pressure which was determined with a gradually increasing pressure up to 30 mmH_2O. Therefore IC values reflect the maximal lung volume during normal inspiration which is increased in emphysematous lungs and decreased by fibrotic lung remodeling. With a step-wise inflation-deflation cycle protocol with defined pressure (p) or volume (V) steps the static compliance and hysteresis area of the pV-loop was determined. Compliance is defined as the ratio of volume change to pressure difference and therefore can be regarded as the ability of the lung to stretch under a defined pressure increase. Low compliance indicates a stiff, rigid lung tissue as seen in lung fibrosis while high compliance values typically indicate presence of emphysema. Lung hysteresis in the pV loops is observed as the relation between pressure and volume during inspiration

differs from that during expiration. During lung inflation higher pressures are needed for a defined lung volume than during expiration. The lung hysteresis area is increased with the degree of emphysema severity. For the measurement of the dynamic compliance, elastance and tissue resistance during a respiratory cycle a sinus-wave with a frequency of 2.5 Hz was applied. Resistance was calculated according to the single compartment model [6].

2.11 Treatment with the NE inhibitor sivelestat

2.11.1 Systemic application via intraperitoneal or subcutaneous injection

Sivelestat (Ono-5046, M = 456.44 g/mol) (Figure 2.3) is a potent alternative substrate inhibitor for NE (IC_{50} = 49 nM) [67]. PR3 is inhibited to a lower extent and only very weak inhibition of CatG has been reported [67, 145]. For systemic application, intraperitoneal (i.p.) and subcutaneous (s.c.) injections were performed twice daily (12h cycle) starting on the day of birth for two weeks with the endpoint on the 14th postnatal day. Sivelestat (Tocris Bio-Techne GmbH, Wiesbaden-Nordenstadt, Germany) was dissolve in 0.9 % NaCl (B. Braun Melsungen AG, Melsungen, Germany) to a concentration of 2.5 mg/ml with pH adjusted to 7.4-7.5. A single dose of 50 µg/g (body weight) was applied in 20 µl/g (body weight) either i.p. or s.c. using 30 G syringes (BD Micro-fine, 0.3 ml, 30 G, BD Medical, Franklin Lakes, USA). For application of sivelestat or 0.9 % NaCl as control, pups were anaesthetized with 3 % isoflurane (Baxter, Deerfield, Ill, USA) in oxygen, injected in the lower left abdomen or s.c. in dorsal skin folds and kept at 37°C until recovery from anesthesia. Endpoint measurements were differential cell count of BAL fluid and lung preparation for histology.

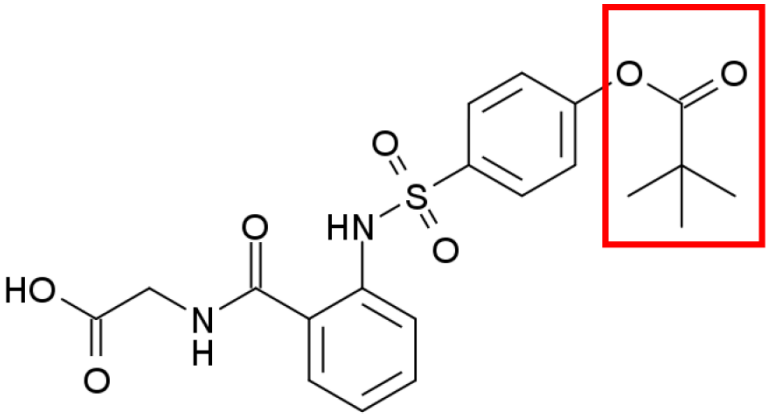

Figure 2.3: Structural formula of the NE inhibitor sivelestat (*N*-{2-[4-(2,2-dimethylpropionyloxy)phenylsulfonylamino]benzoyl}aminoacetic acid). Indicated (red) is the NE acylating group 2,2-dimethylpropoinat which reversibly binds serine in the active center of NE.

2.12 Statistics

Data was derived from at least 3 independent experiments. For statistical evaluation, data was analyzed with SigmaPlot version 12.5 software (Systat Software, Erkrath, Germany) and is reported as mean ± SEM. For multiple group analysis one-way ANOVA was applied with Fisher LSD post-hoc test. Chi Square test was used for genotype distribution analysis. Densitometry of western blot was determined with Image J (Image J 1.48v, NIH, USA). Linear regression was performed for slope determination in MMP-9 activity measurements and for ELISA standard curves with Microsoft Excel 2010 (Microsoft, Redmond, USA). Differences were considered significant at $P \leq 0.05$.

3 Results

3.1 Evaluation of the pathogenic contribution of MMP-9 to CF-like lung disease of βENaC-Tg mice

To evaluate previously described correlation of increased pulmonary MMP-9 levels with disease progression in CF patients, genetic deletion of *Mmp9* in βENaC-Tg mice was used to determine MMP-9-dependent steps in the pathogenesis of CF-like lung disease. A heterozygous breeding strategy enabled the phenotype evaluation of adult WT, *Mmp9*$^{-/-}$ and βENaC-Tg compared to βENaC-Tg/*Mmp9*$^{-/-}$ mice. Additionally, lung function measurements of *NE* or *Mmp9* deficient βENaC-Tg mice were performed to test the independent effects of the respective protease on lung tissue mechanics in adult mice.

3.1.1 MMP-9 protein levels are elevated in BAL fluid of βENaC-Tg mice

To assess the levels of MMP-9 in CF-like lung disease, BAL supernatant was analyzed by gelatin zymography for simultaneous visualization of pro- and active forms of MMP-9 and MMP-2 in lungs of WT, *Mmp9*$^{-/-}$, βENaC-Tg, βENaC-Tg/*Mmp9*$^{-/-}$ mice.

Gelatin zymography of BAL supernatant displayed a predominant band of pro-MMP-9 (92 kDa) in βENaC-Tg mice that was absent in WT, *Mmp9*$^{-/-}$ or βENaC-Tg/*Mmp9*$^{-/-}$ mice. Two forms (82 kDa and 75 kDa) of active MMP-9 were visible in βENaC-Tg mice while not detected in littermate controls. Pro- (72 kDa) and active MMP-2 (62 kDa) bands were observed with approximately similar intensity in all genotypes (Figure 3.1).

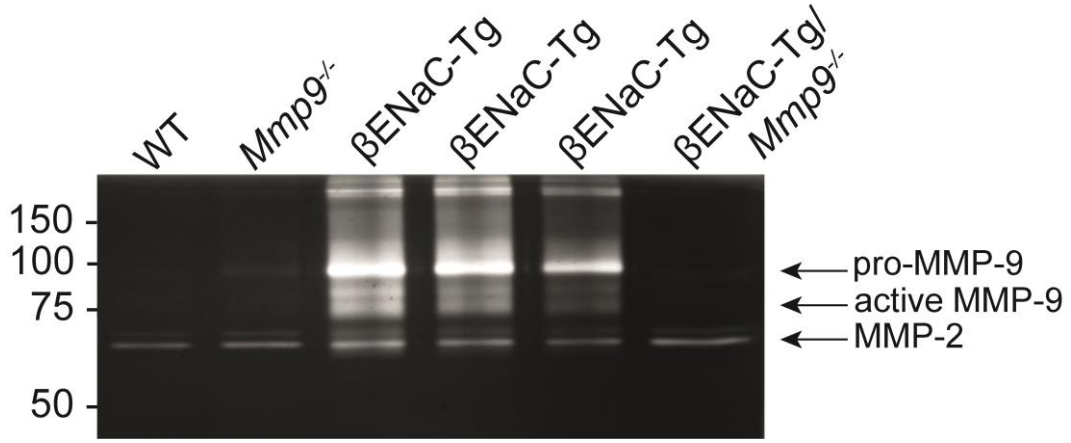

Figure 3.1: MMP-9 levels are elevated in BAL supernatant of βENaC-Tg mice. Gelatin zymography was performed with BAL supernatant of WT, *Mmp9*$^{-/-}$, βENaC-Tg and βENaC-Tg/*Mmp9*$^{-/-}$ mice. Pro-MMP-9 (~92 kDa) and its active forms (~82 and ~75 kDa) are present only in BAL of βENaC-Tg mice. Pro- and active MMP-2 (~72 kDa and ~65 kDa, respectively) are detected in all BAL samples in similar abundance.

3.1.2 Lack of MMP-9 does not reduce mortality in βENaC-Tg mice

In previous studies [42, 43, 66, 89, 92], it was reported that impaired mucociliary clearance in βENaC-Tg mice results in airway mucus obstruction leading to an increased mortality at neonatal age. To investigate the effect of *Mmp9* knockout on mortality of βENaC-Tg mice, we analyzed the genotype frequency of the cross of heterozygous *Mmp9*$^{+/-}$ mice with βENaC-Tg/*Mmp9*$^{+/-}$ mice. By comparing the obtained number of animals that survived until an age of 6 weeks with the number per genotype calculated according to Mendel´s Laws, we deduced the influence of *Mmp9* deletion on spontaneous mortality in βENaC-Tg mice. The percent of obtained βENaC-Tg mice was significantly lower than the calculated value in relation to WT animals. This was not prevented by *Mmp9* deletion as βENaC-Tg/*Mmp9*$^{-/-}$ mice presented a similar mortality (Figure 3.2 A). *Mmp9*$^{-/-}$ and WT mice showed similar survival, indicating that MMP-9 deficiency had no effect on survival. In addition, as a measure of a nutritional status, body weight quantification showed no change comparing all genotypes (Figure 3.2 B).

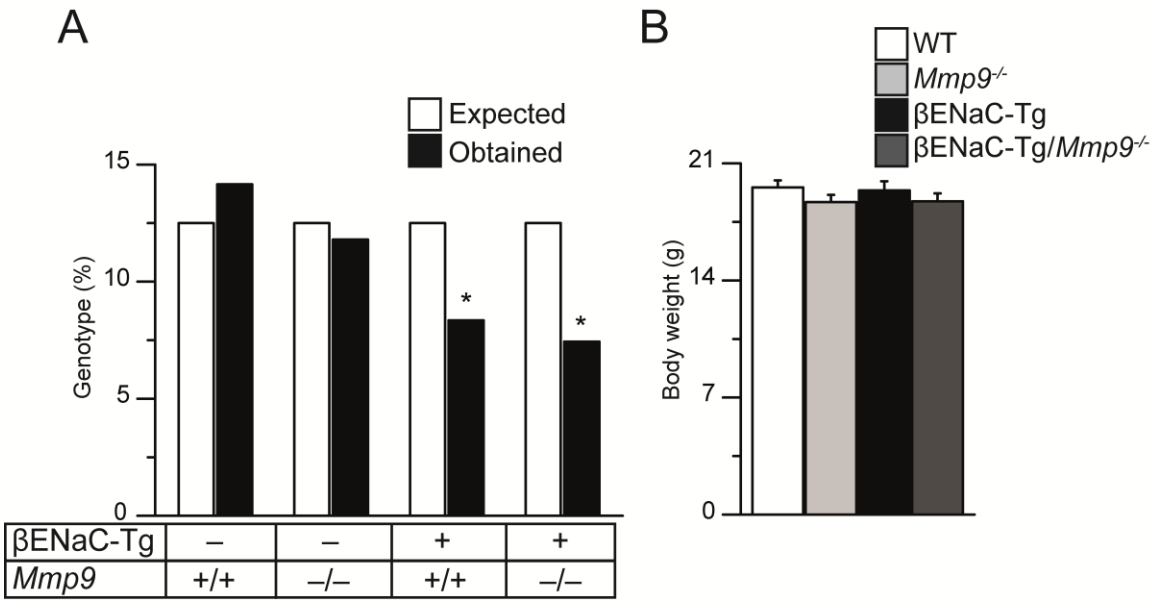

Figure 3.2: *Mmp9* deficiency has no effect on mortality or body weight of βENaC-Tg mice. Comparison of the expected versus obtained genotype frequency (A) of 6 week-old mice was used to determine mortality of WT, *Mmp9*$^{-/-}$, βENaC-Tg and βENaC-Tg/*Mmp9*$^{-/-}$ mice (*P < 0.05 compared to WT, calculated by Chi square test, n = 46-136). Body weight (B) of 6-8 week-old mice (n = 29-32).

3.1.3 Inflammation in βENaC-Tg mice develops independently of MMP-9

To determine the role of MMP-9 in leukocyte recruitment during chronic pulmonary inflammation, leukocyte counts in BAL fluid were compared between WT, *Mmp9*$^{-/-}$, βENaC-Tg and βENaC-Tg/*Mmp9*$^{-/-}$ mice.

Macrophages were the predominant population in BAL fluid of WT or *Mmp9*$^{-/-}$ mice while neutrophils, eosinophils and lymphocytes were almost undetectable in these groups. Macrophage counts were not significantly different comparing all genotypes. As expected from previous studies [92, 150], βENaC-Tg mice showed spontaneous pulmonary inflammation with significantly increased total leukocyte counts in BAL fluid.
The augmented recruitment of neutrophils and eosinophils accounted for most of the increased leukocyte counts in lungs of 6-8 week-old βENaC-Tg compared to WT mice (Figure 3.3 A-D). The inflammatory infiltration was not changed by *Mmp9* deletion suggesting a MMP-9 independent leukocyte influx into the lungs of βENaC-Tg mice. Lymphocyte counts reached significantly higher levels in βENaC-Tg and βENaC-Tg/*Mmp9*$^{-/-}$ mice compared to WT or *Mmp9*$^{-/-}$ mice but their total number was considerably lower relative to other leukocytes. (Figure 3.3 E).

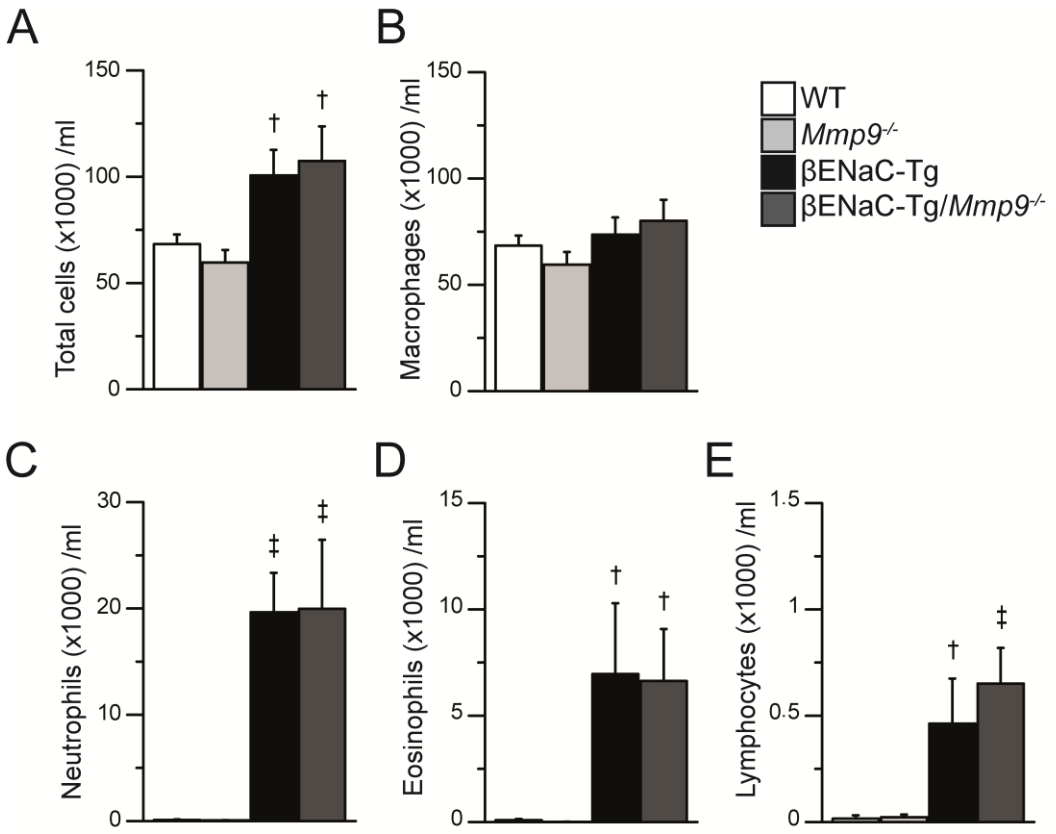

Figure 3.3: Lack of MMP-9 has no effect on leukocyte recruitment in βENaC-Tg mice. Differential cell counts of total cells (A), macrophages (B), neutrophils (C), eosinophils (D) and lymphocytes (E) in BAL of WT, *Mmp9*$^{-/-}$, βENaC-Tg and βENaC-Tg/*Mmp9*$^{-/-}$ mice. Counts are shown as (cell counts/ml BAL volume) x 1000. (†P < 0.01, ‡P < 0.001, compared to WT or *Mmp9*$^{-/-}$, n=12-30).

Chronic pulmonary inflammation is associated with altered cytokine levels in βENaC-Tg mice [92]. To monitor potential alteration in the cytokine profile by *Mmp9* deletion we assessed BAL supernatant using ELISA and CBA kits. The neutrophil chemokines KC, MIP-2 and LIX showed similar levels βENaC-Tg and βENaC-Tg/*Mmp9*$^{-/-}$ mice that were significantly higher compared to controls. This is also reflected in the number of recruited neutrophils (Figure 3.3 C, Figure 3.4 A-C). IL-1α and IL-1β levels were not different comparing βENaC-Tg and βENaC-Tg/*Mmp9*$^{-/-}$ mice but significantly elevated in comparison to WT and *Mmp9*$^{-/-}$ mice. IL-13 concentrations showed comparable levels in lungs of βENaC-Tg and βENaC-Tg/*Mmp9*$^{-/-}$ mice that were increased compared to controls. This is consistent with the respective eosinophil number detected in BAL fluid (Figure 3.3 D, Figure 3.4 F).

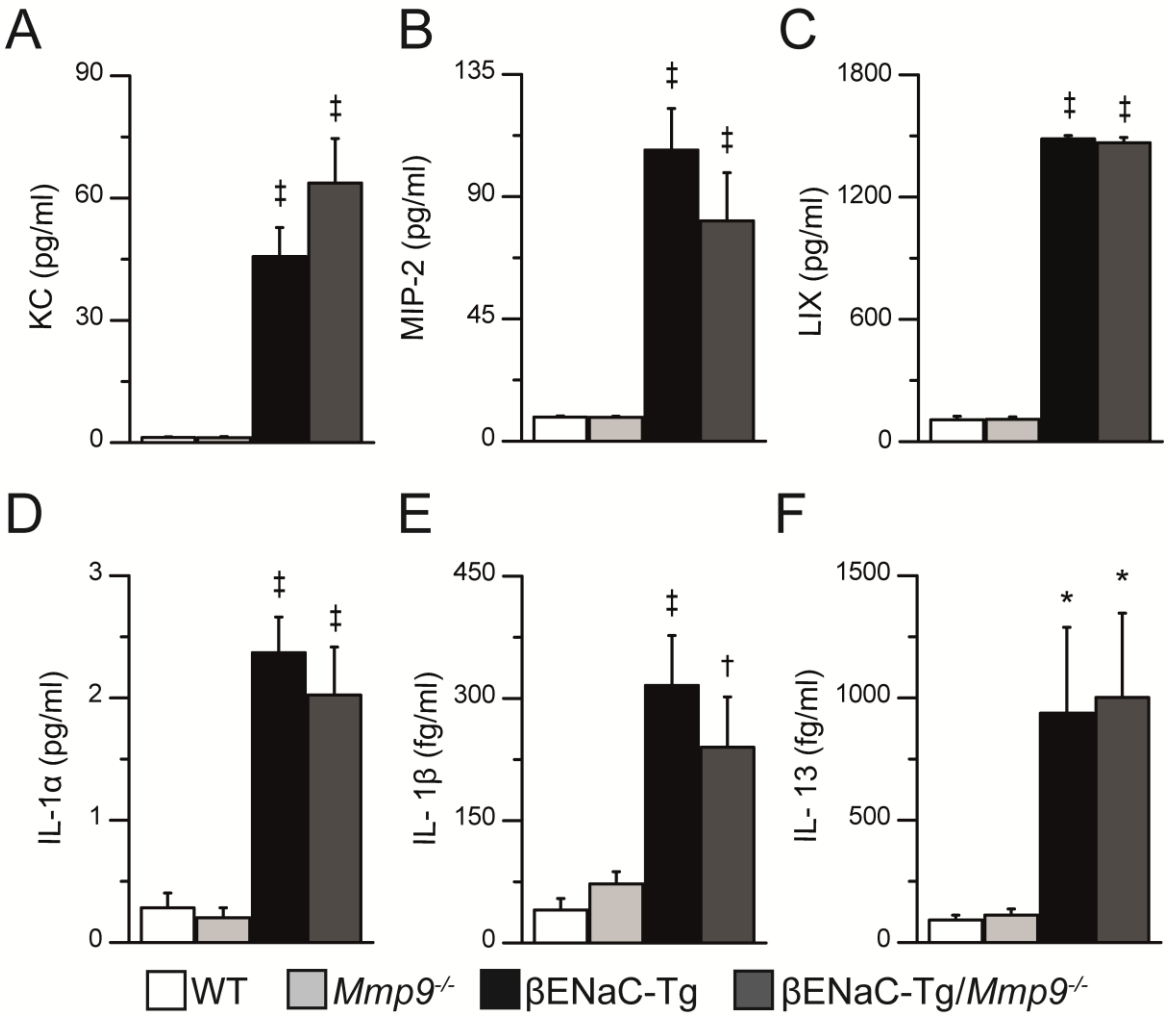

Figure 3.4: Lack of MMP-9 has no effect on pro-inflammatory cytokines levels in βENaC-Tg mice. Concentrations of KC (A), IL-1α (D), IL-1β (E) and IL-13 (F) were measured with CBA kits and MIP-2 (B) and LIX (C) concentrations were determined by ELISA in BAL supernatant of WT, *Mmp9*$^{-/-}$, βENaC-Tg and βENaC-Tg/*Mmp9*$^{-/-}$ mice (*P < 0.05, †P < 0.01, ‡P < 0.001, compared to WT or *Mmp9*$^{-/-}$, n = 10).

In addition to IL-13, chitinase 3 like-1 (*Chi3l1*) was shown to stimulate an alternative activation (M2) of macrophage [81]. On transcript levels *Chi3l1* was present in significantly higher amounts in lungs of βENaC-Tg and βENaC-Tg/*Mmp9*$^{-/-}$ mice compared to controls. Alternative activation of macrophages was confirmed by assessment of M2 marker expression. Transcripts levels of the chitinase *Ym1* and macrophage elastase *Mmp12* were significantly upregulated in βENaC-Tg compared to WT mice which was not affected in *Mmp9* knockout animals (Figure 3.5 A-C).

In summary, βENaC-Tg/*Mmp9*$^{-/-}$ mice display no significant change in inflammatory cell counts or cytokine profile or alternative activation of alveolar macrophages compared to βENaC-Tg mice which suggests that initiation and propagation of inflammation is not dependent on MMP-9.

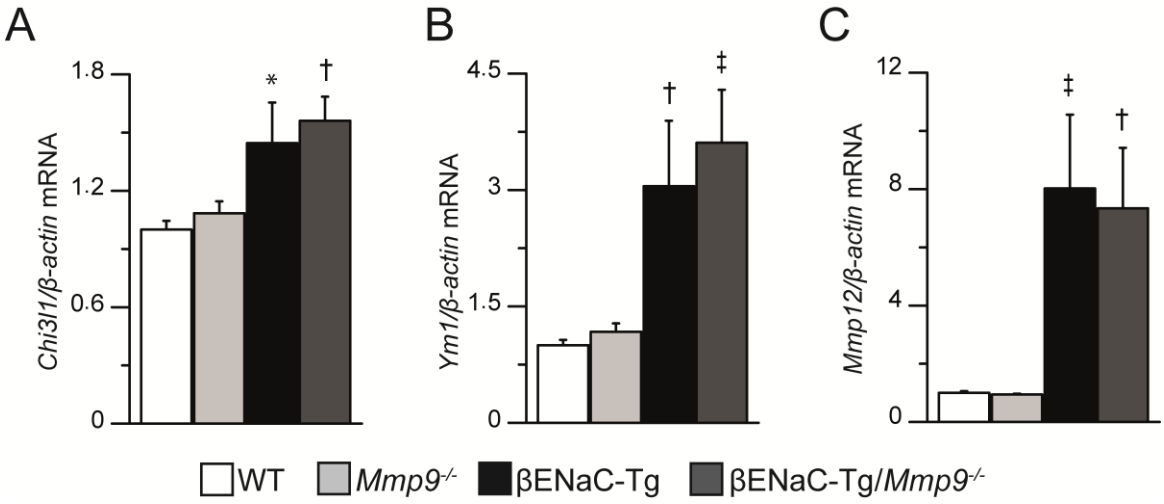

Figure 3.5: *Mmp9* deletion has no effect on mRNA levels of markers for alternative activated macrophages in βENaC-Tg mice. Lung homogenates were assessed for *Chi3l1*, *Ym1* and *Mmp12* expression by qRT-PCR. Expression levels are shown relative to WT values (*P < 0.05 compared to WT, †P < 0.05 compared to WT or *Mmp9*$^{-/-}$, ‡P < 0.01 compared to WT or *Mmp9*$^{-/-}$; n= 9-11).

3.1.4 *Mmp9* deletion partially reduces mucus obstruction while mucin expression is not affected in βENaC-Tg mice

Chronic inflammation and elevated levels of IL-13 and IL-1β are associated with goblet cell metaplasia, mucin hypersecretion and mucus obstruction in airways of patients with chronic obstructive lung diseases and in βENaC-Tg mice [1, 92, 160].

We evaluated AB-PAS stained histological sections of proximal main bronchi of βENaC-Tg, βENaC-Tg/*Mmp9*$^{-/-}$, WT and *Mmp9*$^{-/-}$ mice to determine the effect of *Mmp9* knockout on airway obstruction. An accumulation of AB-PAS positive material in the airway lumen and a thickened epithelium with a high number of goblet cells was present in sections of

βENaC-Tg mice (Figure 3.6 A). In contrast, sections from WT animals showed no luminal mucus and goblet cells constituted only a minor part of the respiratory epithelium. *Mmp9* deletion had no effect on the histological phenotype compared to WT mice. In βENaC-Tg/*Mmp9*$^{-/-}$ mice a lower extent of airway mucus plugging was observed.

Morphometric analysis confirmed a reduced total airway and intraluminal mucus volume density in βENaC-Tg/*Mmp9*$^{-/-}$ compared to βENaC-Tg mice (Figure 3.6 B-D). Of note, this reduction in luminal mucus content was not accompanied by a reduction in goblet cell metaplasia and did not result in a higher survival rates in βENaC-Tg/*Mmp9*$^{-/-}$ compared to βENaC-Tg mice (compare also Figure 3.2). WT and *Mmp9*$^{-/-}$ mice showed similar mucus content and goblet cell counts.

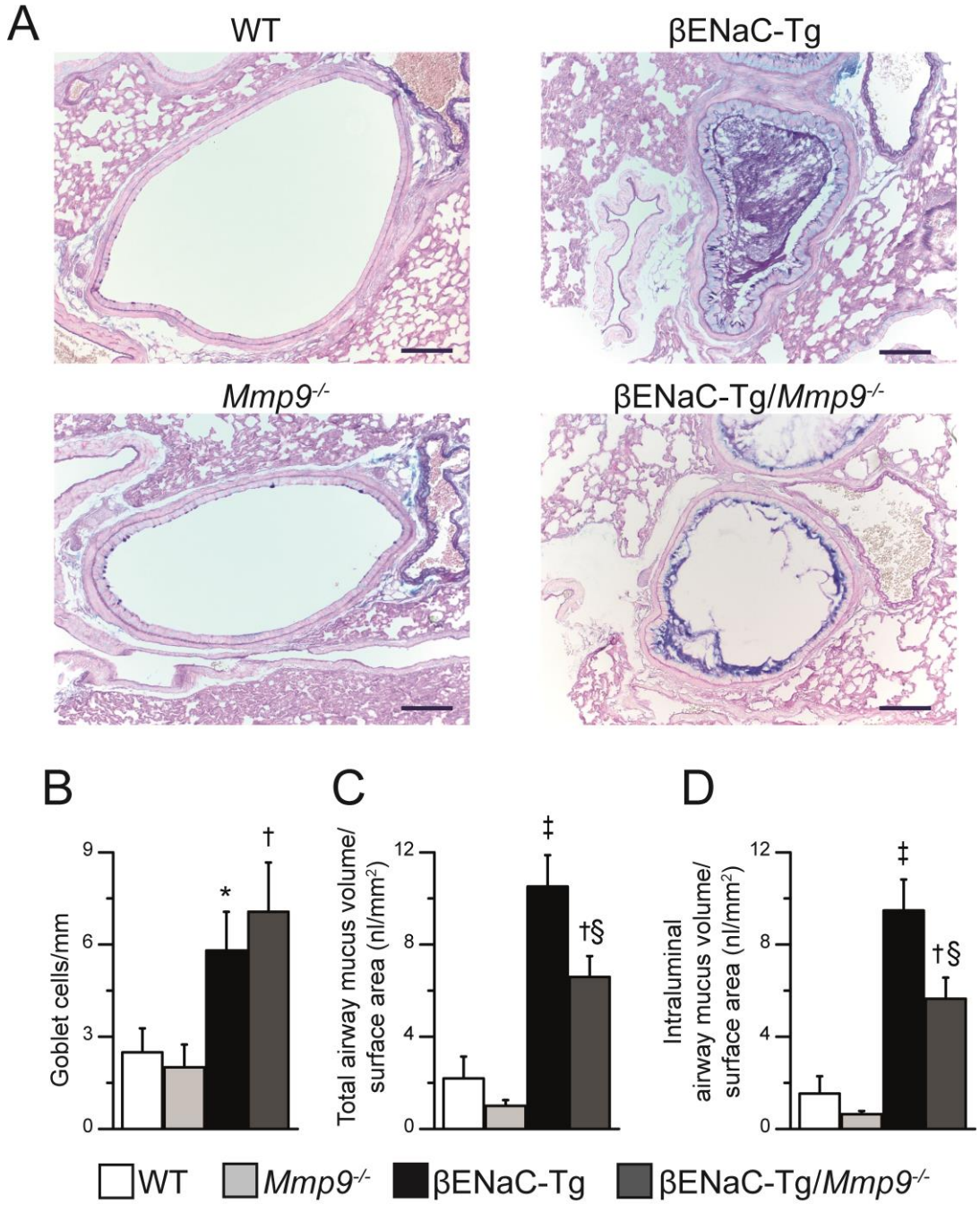

Figure 3.6: *Mmp9* deficient βENaC-Tg mice show reduced airway mucus plugging compared to βENaC-Tg mice. Comparison of AB-PAS stained lung sections at the level of main bronchi of WT, *Mmp9*$^{-/-}$, βENaC-Tg and βENaC-Tg/*Mmp9*$^{-/-}$ mice for the detection of mucus obstruction and goblet cells (A). Counts of AB-PAS positive goblet cells per length of airway basement membrane to quantify the metaplastic response of respiratory epithelia (B). Mucus obstruction by AB-PAS positive material measured by either total airway (C) or intraluminal (D) mucus volume density (*P < 0.05, †P < 0.01, ‡P < 0.001 compared to WT or *Mmp9*$^{-/-}$, §P < 0.05 compared to βENaC-Tg, n = 10-14; scale bar = 100 µm).

Furthermore, to investigate if *Mmp9* deficiency causes a reduced expression of goblet cell markers or major mucus components in βENaC-Tg mice, we performed qRT-PCR with lung tissue lysates. Expression of *Gob5*, as a marker for goblet cells, and mRNA levels of secreted mucins *Muc5ac* and *Muc5b* were significantly higher in βENaC-Tg compared to WT or *Mmp9*$^{-/-}$ mice. *Gob5* expression and mucin hypersecretion was not reduced in βENaC-Tg/*Mmp9*$^{-/-}$ compared to βENaC-Tg mice (Figure 3.7).
In summary, goblet cell counts, goblet cell marker levels and mucin expression were similar in βENaC-Tg and βENaC-Tg/*Mmp9*$^{-/-}$ mice and increased compared to littermate controls. Airway mucus obstruction was partially reduced in βENaC-Tg/*Mmp9*$^{-/-}$ compared to βENaC-Tg mice.

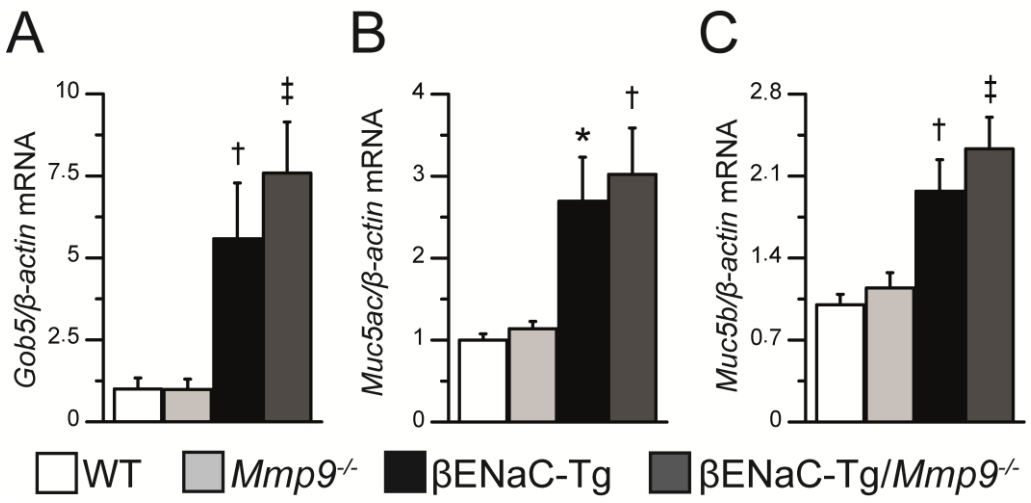

Figure 3.7: Lack of MMP-9 has no effect on mucin expression in βENaC-Tg/*Mmp9*$^{-/-}$ compared with βENaC-Tg mice. mRNA isolated from whole lung tissue was analyzed for goblet cell marker *Gob5* (A) and the main secreted airway mucins *Muc5ac* (B) and *Muc5b* (C) by qRT-PCR (*P < 0.05, †P < 0.01, ‡P < 0.001 compared to WT or *Mmp9*$^{-/-}$, n = 9-11).

3.1.5 Lack of MMP-9 does not reduce lung tissue destruction in βENaC-Tg mice

The measurement lung volume and morphometric assessment of distal lung tissue of βENaC-Tg, βENaC-Tg/*Mmp9*$^{-/-}$ mice and littermate controls were performed to study a potential effector role of MMP-9 in emphysema formation. HE-stained sections of distal lung parenchyma showed regular tissue structure in WT and *Mmp9*$^{-/-}$ mice. Alveolar structure in βENaC-Tg and βENaC-Tg/*Mmp9*$^{-/-}$ mice showed similar emphysematous lesions i.e. less uniform appearance, fewer septa and more hyperinflated areas compared to WT or *Mmp9*$^{-/-}$ mice (Figure 3.8 A).

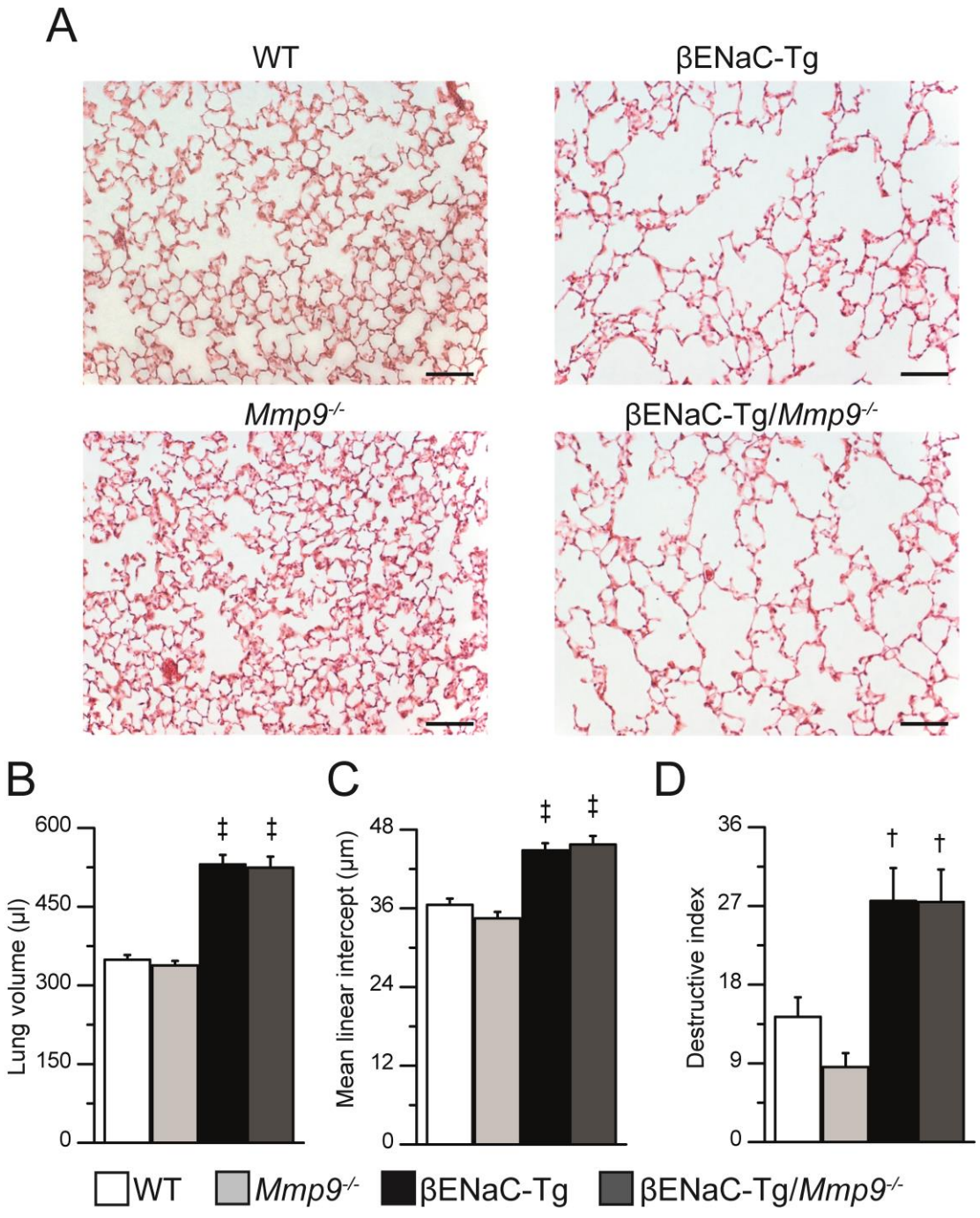

Figure 3.8: Lack of MMP-9 does not reduce emphysema severity in βENaC-Tg mice. Comparison of distal airspace morphology in HE-stained sections of lung parenchyma of indicated genotypes (A). Measurement of lung volume (B), and evaluation of histology by MLI (C) and DI (D) enabled quantification of emphysema severity (†P < 0.01 and ‡P < 0.001 compared to WT or *Mmp9*$^{-/-}$, n = 9-32, scale bar = 100 µm).

Measurement of the lung volume showed comparable values for βENaC-Tg and βENaC-Tg/*Mmp9*$^{-/-}$ mice that were significantly higher compared to littermate controls (Figure 3.8 B). Furthermore, morphometric quantification of tissue sections displayed similarly elevated MLI values in lungs of βENaC-Tg and βENaC-Tg/*Mmp9*$^{-/-}$ mice confirming a significant destruction of alveoli compared to littermate controls (Figure 3.8 C). The additional assessment of alveolar structure by DI measurement showed that the number of interrupted alveolar walls and of emphysematous lesions was unchanged comparing βENaC-Tg and βENaC-Tg/*Mmp9*$^{-/-}$ mice and was significantly increased in comparison to control mice (Figure 3.8 D).
In summary, βENaC-Tg mice exhibit the previously described destruction of alveolar tissue compared to WT mice. Quantification of emphysema severity by lung volume measurement and determination of the MLI and DI showed no alteration in βENaC-Tg/*Mmp9*$^{-/-}$ compared to βENaC-Tg mice.

3.1.6 Lack of MMP-9 does not improve lung function while NE deletion attenuates lung function decline in βENaC-Tg mice

Structural lung damage may alter lung tissue mechanics and therefore impact on lung function. Lung function was tested in NE or MMP-9 deficient βENaC-Tg mice to determine independent and individual contribution of the respective protease on lung tissue properties.
The pressure-volume curves of βENaC-Tg mice showed significantly higher inflation volumes at a given pressure compared to WT mice (Figure 3.9). The excessive lung inflation, reflecting emphysematous lung damage, was not changed in βENaC-Tg/*Mmp9*$^{-/-}$ mice (Figure 3.9 A). Conversely, *NE* deletion partially prevented emphysematous changes in lung function of βENaC-Tg/*NE*$^{-/-}$ mice as shown by a reduced lung inflation at a controlled pressure compared to βENaC-Tg mice (Figure 3.9 B).

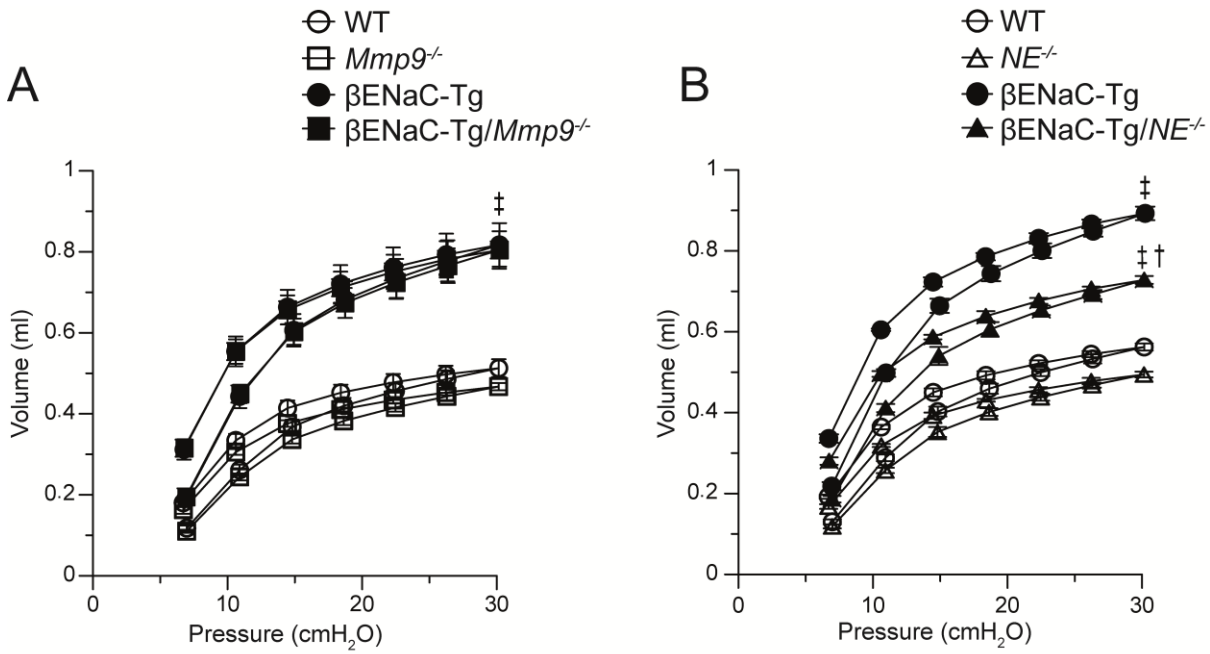

Figure 3.9: *Mmp9* deletion does not preserve lung function while NE deficiency limits lung function decline in βENaC-Tg mice. The pressure-volume curves display with the measured slope and inclination the degree of emphysema that is present in lungs of WT, *Mmp9*$^{-/-}$, βENaC-Tg and βENaC-Tg/*Mmp9*$^{-/-}$ mice (A) and WT, *NE*$^{-/-}$, βENaC-Tg and βENaC-Tg/*NE*$^{-/-}$ mice (B) (†P < 0.01 compared to βENaC-Tg mice, ‡P < 0.001 compared to WT, *NE*$^{-/-}$ *or Mmp9*$^{-/-}$, n=8-14).

The inspiratory capacity and static compliance were not changed in βENaC-Tg/*Mmp9*$^{-/-}$ compared to βENaC-Tg mice and both were significantly elevated relative to WT or *Mmp9*$^{-/-}$ animals (Figure 3.10 A,B). NE deficiency in βENaC-Tg mice reduced both inspiratory capacity and static compliance compared to βENaC-Tg mice (Figure 3.10 E,F). Despite a partial reduction in βENaC-Tg/*NE*$^{-/-}$ mice inspiratory capacity and static compliance remained higher compared to WT and *NE*$^{-/-}$ mice. The hysteresis area of the pressure-volume curve was not affected in βENaC-Tg/*Mmp9*$^{-/-}$ compared βENaC-Tg mice (Figure 3.10 C). Conversely, hysteresis area of βENaC-Tg/*NE*$^{-/-}$ mice reached levels close to WT animals while remained increased compared to *NE*$^{-/-}$ mice (Figure 3.10 G). Lung tissue elastance was not change in βENaC-Tg/*Mmp9*$^{-/-}$ compared to βENaC-Tg mice but significantly decreased compared to WT or *Mmp9*$^{-/-}$ littermates (Figure 3.10 D). NE deficient βENaC-Tg mice preserved higher tissue elastance relative to βENaC-Tg mice although lower compared to WT or *NE*$^{-/-}$ mice (Figure 3.10 H).
In summary, *Mmp9* deletion had no effect on lung tissue mechanics in βENaC-Tg mice. Conversely, βENaC-Tg/*NE*$^{-/-}$ mice showed improved lung function compared to βENaC-

Tg mice. This suggests an independent contribution of these proteases to lung function decline in mice with CF-like lung disease.

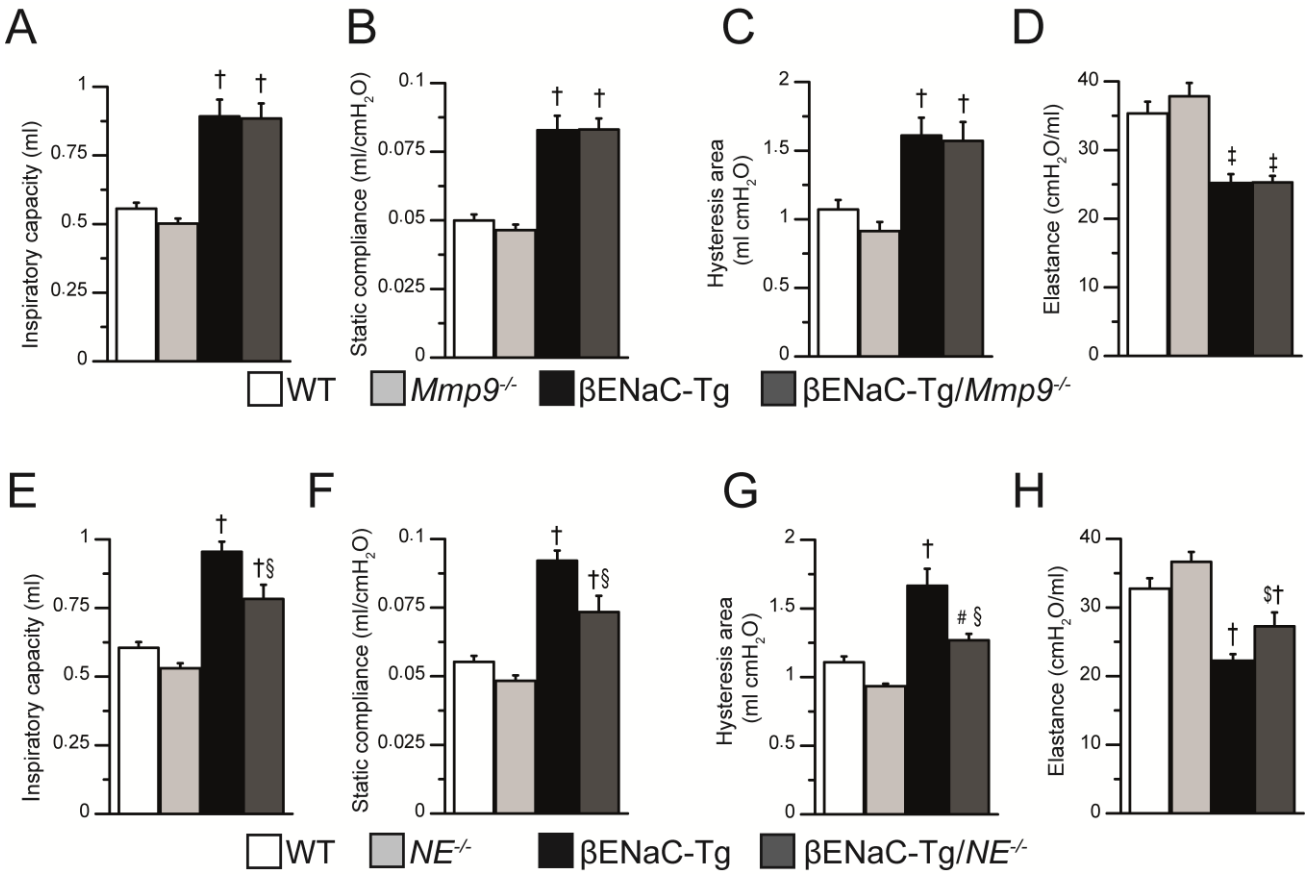

Figure 3.10: Lack of *Mmp9* results in no improvement of lung function parameters in βENaC-Tg mice while βENaC-Tg/*NE*$^{-/-}$ mice display partially preserved lung tissue mechanics. Lung function parameters were measured in anaesthetized, live WT, *Mmp9*$^{-/-}$, βENaC-Tg and βENaC-Tg/*Mmp9*$^{-/-}$ mice and WT, *NE*$^{-/-}$, βENaC-Tg and βENaC-Tg/*NE*$^{-/-}$ mice. Inspiratory capacity, static compliance, area of pressure-volume curve hysteresis and elastance are shown for MMP-9 (A-D) or NE (E-F) deficient βENaC-Tg mice and littermate controls (†P < 0.01 compared to WT, *NE*$^{-/-}$ or *Mmp9*$^{-/-}$, ‡P < 0.001 compared to WT, *NE*$^{-/-}$ or *Mmp9*$^{-/-}$, §P < 0.01 compared to βENaC-Tg mice, $P < 0.05 compared to βENaC-Tg; #P < 0.05 compared to *NE*$^{-/-}$; n=8-14).

3.1.7 Lack of *Mmp9* does not induce compensatory expression of *Mmp2, Mmp8* or *Mmp13* in βENaC-Tg mice

Deletion of *Mmp9* may lead to a compensatory expression of other matrix metalloproteinases which have overlapping substrate specificity. In particular, *Mmp2*, *Mmp8*, *Mmp12* (see Figure 3.5) and *Mmp13* are potential candidates previously proposed to compensate for *Mmp9* deletion in other disease conditions [21, 35, 79].

Expression of compensatory candidates was assessed by qRT-PCR using RNA isolated from lung lysates. Similar to the result shown by gelatin zymography (Figure 3.1), mRNA levels of *Mmp2* presented a constitutive expression across all assessed genotypes (Figure 3.11). Other candidates, *Mmp8* and *Mmp13*, were not differentially regulated on mRNA level in lungs of WT, *Mmp9*$^{-/-}$, βENaC-Tg and βENaC-Tg/*Mmp9*$^{-/-}$ mice.

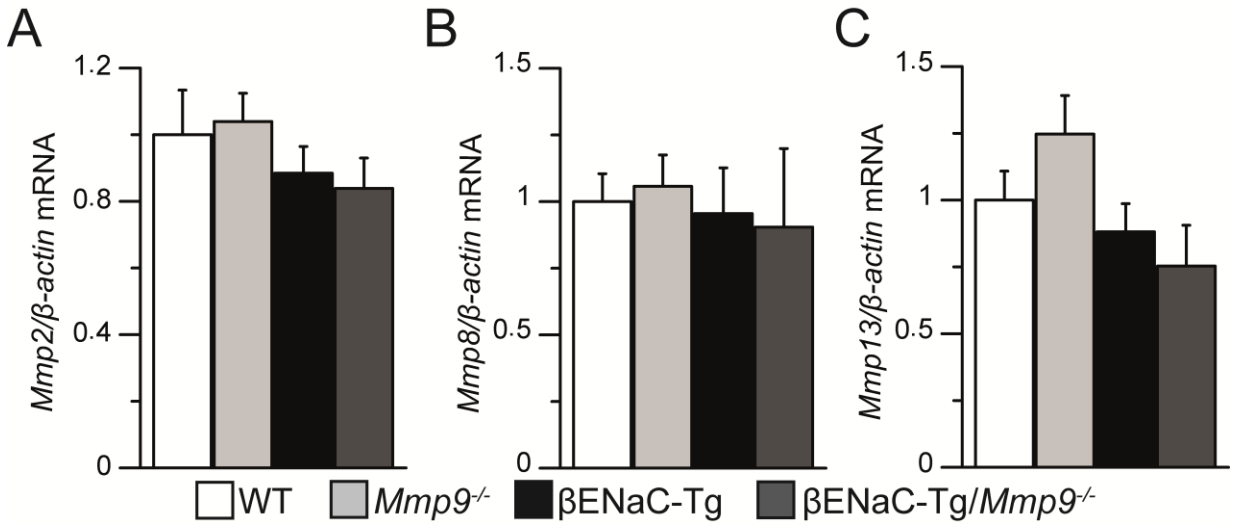

Figure 3.11: Effect of *Mmp9* deletion on expression of *Mmp2*, *Mmp8* or *Mmp13*. RNA was isolated from whole lungs and expression of *Mmp2* (A), *Mmp8* (B) and *Mmp13* (C) was quantified by qRT-PCR and normalized to WT values (n = 9-11).

3.1.8 Secreted MMP-9 is not active in BAL supernatant of βENaC-Tg mice

Gelatin zymography enables the simultaneous detection of pro- and active MMP-9, whereas the actual activity *in vivo* is modulated by presence of protease inhibitors. We used DQ-gelatin, a quenched gelatin-based fluorescence reporter, to assess soluble gelatinase activities of MMP-9 and MMP-2 in BAL supernatant of WT, *Mmp9*$^{-/-}$, βENaC-Tg and βENaC-Tg/*Mmp9*$^{-/-}$ mice. The reporter assay could not detect gelatinase activity in any of the BAL fluids of the tested genotypes, while 0.02 ng/µl of activated rmMMP-9 served as a positive control (Figure 3.12). The lack of gelatinase activity might reflect the sensitivity of the reporter assay or more likely depend on the presence of gelatinase inhibitors in BAL fluid.

To test this hypothesis we performed ELISA measurement of the main MMP-9 inhibitor, TIMP1, and detected elevated levels in BAL supernatant of βENaC-Tg and βENaC-Tg/*Mmp9*$^{-/-}$ mice compared to controls (Figure 3.12 B). To estimate MMP-9 activity *in vivo*, we monitored potential cleavage pattern of the MMP-9 substrate A1AT in BAL supernatant. BAL of βENaC-Tg mice showed no detectable cleavage of A1AT. The

double band of A1AT likely reflects two glycosylation forms which were also observed in WT or MMP-9 deficient mice. Semi-quantitative determination of band intensities revealed a trend to higher A1AT levels in BAL fluid of *Mmp9*$^{-/-}$, βENaC-Tg and βENaC-Tg/*Mmp9*$^{-/-}$ mice compared to WT animals (Figure 3.12 C,D).

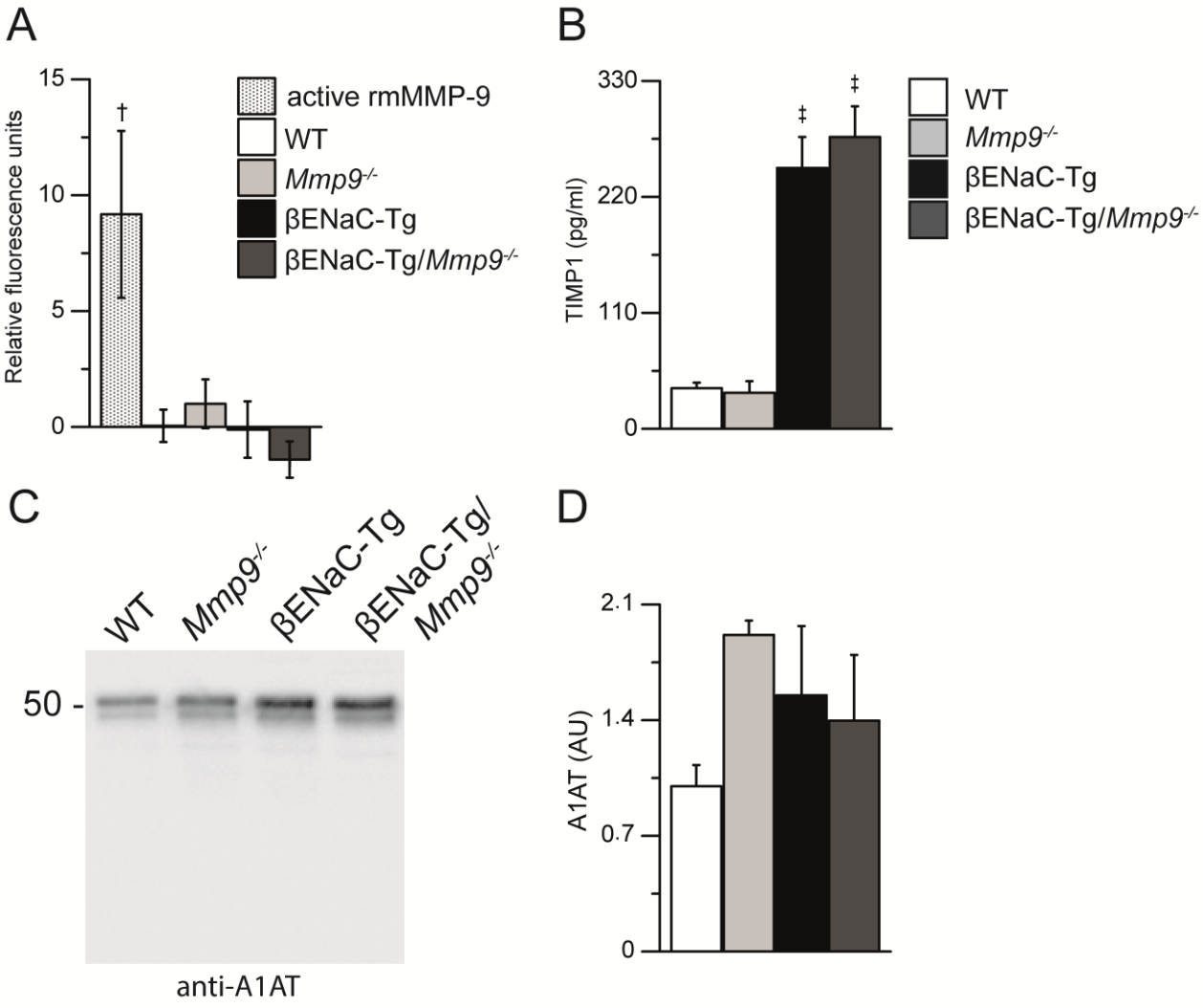

Figure 3.12: Soluble MMP-9 is not active in BAL supernatant of βENaC-Tg mice. To monitor gelatinase activity *in vitro* cleavage of the reporter DQ-gelatin is shown as fluorescence change over incubation time with BAL supernatant or activated recombinant murine MMP-9 (0.02 ng/µl) (A). TIMP1 levels were measure by ELISA in BAL supernatant of WT, *Mmp9*$^{-/-}$, βENaC-Tg and βENaC-Tg/*Mmp9*$^{-/-}$ mice (B). *In vivo* cleavage of A1AT was evaluated by assessment of BAL supernatant in western blot. Full-length A1AT is detected in two different glycosylated variants (C). Semi-quantitative evaluation of A1AT band intensity in western blots (D) (†P < 0.01 compared to BAL samples; ‡P < 0.001 compared to WT, *Mmp9*$^{-/-}$; A, n = 5; B, n = 10; C-D, n = 3-5).

In summary, although elevated MMP-9 levels are present in BAL supernatant βENaC-Tg mice, increased TIMP1 levels prevent soluble gelatinase activity *in vitro* and *in vivo* indicating a balanced antiprotease-protease ratio in βENaC-Tg mice.

3.2 Treatment studies with the neutrophil elastase inhibitor sivelestat

NE deficiency improved lung function of βENaC-Tg mice. In combination with previous studies [49], this suggests that NE, in contrast to MMP-9, is a promising candidate for therapeutic intervention. Therefore, preclinical trials using the NE inhibitor sivelestat were performed. Newborn WT and βENaC-Tg mice were treated with sivelestat or vehicle (0.9 % NaCl) either by intraperitoneal or by subcutaneous injection every 12 h for a period of 2 weeks.

3.2.1 Intraperitoneal application of sivelestat does not prevent onset of lung disease in βENaC-Tg mice

Sivelestat treatment by intraperitoneal (i.p.) injections was well tolerated. Quantification of total cell counts in BAL fluid and in particular of neutrophil counts showed no difference in sivelestat-treated βENaC-Tg mice in comparison to vehicle controls (Figure 3.13 A). However, histologic evaluation of AB-PAS-stained lung sections of 2 week-old mice showed that sivelestat treatment reduced mucus obstruction in main bronchi of βENaC-Tg mice compared to vehicle controls. Moreover, quantification of lung tissue damage by MLI measurement in HE-stained tissue sections revealed no significant change in sivelestat-treated βENaC-Tg mice compared to vehicle controls (Figure 3.13 B,C).

In summary, treatment with the neutrophil serine protease inhibitor sivelestat by i.p. injections reduced mucus obstruction but did not prevent the development of chronic inflammatory lung disease in juvenile βENaC-Tg mice.

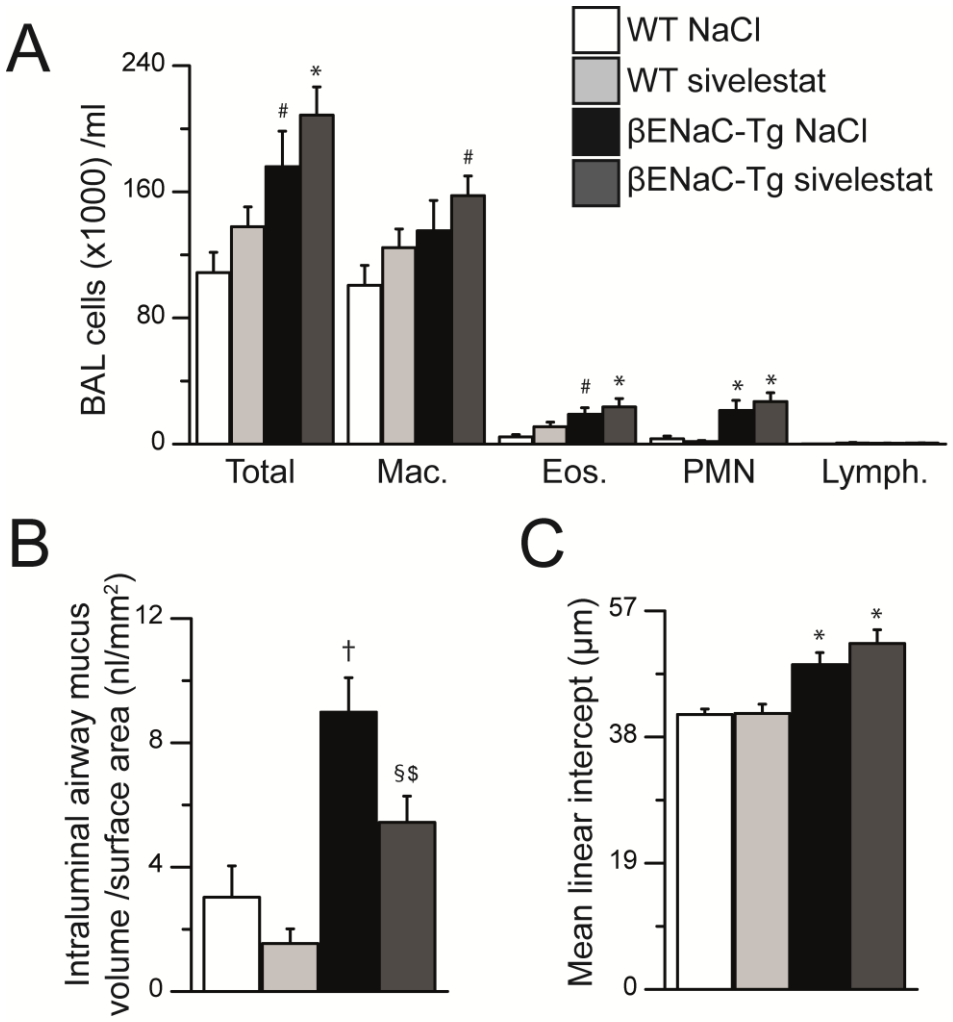

Figure 3.13: Intraperitoneal treatment with sivelestat attenuates airway mucus plugging but does not prevent inflammation or emphysema development in βENaC-Tg mice. Sivelestat (100 mg/kg body weight per day) was applied by intraperitoneal injection in newborn mice over a period of 2 weeks. Inflammatory leukocyte recruitment was assessed by differential cell count in BAL fluid of WT and βENaC-Tg mice treated with sivelestat or vehicle 0.9 % NaCl (A). Lung histology was evaluated for airway mucus obstruction by measurement of intraluminal airway mucus volume density (B) and for emphysematous changes by determination of mean linear intercepts (C). Total = total BAL cells, Mac. = macrophages, Eos. = eosinophils, PMN = neutrophils, Lymph. = lymphocytes. (*P < 0.05 compared to WT treated with vehicle or sivelestat; †P < 0.001 compared to WT treated with vehicle or sivelestat; #P < 0.05 compared to WT treated with vehicle; §P < 0.01 compared to βENaC-Tg treated with vehicle; $P < 0.01 compared to WT treated with sivelestat; n = 14-20).

3.2.2 Subcutaneous application of sivelestat has no impact on disease development of βENaC-Tg mice

To circumvent potential hepatic first-pass effects of sivelestat, we used the i.p. treatment protocol for subcutaneous (s.c.) application. After 14 day of s.c. treatment with sivelestat, differential cell count of BAL fluid showed an induced recruitment of macrophages, eosinophils and neutrophils into the lungs of vehicle treated βENaC-Tg mice which was not changed in the sivelestat treated group (Figure 3.14 A).

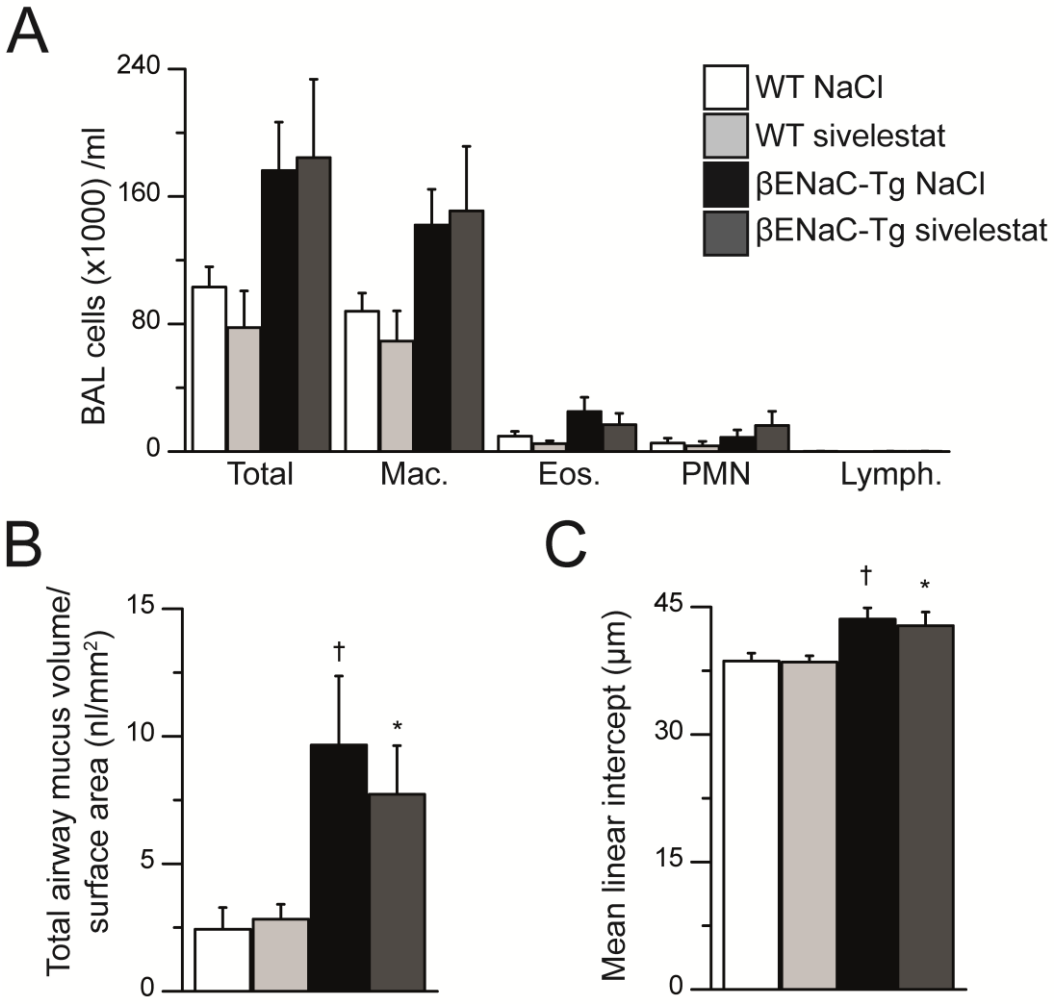

Figure 3.14: Subcutaneous delivery of sivelestat shows no impact on lung pathophysiology of βENaC-Tg mice. Differential cell counts of BAL fluid (A) was used to determine the levels of total, macrophages (Mac.), eosinophils (Eos.), neutrophils (PMN) and lymphocytes (Lymph.) in sivelestat or vehicle (0.9% NaCl) treated WT and βENaC-Tg mice (n= 5-8). Mucus obstruction was quantified in AB-PAS stained airway sections by total airway mucus volume density (B) (n= 9-15). Distal lung histology was assessed by measurement of mean linear intercepts (C) (n= 8-14). (*$P < 0.05$ compared to WT treated with vehicle or sivelestat; †$P < 0.01$ compared to WT treated with vehicle or sivelestat).

Assessment of airway mucus plugging revealed increased mucus obstruction in proximal main bronchi of vehicle treated βENaC-Tg mice that was not reduced by s.c. sivelestat treatment. Additionally, quantification of lung destruction showed significantly higher mean linear intercepts in vehicle treated and no alteration in sivelestat treated βENaC-Tg mice (Figure 3.14 B,C). In total, the subcutaneous treatment with sivelestat did not prevent or delay the disease onset or severity in 2 week-old βENaC-Tg mice.

In conclusion, sivelestat treatment of βENaC-Tg mice showed no effect on pulmonary inflammation or proteolytic lung tissue destruction. Therefore, further studies are needed using more potent inhibitors for targeting NE in CF-like lung disease.

4 Discussion

4.1 Role of MMP-9 in the pathogenesis of βENaC-Tg mice

Several studies suggest a potential pathogenic role of MMP-9 in inflammatory lung diseases (see chapter 1.4.3). However, *in vivo* studies that investigate MMP-9-dependent effects in the context of CF lung disease are lacking. The present study investigated i) MMP-9-dependent phenotypic alterations in mice with CF-like lung disease, ii) the impact of *Mmp9* or *NE* deletion on lung function in βENaC-Tg mice and iii) evaluates NE as therapeutic target in preclinical trials with the protease inhibitor sivelestat as preventive treatment.

4.1.1 Elevated MMP-9 levels in BAL fluid in βENaC-Tg mice likely originate from activated neutrophils

In the present study, pro- and active forms of MMP-9 protein were detected by gelatin zymography exclusively in BAL supernatant of βENaC-Tg mice (Figure 3.1). Previous studies of βENaC-Tg mice showed no differential regulation of *Mmp9* or *NE* mRNA levels compared to WT mice [137, 150]. Instead, *Mmp12* mRNA levels, as only leukocyte-derived protease, were highly elevated in βENaC-Tg mice. Neutrophils express *Mmp9* and *NE* only during maturation in the bone marrow and proteases are stored in granules [25]. Therefore, neutrophil granules are likely the major source of MMP-9 protein in βENaC-Tg mice, since *Mmp9* transcription is not induced. Zymography also demonstrated that pro-MMP-9 is converted *in vivo* into its active form in βENaC-Tg mice. Numerous proteases are able to cleave pro-MMP-9, of which previously only active NE was detected in βENaC-Tg mice [49, 63, 154]. Of note, zymography does not display the actual proteolytic activity *in vivo* since proteases are separated from their endogenous inhibitors during SDS PAGE (see Material and Methods 2.4). Instead, gelatin zymography enable the detection of gelatinase protein levels in the picogram range [156]. The second gelatinase MMP-2 was observed in similar band intensity in all genotypes which indicates a constitutive expression and no induction by inflammatory stimuli (Figure 3.1, Figure 3.11).

4.1.2 MMP-9 is not active in BAL supernatant of βENaC-Tg mice

Presence of active MMP-9 bands in zymograms of CF sputum has been used synonymously with MMP-9 activity in some studies [48] although this is misleading. Using a soluble gelatin-based reporter enabled the inference on MMP-9 activity in lungs of βENaC-Tg mice. In all tested genotypes no free gelatinase activity was detected in BAL supernatant (Figure 3.12). Additionally, βENaC-Tg mice displayed higher

concentrations of TIMP1 which reflects an intact antiprotease shield and explains the lack of free MMP-9 activity. The monitoring of A1AT band pattern by western blot revealed no detectable substrate cleavage by MMP-9 in BAL supernatant or *in vivo* (Figure 3.12). Collectively, this indicates that soluble MMP-9 is not active in bronchial secretions of βENaC-Tg mice.

These results are similar to observations monitoring free MMP-12 and NE activity in βENaC-Tg mice [49, 150]. Both studies reported an absence of free protease activity in BAL supernatant. However, both studies demonstrated a reduction in emphysema severity by either *NE* or *Mmp12* deletion in βENaC-Tg mice [49, 150]. In these studies, MMP-12 and NE activity was only detected on the surface of macrophages or neutrophil, respectively. A recent study supports the view of a pathogenic contribution of cell surface NE activity. In this study, Dittrich et al. reported an inverse correlation of FEV_1 with either free NE activity in sputum supernatant or NE activity on surfaces of neutrophils in CF patients [33]. A limitation of the current study is that MMP-9 activity was not assessed on the surface of neutrophils in βENaC-Tg mice. This could be addressed by *in situ* gelatin zymography which is also suited to determine gelatinase activity in tissue sections [156]. Therefore, a potential surface MMP-9 activity on leukocytes in βENaC-Tg mice cannot be excluded. Nevertheless, the present study does not suggest an important pathogenic role of a putative cell surface-bound activity of MMP-9 in βENaC-Tg mice.

4.1.3 *Mmp9* deletion reduces mucus obstruction but has no effect on mortality in βENaC-Tg mice

βENaC-Tg mice show an increased mortality mainly within the first two weeks after birth [66, 89]. βENaC-Tg expression causes fatal mucus obstruction predominantly in the trachea in newborn mice [43, 92]. The analysis of the genotype frequencies of crossing *Mmp9*$^{-/-}$ with βENaC-Tg mice revealed no protective effect by *Mmp9* knockout in βENaC-Tg mice (Figure 3.2). Conversely, MMP-9 deficiency reduced airway mucus obstruction in adult βENaC-Tg mice while goblet cell metaplasia and mucin hypersecretion was unaffected in βENaC-Tg/*Mmp9*$^{-/-}$ compared to βENaC-Tg mice (Figure 3.6 and 3.7). This suggests that reduced airway mucus obstruction is present in adult but not in neonatal βENaC-Tg/*Mmp9*$^{-/-}$ mice. Furthermore, death causing mucus plugs are found in the trachea of neonatal βENaC-Tg mice while the mucus obstruction has been measure in main bronchi in the present study. Proximal and distal trachea epithelia were shown to differ in cell composition and ion channel expression [103] and the difference might be even stronger when comparing trachea and bronchi. This spatiotemporal difference might explain the lack of an association between the observed reduction in airway obstruction in adult βENaC-Tg/*Mmp9*$^{-/-}$ mice and neonatal mortality.

Reduced airway mucus obstruction in adult βENaC-Tg/*Mmp9*$^{-/-}$ mice might be a result of changed MCC and/or altered airway epithelial ion channel permeability compared to βENaC-Tg mice. Alternatively, mucus composition could be altered which changes its rheology. DNA and actin, e.g. of necrotic or NETing neutrophils, have a disproportional strong effect on mucus viscosity [78]. Although MMP-9 has not been implicated directly in NET generation, its association with DNA in NETs has been documented [13]. Also, oxidation of mucins, e.g. by oxidative burst of leukocytes, was shown to increase cross-linking, thereby stiffen mucus polymers and potentially compromising its clearance [177]. How MMP-9 may be implicated in these processes is unknown. Previous studies in βENaC-Tg/NE$^{-/-}$ mice reported reduced DNA content in BAL, diminished goblet cell metaplasia and mucin expression but invariantly increased airway mucus obstruction compared to βENaC-Tg mice [49]. ENaC-mediated Na^+ currents were unchanged and the resulting ASL depletion was sufficient to cause airway mucus obstruction. This was also reflected by similar mortality in βENaC-Tg/NE$^{-/-}$ and βENaC-Tg mice. These results suggest that alterations in ENaC conductance are the main determinant for the development of airway mucus plugging while lower mucin secretion or changes in mucus composition, i.e. lower DNA content, are not protective in βENaC-Tg mice.

Performing electrophysiological measurement of isolated trachea epithelia by Ussing chamber could enables direct quantification of potentially altered ENaC-mediated Na^+ absorption in airway epithelia of βENaC-Tg/*Mmp9*$^{-/-}$ mice. Complementary measurement of MCC by monitoring clearance of fluorescent tracers after instillation or applied directly on trachea epithelia could be used to detect differences in mucus clearance between βENaC-Tg/*Mmp9*$^{-/-}$ and βENaC-Tg mice.

4.1.4 *Mmp9* deficiency has no effect on chronic inflammatory lung disease in βENaC-Tg mice

IL-1α is released upon cell necrosis and has been reported as sterile trigger for inflammation in βENaC-Tg mice [43]. Further propagation of inflammation involves IL-1β signaling. Secreted proteases including MMP-9 were shown to convert pro-IL-1β and thereby might contribute to subsequent inflammatory responses [141]. In the present study, IL-1α and IL-1β concentrations are similarly elevated in βENaC-Tg and βENaC-Tg/*Mmp9*$^{-/-}$ mice (Figure 3.4 D, E). This may indicate a persistent pro-inflammatory stimulus by necrotic cells and MMP-9-independent generation of IL-1β e.g. by inflammasomes [80]. MMP-9 was shown to be involved in the migration of cultured airway epithelial cells in wound healing models [15, 82]. In these models, large wounds are induced by NaOH application *in vitro* which is different to the single cell necrosis present in airways of βENaC-Tg mice [92]. An important distinction might be that airway

epithelial basement membranes are intact in βENaC-Tg mice. Thus, replacement of epithelial cells by basal cells is likely unaffected and not dependent on MMP-9. βENaC-Tg mice were shown to develop spontaneous pulmonary bacterial infections which may potentiate the immune response [49, 86]. In this context, it is worth noticing that *Mmp9* deletion has not been implicated in an impairment of bacterial killing [8, 154].

Damaged epithelia release cytokines, e.g. IL-33 and IL-13, which initiates wound healing and tissue repair [42, 105]. This pathway is predominant in βENaC-Tg mice as illustrated by elevated expression of macrophage M2 signature genes [137, 150]. IL-13 concentrations were similar in βENaC-Tg and βENaC-Tg/*Mmp9*$^{-/-}$ mice (Figure 3.4. F). Alternative activation of macrophages was not changed as indicated by equally elevated *Mmp12* and *Ym1* levels in both genotypes (Figure 3.5.). MMP-9 expression has been linked both to M1 or M2 macrophages [114, 139] and therefore cannot be regarded as a reliable marker for polarization.

The resulting inflammatory response in adult βENaC-Tg mice was not affected by *Mmp9* knockout (Figure 3.3 and 3.4). In the presence of raised levels of neutrophil chemoattractants no alteration of neutrophil recruitment is observed in the lungs of βENaC-Tg/*Mmp9*$^{-/-}$ mice compared to βENaC-Tg mice (Figure 3.3). Similarly, eosinophil and lymphocyte migration was not affected by *Mmp9* deletion in βENaC-Tg mice.

The direct role of MMP-9 in leukocyte recruitment to inflammatory sites is still controversial [8, 32]. *In vitro* studies suggest an involvement of MMP-9 in transmigration of eosinophils and neutrophils across artificial basement membranes [31, 108]. Although MMP-9 may degrade basement membrane collagen type IV, to date no study using protease inhibitors or genetic deletion has conclusively demonstrated the necessity for MMP-9 to transverse basement membranes *in vivo* [72]. Several studies modeling acute inflammation reported no difference in neutrophil infiltration into lung, peritoneum or skin tissues when comparing *Mmp9*$^{-/-}$ and WT mice [4, 8, 165]. Interestingly, transgenic pulmonary IL-13 expression resulted in enhanced recruitment of neutrophils in *Mmp9*$^{-/-}$ compared to WT mice [79]. In asthma models, it was shown that less leukocytes are recruited in *Mmp9*$^{-/-}$ mice while a different study using the same model demonstrated no difference in neutrophil but even higher eosinophil numbers in lungs of *Mmp9*$^{-/-}$ compared to WT mice [17, 99]. A potential difference between these studies might be the applied experimental conditions and the used stimuli inducing different levels of acute or chronic inflammatory responses. Moreover, lung infiltrating leukocytes transmigrate at alveolar capillaries and not primarily at post-capillary venules as in other organs [130]. Leukocytes are thought to cross endothelia at tricellular borders where junction proteins are discontinuous [72]. Furthermore, IL-1β was shown to alter epithelial resistance and IL-13 may promote cellular tight junction disruption [26, 172]. In conclusion, prolonged

cytokine exposure may be sufficient to interfere with endothelial and epithelial barrier function which may permit MMP-9-independent leukocyte transmigration into airspaces in βENaC-Tg mice.

Chronic inflammation in βENaC-Tg/*Mmp9*$^{-/-}$ and βENaC-Tg mice lead to a similar degree of alveolar destruction as quantified by lung volume measurement and by morphometric parameters i.e. MLI and DI (Figure 3.8). The data indicate no crucial contribution of MMP-9 to lung morphogenesis or proteolytic destruction during chronic, neutrophilic inflammation in βENaC-Tg mice. NE deletion in βENaC-Tg mice reduced emphysema severity by approximately 50 % [49]. The hypothesis of MMP-9 as effector of NE activity is not supported by the current results. Hence, a contribution of MMP-9 to residual emphysema in βENaC-Tg/NE$^{-/-}$ mice is unlikely. A redundancy in the protease web could explain the lack of prominent influence of MMP-9 deficiency in βENaC-Tg mice. In fact, most *Mmp* deletions do not result in a notable phenotype which points to functional overlap and robustness in the proteolytic system [24, 125]. In βENaC-Tg mice *Mmp12* deletion reduced emphysema but not mucus obstruction or inflammation compared to βENaC-Tg mice [150]. Of note, MMP-12 has additional intracellular functions in regulating transcription which might also modulate lung disease in βENaC-Tg mice [96]. According to the current view versatile interactions between proteases and inhibitors constitute the protease web [41]. Identification of node points in the protease web could enable intervention in pathophysiologic processes. However, the current and previous studies in βENaC-Tg mice point to the involvement of several proteases in parallel pathogenic processes leading to similar disease states e.g. emphysema and/or mucus obstruction [49, 150]. In addition, overlapping substrate specificity with MMP-9 might be sufficient to compensate for genetic deletion of *Mmp9* in βENaC-Tg mice. MMP-8 is in particular an interesting candidate for compensation. *Mmp8* is not upregulated on mRNA level in βENaC-Tg/*Mmp9*$^{-/-}$ mice compared to βENaC-Tg mice (Figure 3.11). However, MMP-9 and MMP-8 are both found in secondary granules of neutrophils and therefore secreted simultaneously [25]. Furthermore, protease function might differ between disease states. Hence, MMP-9 could have essential function in pathophysiological processes that are not represented in βENaC-Tg mice in particular during infection with CF-related pathogens.

Alternative protease-independent mechanisms linking activated leukocytes, oxidative lung damage and increase epithelial apoptosis to emphysema formation are discussed [117]. Structural lung damage may also be induced or enhanced by environmental exposures in particular by bacterial infections [5, 127]. In a mouse model of chronic low-dose LPS exposure an increased count of apoptotic alveolar epithelial cells was detected and proposed as underlying cause of emphysema. Of note, MMP-9 deficient mice were

not protected from epithelial apoptosis and emphysema formation triggered by LPS inhalation [12].

Alveolar and also airway epithelial damage may also be caused by oxidative stress which is associated with an oxidant-antioxidant imbalance [5, 117]. Oxidative stress may arise from ROS release by phagocytes during killing of large, indigestible pathogens [164]. It has also been suggested that hypoxia contributes to oxidative lung damage by impairing oxidant-antioxidant balance and/or generation of ROS from mitochondria [3]. Glutathione (GSH), vitamin C and also mucins may serve as oxidant scavengers in the lung [117]. In fact, oxidative stress was reported in βENaC-Tg mice as indicated by reduced GSH to oxidized glutathione GSSG ratios which could be reversed by thiocyanate treatment [18]. In summary, the present study suggests that MMP-9 is not directly involved in chronic inflammation or alveolar tissue destruction and residual emphysema in NE deficient βENaC-Tg mice might be explained by the activity of other proteases, epithelial apoptosis or oxidative lung damage.

4.1.5 Lung function testing of βENaC-Tg mice indicate no overlapping effects of *Mmp9* or *NE* deletion on lung tissue mechanics

The analysis of lung function in βENaC-Tg/*NE*$^{-/-}$ and βENaC-Tg/*Mmp9*$^{-/-}$ mice further investigated NE- and MMP-9-dependent pathogenic effects in βENaC-Tg mice. Like NE, MMP-9 degrades elastin but also other ECM components e.g. fibronectin, laminin and collagen [124, 128]. Elastin and collagen fibers are organized in a complex network within the lung which determine the mechanical characteristics [163, 167, 171].

So far, the individual role of either protease on lung tissue mechanics has not been studied in CF-like lung disease. Lack of MMP-9 did not prevent lung function decline but NE deletion improved lung function in all tested parameters in βENaC-Tg mice (Figure 3.9, 3.10). This suggests that MMP-9 does not contribute significantly to NE dependent lung disease in βENaC-Tg mice. In reverse, *Mmp9* deletion might result in enhanced compensatory NE activity. In this case higher proteolytic lung damage would be expected in βENaC-Tg/*Mmp9*$^{-/-}$ compared to βENaC-Tg mice. Hence, invariantly increased NE activity in βENaC-Tg/*Mmp9*$^{-/-}$ mice likely mediates, at least in part, the observed lung function impairment similarly to βENaC-Tg mice.

Histology and lung function measurements showed that βENaC-Tg mice display emphysematous, enlarged distal airspaces (Figure 3.8 - 3.10) [92, 150]. This is in divergence to CF patients who develop predominantly bronchiectasis. Species-specific difference between mice and humans in the anatomical lung structure including bronchial size and branching pattern might explain these different observations [92, 132]. It has been hypothesized that the lower number of airway branching in mice compared to the

human lung might favor a faster distribution of damaging factor from inflamed airways to distal alveolar parenchyma in mice [162].

In CF patients, several correlative studies with FEV_1 measurements as main determinant of lung function and MMP-9 levels in sputum have been performed. The first published study by Delacourt et al. demonstrated a significant inverse correlation of MMP-9 activity in sputum supernatant and FEV_1 in clinically stable CF patients [30]. However, NE activity was not assessed in this study. In a subsequent study, MMP-9 activity was only significantly higher during exacerbations but no association with lung function alterations were detected in CF patients [46]. In a study by Sagel et al., an association of lower FEV_1 with higher MMP-9 protein levels were determined [135]. This result was not confirmed in a subsequent prospective study over 4 years by the same group. In particular, this study showed that annual FEV_1 decline in CF patients with relatively conserved lung function correlated with NE but not MMP-9 concentrations in sputum [136]. The different detection methods of either MMP-9 protein levels or activity and difference in the patient cohort impede a conclusive comparison of the mentioned studies. The divergent stage of lung function impairment in the studied CF cohorts and the lack of NE activity measurements further complicate the interpretation. Conversely, numerous studies reported an association of NE and structural lung damage or lung function decline in CF patients [33, 97, 136, 142].

In conclusion, the current data suggest that NE is directly involved in lung function impairment while MMP-9 has a minor role as disease promoting factor in βENaC-Tg mice. Therefore, diminished spirometric parameters in CF patients might be essentially related to higher neutrophil counts and secretion of NE whereas the concomitant release of MMP-9 might be less important. Therefore, the specific inhibition of MMP-9, in contrast to NE, is unlikely to be an effective treatment for the lung disease of βENaC-Tg mice and potentially of CF patients.

4.1.6 Comparison of the studies on the role of MMP-9 in βENaC-Tg mice to CF lung disease in patients

The classical concept explaining lung damage and lung function decline in several obstructive lung diseases is based on the finding of high concentrations of proteases with simultaneously reduced anti-protease levels in bronchial secretions [60, 107, 117, 136].

With regard to MMP-9, MMP-12 and NE, endogenous antiproteases completely inhibit soluble protease activity in pulmonary secretions of βENaC-Tg mice (see Figure 3.12) [49, 150]. This poised protease-antiprotease ratio in βENaC-Tg mice points to a significant difference to CF patients, especially in later disease stages. Young CF

patients (~ 12 years) showed an induction of TIMP1 protein amount while in adults with CF (~ 22 years) TIMP1 protein was depleted from bronchial secretions compared to healthy controls [46, 135]. In older patients, as CF lung disease progresses higher neutrophil counts in sputum are observed and therefore more secreted NE is detected which likely degrades TIMP1 [33, 91, 135]. Adult βENaC-Tg mice show a neutrophil percentage in BAL fluid which is more representative of early CF lung disease [69, 92]. The ~2- to 7-fold higher ratio of blood neutrophils to total white blood cells in humans compared to mice likely contributes to a lower lung neutrophilia in adult βENaC-Tg mice compared to CF patients [101]. In young CF patients, higher neutrophil protease levels are especially found during bacterial respiratory infections [48]. These exacerbations may cause an intermittent disruption of the antiprotease shield in young CF patients which is not represented in βENaC-Tg mice.

Several studies suggest that during chronic inflammation with gradually increasing neutrophil counts and associated release of granule contents, NE concentrations may exceed antiprotease levels and free NE activity may trigger pro-MMP-9 activation in older CF patients [46, 136]. This unopposed protease activity is thought to cause structural lung damage by disrupting epithelial function, aggravating airway mucus obstruction and further promoting inflammation [107, 159]. In contrast to the current study, previous studies in CF patients suggest that unopposed NE *and* MMP-9 activity cause lung tissue damage [48, 142]. Garrat et al. reported that increased MMP-9 levels correlated moderately with the progression of bronchiectasis within 12 months in CF patients. This correlation was based on MMP-9 protein amount detected by gelatin zymography and not activity [48]. Furthermore, the cohort in this study was carefully composed of similar group size of patients with NE activity in BAL and those without. Secretion of NE-containing azurophil granules require higher stimuli concentrations than for MMP-9 containing granules [122]. As expected, MMP-9 protein levels and NE activity showed a positive correlation in CF BAL fluid [48]. Therefore, presence of NE activity might have been a confounding factor introduced by group sampling in their analysis. In mouse models for chronic obstructive pulmonary disease (COPD), MMP-9 deficiency had no protective effect in mice with smoke-induced emphysema [4]. Furthermore, emphysema severity in COPD patients did not correlate with *Mmp9* mRNA levels in lung tissue.

The current study in βENaC-Tg/*Mmp9*$^{-/-}$ mice questions the role of MMP-9 in CF lung disease. However, based on the current results definitive conclusions about a pathogenic role of MMP-9 in patients cannot be drawn because several characteristics of CF lung disease, e.g. intermittent infections and the degree of neutrophilic inflammation, are not be represented in βENaC-Tg mice. The role of NE and MMP-9 and their

interaction during exacerbations could be further studied by challenging βENaC-Tg mice with LPS or bacterial pathogens. This might create temporarily disrupted protease-antiprotease balance. Thereby, unopposed free NE could generate high levels of soluble MMP-9 activity and enable the study of the role of MMP-9 during inflammation with high neutrophil counts in βENaC-Tg mice.

4.2 Preclinical trials revealed no improvement of key characteristics by sivelestat treatment in mice with CF-like lung disease

The studies of NE deficient βENaC-Tg mice suggest that inhibiting NE activity with small molecule compounds might delay or prevent lung disease in βENaC-Tg mice. To date no protease inhibitor has an approval for the treatment of CF lung disease [123]. In Japan and Korea, sivelestat has been approved for the treatment of acute lung injury (ALI) associated with systemic inflammatory response syndrome [57]. Sivelestat inhibits two major neutrophil serine proteases NE and PR3 while CatG activity is reduced only at higher inhibitor concentrations [145]. The performed preclinical trials using sivelestat were designed to assess the concept of pharmacologic targeting of neutrophil serine proteases in mice with CF-like lung disease.

Intraperitoneal application of sivelestat resulted in a reduction of mucus obstruction but did not reduce inflammation or prevent emphysema development in 2-week old βENaC-Tg mice compared to vehicle controls (Figure 3.13). The subsequent s.c. study showed no improved therapeutic effect compared to i.p. injection of sivelestat in βENaC-Tg mice (Figure 3.14). This indicates that hepatic first-pass effects were likely not responsible for the inefficiency of sivelestat.

Nevertheless, the negative results may be related to pharmacokinetic properties of sivelestat since *in vitro* inhibition of NE is well characterized [67]. In the current study, a single applied dose (50 mg/kg body weight) exceeded the IC_{50} for NE (49 nM) by ~ 2200 fold assuming a uniform distribution within the whole body (see also Methods 2.11.1). Of note, the published IC_{50} [67] is based on *in vitro* titration and likely differs from *in vivo* values (see below). The pharmacokinetic parameters for sivelestat are not well documented in the literature. Treatment of ALI patients with sivelestat requires continuous intravenous perfusion over days to assure therapeutic levels [57]. This may be related to a short half-life time of approximately 2 hours [98]. At physiologic blood pH, sivelestat is present mainly as anion due to the carboxyl groups in its structure (see Figure 2.3.). The plasma membrane permeation of sivelestat as charged molecule is

likely restricted and in particular diffusion into blood vessels and from blood into pulmonary tissue might be limited. During inflammation capillaries become more permeable which results in higher plasma content at inflammatory sites. In fact, patients with ALI due to systemic inflammation, e.g. sepsis, typically suffer from pulmonary edema what explains the effectiveness of sivelestat in this disease condition [19, 57]. In studies with murine models of pulmonary diseases the same sivelestat dose as used in the current studies achieved therapeutic effects when applied by i.p. injections. In an asthma model or ALI model sivelestat treatment reduced pulmonary inflammation and goblet cell metaplasia or decreased neutrophil infiltration and alveolar damage, respectively [70, 138]. However, in these and other studies an acute inflammatory responses was induced in adult mice and sivelestat was applied directly before inflammatory stimulation and only for a short study period [62]. The current study indicates that the chronic lung disease that develops over the first two weeks in βENaC-Tg mice could not be reduced by sivelestat treatment. Sivelestat primarily inhibits NE and is a less potent inhibitor for PR3 while CatG is not targeted at therapeutic doses. Unopposed CatG activity could be an additional explanation for the limited effects by sivelestat treatment in βENaC-Tg mice.

In newborn mice i.p. or s.c. injections are the only practical application methods for systemic drug delivery. With a 12 h application cycle in combination with a slow drug absorption, in particular after s.c. injection, a prolonged plasma sivelestat concentration can be assumed [151]. In general, absorption of water soluble drugs is expected to be more rapid after i.p. than with s.c. injections [50]. However, the exact bioavailability depends on drug properties and is not published for sivelestat. I.p. injection of sivelestat might result in more rapid absorption and higher blood peak levels compared to s.c. application. Therefore, higher blood sivelestat levels after i.p. application might partially inhibit NE in pulmonary tissue and thereby reducing NE-mediated mucin expression [159]. This might explain the diminished mucus obstruction in βENaC-Tg mice treated with sivelestat by i.p. injections but not by s.c. application.

In previous studies, NE was shown to be active solely on the surface of neutrophils in βENaC-Tg mice and not in BAL supernatant [49]. Cell surface-bound NE was shown to be highly resistant to inhibition by endogenous inhibitors, like A1AT, but also small molecular weight inhibitors were less effective in limiting activity of surface-bound NE [116]. This may explain the preserved surface NE activity on neutrophils in βENaC-Tg mice reported in previous studies [49]. In addition, this observation suggests that significantly higher sivelestat concentrations are necessary to fully inhibit neutrophil surface-bound in comparison to soluble NE activity. The polar nature of sivelestat restricts NE inhibition to the extracellular location and excludes accumulation within

primary neutrophil granules prior to secretion. NE is stored in azurophil granules in mM concentrations which results upon secretion in a transient mismatch between NE and inhibitor concentration [84]. This process, termed quantum proteolysis, predicts NE activity in the surrounding of neutrophils even in the presence of high levels of inhibitors. Additionally, neutrophils may form an integrin-based seal around contact sites to ECM substrates which restricts access of inhibitors to secreted proteases [118, 176]. The performed preclinical trial using sivelestat could not reproduce the results of NE deletion in βENaC-Tg mice. Lack of NE reduced neutrophil infiltration and emphysema severity but had no effect on airway mucus obstruction in adult βENaC-Tg mice [49]. The contradictory result of the preclinical sivelestat trial might reflect insufficient sivelestat levels in pulmonary tissue to achieve effective NE inhibition in particular on the surface of neutrophils. A limitation of the performed treatment studies is that the concentrations of sivelestat in lung tissue or blood have not been assessed. Local application by intranasal (i.n.) instillation could be performed to enable sufficient pulmonary sivelestat levels. A disadvantage of i.n. instillation is that only low volumes and therefore only low drug doses can be applied. MCC in murine airway may prevent sustained pulmonary drug levels. In addition, airway mucus plugging in βENaC-Tg mice could also impede sivelestat delivery into lower airspaces.

The difficulty to inhibit NE activity in CF lung disease may be reflected in the low number of clinical trials conducted so far. These trials using different NE inhibitors reported only limited effects on lung disease in CF patients [36, 51] (see also introduction 1.6). The preclinical trials with sivelestat revealed that effective treatment requires inhibitor concentrations that are high enough to target neutrophil serine proteases in solution and on cell surfaces. To achieve this, a membrane permeable inhibitor e.g. GW311616A [87] that may accumulate within azurophil granules of blood neutrophils could be more effective. Alternatively, prevention of neutrophil serine protease activation by cathepsin C inhibition within bone marrow neutrophils was shown to abrogate levels of all neutrophil-derived serine proteases without impairing neutrophil recruitment into the lungs [53]. Cathepsin C deficiency cause Papillon-Lefèvre syndrome in humans. Main symptoms are periodontitis and subsequent loss of teeth at young age [131]. Thus, adverse effects of simultaneous targeting all neutrophil serine proteases seem to be limited.

5 Conclusions

Increased protease activity is thought to contribute to the reported differences in the progression of lung disease in CF patients. The evaluation of the role of individual proteases as disease promoting factor is crucial for the development of targeted therapies to treat CF lung disease. Most research has focused on the neutrophil-derived serine protease NE while less is known about the involvement of other proteases. The present work elucidates the role of the putative NE effector MMP-9 in βENaC-Tg mice and evaluates protease inhibitor treatment as a therapeutic strategy for CF patients.

Monitoring of MMP-9 protein levels indicated high abundance in BAL fluid of βENaC-Tg mice. The further analysis of MMP-9 deficient βENaC-Tg mice showed reduced airway mucus obstruction which did not result in lower mortality, nor attenuate inflammation or decrease distal airspace enlargement compared to βENaC-Tg mice. Furthermore, comparison of lung function in βENaC-Tg, βENaC-Tg/*NE*$^{-/-}$ and βENaC-Tg/*Mmp9*$^{-/-}$mice indicated that *Mmp9* deletion did not ameliorate lung function parameters relative to βENaC-Tg mice while NE deficiency reduced lung function decline. The current data demonstrate that the mere presence of MMP-9 in BAL fluid of βENaC-Tg mice does not predict a pathological role. In summary, the study indicates that MMP-9 is not a pivotal pathogenic factor while NE significantly contributes to lung disease of βENaC-Tg mice.

Implications of these results were applied and tested in a preventive, preclinical trial using the NE inhibitor sivelestat in newborn WT and βENaC-Tg mice. Intraperitoneal application of sivelestat reduced airway mucus obstruction but failed to prevent inflammation or lung tissue destruction in βENaC-Tg mice. These results may be related to pharmacokinetic characteristics of sivelestat or the persistence of inhibitor-resistant NE activity on neutrophil-surface or in sequestered locations in lung tissue.

In summary, the data suggest that *Mmp9* deletion does not attenuate lung disease in βENaC-Tg mice. To the extent that βENaC-Tg mice resemble CF lung disease, these results question the proposed pathogenic role of MMP-9 in patients. The performed trials with sivelestat indicate that further treatment studies are needed using compounds with improved pharmacokinetic properties to target neutrophil-surface protease activity and to translate the findings of protease-deficient βENaC-Tg mice into clinical practice.

6 References

1. Alevy YG, Patel AC, Romero AG, Patel DA, Tucker J, Roswit WT, Miller CA, Heier RF, Byers DE, Brett TJ, Holtzman MJ (2012) IL-13–induced airway mucus production is attenuated by MAPK13 inhibition. Journal of Clinical Investigation 122:4555–4568. doi: 10.1172/JCI64896

2. Amitani R, Wilson R, Rutman A, Read R, Ward C, Burnett D, Stockley RA, Cole PJ (1991) Effects of Human Neutrophil Elastase and *Pseudomonas aeruginosa* Proteinases on Human Respiratory Epithelium. American Journal of Respiratory Cell and Molecular Biology 4:26–32. doi: 10.1165/ajrcmb/4.1.26

3. Araneda OF, Tuesta M (2012) Lung Oxidative Damage by Hypoxia. Oxidative Medicine and Cellular Longevity 2012:1–18. doi: 10.1155/2012/856918

4. Atkinson JJ, Lutey BA, Suzuki Y, Toennies HM, Kelley DG, Kobayashi DK, Ijem WG, Deslee G, Moore CH, Jacobs ME, Conradi SH, Gierada DS, Pierce RA, Betsuyaku T, Senior RM (2011) The Role of Matrix Metalloproteinase-9 in Cigarette Smoke–induced Emphysema. American Journal of Respiratory and Critical Care Medicine 183:876–884. doi: 10.1164/rccm.201005-0718OC

5. Barnes PJ, Burney PGJ, Silverman EK, Celli BR, Vestbo J, Wedzicha JA, Wouters EFM (2015) Chronic obstructive pulmonary disease. Nature Reviews Disease Primers 15076. doi: 10.1038/nrdp.2015.76

6. Bates JHT, Irvin CG (2003) Measuring lung function in mice: the phenotyping uncertainty principle. Journal of Applied Physiology 94:1297–1306. doi: 10.1152/japplphysiol.00706.2002

7. Belaaouaj A (2002) Neutrophil elastase-mediated killing of bacteria: lessons from targeted mutagenesis. Microbes and infection 4:1259–1264

8. Betsuyaku T, Michael Shipley J, Liu Z, Senior RM (1999) Neutrophil Emigration in the Lungs, Peritoneum, and Skin Does Not Require Gelatinase B. American Journal of Respiratory Cell and Molecular Biology 20:1303–1309. doi: 10.1165/ajrcmb.20.6.3558

9. Borregaard N, Cowland JB (1997) Granules of the human neutrophilic polymorphonuclear leukocyte. Blood 89:3503–3521

10. Brandes ME, Mai UE, Ohura K, Wahl SM (1991) Type I transforming growth factor-beta receptors on neutrophils mediate chemotaxis to transforming growth factor-beta. J Immunol 147:1600

11. Branzk N, Lubojemska A, Hardison SE, Wang Q, Gutierrez MG, Brown GD, Papayannopoulos V (2014) Neutrophils sense microbe size and selectively release neutrophil extracellular traps in response to large pathogens. Nature Immunology 15:1017–1025. doi: 10.1038/ni.2987

12. Brass DM, Hollingsworth JW, Cinque M, Li Z, Potts E, Toloza E, Foster WM, Schwartz DA (2008) Chronic LPS Inhalation Causes Emphysema-Like Changes in Mouse Lung that Are Associated with Apoptosis. American Journal of Respiratory Cell and Molecular Biology 39:584–590. doi: 10.1165/rcmb.2007-0448OC

13. Brinkmann V (2004) Neutrophil Extracellular Traps Kill Bacteria. Science 303:1532–1535. doi: 10.1126/science.1092385

14. Bruce MC, Poncz L, Klinger JD, Stern RC, Tomashefski JF, Dearborn DG (1985) Biochemical and Pathologic Evidence for Proteolytic Destruction of Lung Connective Tissue in Cystic Fibrosis. Am Rev Respir Dis 132:529–535. doi: 10.1164/arrd.1985.132.3.529

15. Buisson A-C, Zahm J-M, Polette M, Pierrot D, Bellon G, Puchelle E, Birembaut P, Tournier J-M (1996) Gelatinase B is involved in the in vitro wound repair of human respiratory epithelium. Journal of Cellular Physiology 166:413–426. doi: 10.1002/(SICI)1097-4652(199602)166:2<413::AID-JCP20>3.0.CO;2-A

16. Button B, Cai L-H, Ehre C, Kesimer M, Hill DB, Sheehan JK, Boucher RC, Rubinstein M (2012) A Periciliary Brush Promotes the Lung Health by Separating the Mucus Layer from Airway Epithelia. Science 337:937–941. doi: 10.1126/science.1223012

17. Cataldo DD, Tournoy KG, Vermaelen K, Munaut C, Foidart J-M, Louis R, Noël A, Pauwels RA (2002) Matrix metalloproteinase-9 deficiency impairs cellular infiltration and bronchial hyperresponsiveness during allergen-induced airway inflammation. The American journal of pathology 161:491–498

18. Chandler JD, Min E, Huang J, McElroy CS, Dickerhof N, Mocatta T, Fletcher AA, Evans CM, Liang L, Patel M, Kettle AJ, Nichols DP, Day BJ (2015) Antiinflammatory and Antimicrobial Effects of Thiocyanate in a Cystic Fibrosis Mouse Model. American Journal of Respiratory Cell and Molecular Biology 53:193–205. doi: 10.1165/rcmb.2014-0208OC

19. Chawla LS, Fink M, Goldstein SL, Opal S, Gómez A, Murray P, Gómez H, Kellum JA (2016) The Epithelium as a Target in Sepsis: SHOCK 45:249–258. doi: 10.1097/SHK.0000000000000518

20. Chen GY, Nuñez G (2010) Sterile inflammation: sensing and reacting to damage. Nature Reviews Immunology 10:826–837. doi: 10.1038/nri2873

21. Chiao YA, Ramirez TA, Zamilpa R, Okoronkwo SM, Dai Q, Zhang J, Jin Y-F, Lindsey ML (2012) Matrix metalloproteinase-9 deletion attenuates myocardial fibrosis and diastolic dysfunction in ageing mice. Cardiovascular Research 96:444–455. doi: 10.1093/cvr/cvs275

22. Clark I, Swingler T, Sampieri C, Edwards D (2008) The regulation of matrix metalloproteinases and their inhibitors. The International Journal of Biochemistry & Cell Biology 40:1362–1378. doi: 10.1016/j.biocel.2007.12.006

23. Colotta F, Re F, Polentarutti N, Sozzani S, Mantovani A (1992) Modulation of granulocyte survival and programmed cell death by cytokines and bacterial products. Blood 80:2012

24. Coussens LM, Shapiro SD, Soloway PD, Werb Z (2001) Models for gain-of-function and loss-of-function of MMPs. Transgenic and gene targeted mice. Methods Mol Biol 151:149–179

25. Cowland JB, Borregaard N (2016) Granulopoiesis and granules of human neutrophils. Immunological Reviews 273:11–28. doi: 10.1111/imr.12440

26. Coyne CB (2002) Regulation of Airway Tight Junctions by Proinflammatory Cytokines. Molecular Biology of the Cell 13:3218–3234. doi: 10.1091/mbc.E02-03-0134

27. Cutting GR (2015) Cystic fibrosis genetics: from molecular understanding to clinical application. Nature Reviews Genetics 16:45–56. doi: 10.1038/nrg3849

28. De Filippo K, Henderson RB, Laschinger M, Hogg N (2008) Neutrophil Chemokines KC and Macrophage-Inflammatory Protein-2 Are Newly Synthesized by Tissue Macrophages Using Distinct TLR Signaling Pathways. The Journal of Immunology 180:4308–4315. doi: 10.4049/jimmunol.180.6.4308

29. Dean RA, Cox JH, Bellac CL, Doucet A, Starr AE, Overall CM (2008) Macrophage-specific metalloelastase (MMP-12) truncates and inactivates ELR+ CXC chemokines and generates CCL2, -7, -8, and -13 antagonists: potential role of the macrophage in terminating polymorphonuclear leukocyte influx. Blood 112:3455–3464. doi: 10.1182/blood-2007-12-129080

30. Delacourt C, Le Bourgeois M, D'Ortho MP, Doit C, Scheinmann P, Navarro J, Harf A, Hartmann DJ, Lafuma C (1995) Imbalance between 95 kDa type IV collagenase and tissue inhibitor of metalloproteinases in sputum of patients with cystic fibrosis. Am J Respir Crit Care Med 152:765–774. doi: 10.1164/ajrccm.152.2.7633740

31. Delclaux C, Delacourt C, D'Ortho MP, Boyer V, Lafuma C, Harf A (1996) Role of gelatinase B and elastase in human polymorphonuclear neutrophil migration across basement membrane. American Journal of Respiratory Cell and Molecular Biology 14:288–295. doi: 10.1165/ajrcmb.14.3.8845180

32. D'Haese A, Wuyts A, Dillen C, Dubois B, Billiau A, Heremans H, Van Damme J, Arnold B, Opdenakker G (2000) In Vivo Neutrophil Recruitment by Granulocyte Chemotactic Protein-2 Is Assisted by Gelatinase B/MMP-9 in the Mouse. Journal of Interferon & Cytokine Research 20:667–674. doi: 10.1089/107999000414853

33. Dittrich AS, Kühbandner I, Gehrig S, Rickert-Zacharias V, Twigg M, Wege S, Taggart CC, Herth F, Schultz C, Mall MA (2018) Elastase activity on sputum neutrophils correlates with severity of lung disease in cystic fibrosis. European Respiratory Journal 51:1701910. doi: 10.1183/13993003.01910-2017

34. Doerschuk CM (2001) Mechanisms of Leukocyte Sequestration in Inflamed Lungs. Microcirculation 8:71–88. doi: 10.1111/j.1549-8719.2001.tb00159.x

35. Ducharme A, Frantz S, Aikawa M, Rabkin E, Lindsey M, Rohde LE, Schoen FJ, Kelly RA, Werb Z, Libby P, Lee RT (2000) Targeted deletion of matrix metalloproteinase-9 attenuates left ventricular enlargement and collagen accumulation after experimental myocardial infarction. Journal of Clinical Investigation 106:55–62. doi: 10.1172/JCI8768

36. Elborn JS, Perrett J, Forsman-Semb K, Marks-Konczalik J, Gunawardena K, Entwistle N (2012) Efficacy, safety and effect on biomarkers of AZD9668 in cystic fibrosis. European Respiratory Journal 40:969–976. doi: 10.1183/09031936.00194611

37. Escolar JDD, Escolar A (2004) Lung histeresis: A morphological view

38. Fahy JV, Dickey BF (2010) Airway Mucus Function and Dysfunction. New England Journal of Medicine 363:2233–2247. doi: 10.1056/NEJMra0910061

39. Faurschou M, Borregaard N (2003) Neutrophil granules and secretory vesicles in inflammation. Microbes and Infection 5:1317–1327. doi: 10.1016/j.micinf.2003.09.008

40. Feliciano GT, da Silva AJR (2015) Unravelling the reaction mechanism of matrix metalloproteinase 3 using QM/MM calculations. Journal of Molecular Structure 1091:125–132. doi: 10.1016/j.molstruc.2015.02.079

41. Fortelny N, Cox JH, Kappelhoff R, Starr AE, Lange PF, Pavlidis P, Overall CM (2014) Network Analyses Reveal Pervasive Functional Regulation Between Proteases in the Human Protease Web. PLoS Biology 12:e1001869. doi: 10.1371/journal.pbio.1001869

42. Fritzsching B, Hagner M, Dai L, Christochowitz S, Agrawal R, van Bodegom C, Schmidt S, Schatterny J, Hirtz S, Brown R, Goritzka M, Duerr J, Zhou-Suckow Z, Mall MA (2017) Impaired mucus clearance exacerbates allergen-induced type 2 airway inflammation in juvenile mice. Journal of Allergy and Clinical Immunology 140:190–203.e5. doi: 10.1016/j.jaci.2016.09.045

43. Fritzsching B, Zhou-Suckow Z, Trojanek JB, Schubert SC, Schatterny J, Hirtz S, Agrawal R, Muley T, Kahn N, Sticht C, Gunkel N, Welte T, Randell SH, Länger F, Schnabel P, Herth FJF, Mall MA (2015) Hypoxic Epithelial Necrosis Triggers Neutrophilic Inflammation via IL-1 Receptor Signaling in Cystic Fibrosis Lung Disease. American Journal of Respiratory and Critical Care Medicine 191:902–913. doi: 10.1164/rccm.201409-1610OC

44. Fujisawa T, Chang MM-J, Velichko S, Thai P, Hung L-Y, Huang F, Phuong N, Chen Y, Wu R (2011) NF-κB Mediates IL-1β– and IL-17A–Induced *MUC5B* Expression in Airway Epithelial Cells. American Journal of Respiratory Cell and Molecular Biology 45:246–252. doi: 10.1165/rcmb.2009-0313OC

45. Gaggar A, Jackson PL, Noerager BD, O'Reilly PJ, McQuaid DB, Rowe SM, Clancy JP, Blalock JE (2008) A novel proteolytic cascade generates an extracellular matrix-derived chemoattractant in chronic neutrophilic inflammation. J Immunol 180:5662–5669

46. Gaggar A, Li Y, Weathington N, Winkler M, Kong M, Jackson P, Blalock JE, Clancy JP (2007) Matrix metalloprotease-9 dysregulation in lower airway secretions of cystic fibrosis patients. American Journal of Physiology-Lung Cellular and Molecular Physiology 293:L96–L104. doi: 10.1152/ajplung.00492.2006

47. Garratt LW, Sutanto EN, Ling K-M, Looi K, Iosifidis T, Martinovich KM, Shaw NC, Buckley AG, Kicic-Starcevich E, Lannigan FJ, Knight DA, Stick SM, Kicic A (2016) Alpha-1 Antitrypsin Mitigates the Inhibition of Airway Epithelial Cell Repair by Neutrophil Elastase. American Journal of Respiratory Cell and Molecular Biology 54:341–349. doi: 10.1165/rcmb.2015-0074OC

48. Garratt LW, Sutanto EN, Ling K-M, Looi K, Iosifidis T, Martinovich KM, Shaw NC, Kicic-Starcevich E, Knight DA, Ranganathan S, Stick SM, Kicic A (2015) Matrix metalloproteinase activation by free neutrophil elastase contributes to bronchiectasis progression in early cystic fibrosis. European Respiratory Journal 46:384–394. doi: 10.1183/09031936.00212114

49. Gehrig S, Duerr J, Weitnauer M, Wagner CJ, Graeber SY, Schatterny J, Hirtz S, Belaaouaj A, Dalpke AH, Schultz C, Mall MA (2014) Lack of Neutrophil Elastase Reduces Inflammation, Mucus Hypersecretion, and Emphysema, but Not Mucus Obstruction, in Mice with Cystic Fibrosis–like Lung Disease. American Journal of Respiratory and Critical Care Medicine 189:1082–1092. doi: 10.1164/rccm.201311-1932OC

50. Gibaldi M, Perrier D (1975) Route of Administration and Drug Disposition. Drug Metabolism Reviews 3:185–199. doi: 10.3109/03602537408993742

51. Griese M, Latzin P, Kappler M, Weckerle K, Heinzlmaier T, Bernhardt T, Hartl D (2006) 1-Antitrypsin inhalation reduces airway inflammation in cystic fibrosis patients. European Respiratory Journal 29:240–250. doi: 10.1183/09031936.00047306

52. Griffin KL, Fischer BM, Kummarapurugu AB, Zheng S, Kennedy TP, Rao NV, Foster WM, Voynow JA (2014) 2-O, 3-O-Desulfated Heparin Inhibits Neutrophil Elastase–Induced HMGB-1 Secretion and Airway Inflammation. American Journal of Respiratory Cell and Molecular Biology 50:684–689. doi: 10.1165/rcmb.2013-0338RC

53. Guarino C, Hamon Y, Croix C, Lamort A-S, Dallet-Choisy S, Marchand-Adam S, Lesner A, Baranek T, Viaud-Massuard M-C, Lauritzen C, Pedersen J, Heuzé-Vourc'h N, Si-Tahar M, Fıratlı E, Jenne DE, Gauthier F, Horwitz MS, Borregaard N, Korkmaz B (2017) Prolonged pharmacological inhibition of cathepsin C results in elimination of neutrophil serine proteases. Biochemical Pharmacology 131:52–67. doi: 10.1016/j.bcp.2017.02.009

54. Halverson TWR, Wilton M, Poon KKH, Petri B, Lewenza S (2015) DNA Is an Antimicrobial Component of Neutrophil Extracellular Traps. PLOS Pathogens 11:e1004593. doi: 10.1371/journal.ppat.1004593

55. Hankinson JL, Odencrantz JR, Fedan KB (1999) Spirometric Reference Values from a Sample of the General U.S. Population. American Journal of Respiratory and Critical Care Medicine 159:179–187. doi: 10.1164/ajrccm.159.1.9712108

56. Harkema JR, Plopper CG, Hyde DM, St George JA (1987) Regional differences in quantities of histochemically detectable mucosubstances in nasal, paranasal, and nasopharyngeal epithelium of the bonnet monkey. Journal of Histochemistry & Cytochemistry 35:279–286. doi: 10.1177/35.3.2434556

57. Hayakawa M, Katabami K, Wada T, Sugano M, Hoshino H, Sawamura A, Gando S (2010) SIVELESTAT (SELECTIVE NEUTROPHIL ELASTASE INHIBITOR) IMPROVES THE MORTALITY RATE OF SEPSIS ASSOCIATED WITH BOTH ACUTE RESPIRATORY DISTRESS SYNDROME AND DISSEMINATED INTRAVASCULAR COAGULATION PATIENTS: Shock 33:14–18. doi: 10.1097/SHK.0b013e3181aa95c4

58. Hilgendorff A, Parai K, Ertsey R, Jain N, Navarro EF, Peterson JL, Tamosiuniene R, Nicolls MR, Starcher BC, Rabinovitch M, Bland RD (2011) Inhibiting Lung Elastase Activity Enables Lung Growth in Mechanically Ventilated Newborn Mice. American Journal of Respiratory and Critical Care Medicine 184:537–546. doi: 10.1164/rccm.201012-2010OC

59. Hilgendorff A, Parai K, Ertsey R, Juliana Rey-Parra G, Thébaud B, Tamosiuniene R, Jain N, Navarro EF, Starcher BC, Nicolls MR, Rabinovitch M, Bland RD (2012) Neonatal mice genetically modified to express the elastase inhibitor elafin are protected against the adverse effects of mechanical ventilation on lung growth. American Journal of Physiology-Lung Cellular and Molecular Physiology 303:L215–L227. doi: 10.1152/ajplung.00405.2011

60. Hill AT, Bayley D, Stockley RA (1999) The Interrelationship of Sputum Inflammatory Markers in Patients with Chronic Bronchitis. American Journal of Respiratory and Critical Care Medicine 160:893–898. doi: 10.1164/ajrccm.160.3.9901091

61. Hoenderdos K, Lodge KM, Hirst RA, Chen C, Palazzo SGC, Emerenciana A, Summers C, Angyal A, Porter L, Juss JK, O'Callaghan C, Chilvers ER, Condliffe AM (2016) Hypoxia upregulates neutrophil degranulation and potential for tissue injury. Thorax 71:1030–1038. doi: 10.1136/thoraxjnl-2015-207604

62. Iba T, Kidokoro A, Fukunaga M, Takuhiro K, Yoshikawa S, Sugimotoa K (2006) PRETREATMENT OF SIVELESTAT SODIUM HYDRATE IMPROVES THE LUNG MICROCIRCULATION AND ALVEOLAR DAMAGE IN LIPOPOLYSACCHARIDE-INDUCED ACUTE LUNG INFLAMMATION IN HAMSTERS: Shock 26:95–98. doi: 10.1097/01.shk.0000223126.34017.d9

63. Jackson PL, Xu X, Wilson L, Weathington NM, Clancy JP, Blalock JE, Gaggar A (2010) Human Neutrophil Elastase-Mediated Cleavage Sites of MMP-9 and TIMP-1: Implications to Cystic Fibrosis Proteolytic Dysfunction. Molecular Medicine 16:159–166. doi: 10.2119/molmed.2009.00109

64. Jiang D, Wenzel SE, Wu Q, Bowler RP, Schnell C, Chu HW (2013) Human Neutrophil Elastase Degrades SPLUNC1 and Impairs Airway Epithelial Defense against Bacteria. PLoS ONE 8:e64689. doi: 10.1371/journal.pone.0064689

65. Jiang Q, Engelhardt JF (1998) Cellular heterogeneity of CFTR expression and function in the lung: implications for gene therapy of cystic fibrosis. European Journal of Human Genetics 6:12–31. doi: 10.1038/sj.ejhg.5200158

66. Johannesson B, Hirtz S, Schatterny J, Schultz C, Mall MA (2012) CFTR Regulates Early Pathogenesis of Chronic Obstructive Lung Disease in βENaC-Overexpressing Mice. PLoS ONE 7:e44059. doi: 10.1371/journal.pone.0044059

67. Kawabata K, Suzuki M, Sugitani M, Imaki K, Toda M, Miyamoto T (1991) ONO-5046, a novel inhibitor of human neutrophil elastase. Biochem Biophys Res Commun 177:814–820

68. Kerem B, Rommens J, Buchanan J, Markiewicz D, Cox T, Chakravarti A, Buchwald M, Tsui L (1989) Identification of the cystic fibrosis gene: genetic analysis. Science 245:1073–1080. doi: 10.1126/science.2570460

69. Khan TZ, Wagener JS, Bost T, Martinez J, Accurso FJ, Riches DW (1995) Early pulmonary inflammation in infants with cystic fibrosis. American Journal of Respiratory and Critical Care Medicine 151:1075–1082. doi: 10.1164/ajrccm.151.4.7697234

70. Koga H, Miyahara N, Fuchimoto Y, Ikeda G, Waseda K, Ono K, Tanimoto Y, Kataoka M, Gelfand EW, Tanimoto M, Kanehiro A (2013) Inhibition of neutrophil elastase attenuates airway hyperresponsiveness and inflammation in a mouse model of secondary allergen challenge: neutrophil elastase inhibition attenuates allergic airway responses. Respiratory Research 14:8. doi: 10.1186/1465-9921-14-8

71. Kolaczkowska E, Jenne CN, Surewaard BGJ, Thanabalasuriar A, Lee W-Y, Sanz M-J, Mowen K, Opdenakker G, Kubes P (2015) Molecular mechanisms of NET formation and degradation revealed by intravital imaging in the liver vasculature. Nature Communications 6:6673. doi: 10.1038/ncomms7673

72. Kolaczkowska E, Kubes P (2013) Neutrophil recruitment and function in health and inflammation. Nature Reviews Immunology 13:159–175. doi: 10.1038/nri3399

73. Konstan MW, Morgan WJ, Butler SM, Pasta DJ, Craib ML, Silva SJ, Stokes DC, Wohl MEB, Wagener JS, Regelmann WE, Johnson CA (2007) Risk Factors For Rate of Decline in Forced Expiratory Volume in One Second in Children and Adolescents with Cystic Fibrosis. The Journal of Pediatrics 151:134–139.e1. doi: 10.1016/j.jpeds.2007.03.006

74. Korkmaz B, Horwitz MS, Jenne DE, Gauthier F (2010) Neutrophil Elastase, Proteinase 3, and Cathepsin G as Therapeutic Targets in Human Diseases. Pharmacological Reviews 62:726–759. doi: 10.1124/pr.110.002733

75. Kramer EL, Clancy JP (2018) TGFβ as a therapeutic target in cystic fibrosis. Expert Opinion on Therapeutic Targets 22:177–189. doi: 10.1080/14728222.2018.1406922

76. Kreda SM, Davis CW, Rose MC (2012) CFTR, Mucins, and Mucus Obstruction in Cystic Fibrosis. Cold Spring Harbor Perspectives in Medicine 2:a009589–a009589. doi: 10.1101/cshperspect.a009589

77. Lachmann B, Robertson B, Vogel J (1980) In Vivo Lung Lavage as an Experimental Model of the Respiratory Distress Syndrome. Acta Anaesthesiologica Scandinavica 24:231–236. doi: 10.1111/j.1399-6576.1980.tb01541.x

78. Lai SK, Wang Y-Y, Wirtz D, Hanes J (2009) Micro- and macrorheology of mucus. Advanced Drug Delivery Reviews 61:86–100. doi: 10.1016/j.addr.2008.09.012

79. Lanone S, Zheng T, Zhu Z, Liu W, Lee CG, Ma B, Chen Q, Homer RJ, Wang J, Rabach LA, Rabach ME, Shipley JM, Shapiro SD, Senior RM, Elias JA (2002) Overlapping and enzyme-specific contributions of matrix metalloproteinases-9 and -12 in IL-13–induced inflammation and remodeling. Journal of Clinical Investigation 110:463–474. doi: 10.1172/JCI14136

80. Latz E, Xiao TS, Stutz A (2013) Activation and regulation of the inflammasomes. Nature Reviews Immunology 13:397–411. doi: 10.1038/nri3452

81. Lee CG, Hartl D, Lee GR, Koller B, Matsuura H, Da Silva CA, Sohn MH, Cohn L, Homer RJ, Kozhich AA, Humbles A, Kearley J, Coyle A, Chupp G, Reed J, Flavell RA, Elias JA (2009) Role of breast regression protein 39 (BRP-39)/chitinase 3-like-1 in Th2 and IL-13–induced tissue responses and apoptosis. The Journal of Experimental Medicine 206:1149–1166. doi: 10.1084/jem.20081271

82. Legrand C, Gilles C, Zahm J-M, Polette M, Buisson A-C, Kaplan H, Birembaut P, Tournier J-M (1999) Airway Epithelial Cell Migration Dynamics: MMP-9 Role in Cell–Extracellular Matrix Remodeling. The Journal of Cell Biology 146:517–529. doi: 10.1083/jcb.146.2.517

83. Linsdell P (2014) Functional architecture of the CFTR chloride channel. Molecular Membrane Biology 31:1–16. doi: 10.3109/09687688.2013.868055

84. Liou TG, Campbell EJ (1995) Nonisotropic Enzyme-Inhibitor Interactions: A Novel Nonoxidative Mechanism for Quantum Proteolysis by Human Neutrophils. Biochemistry 34:16171–16177. doi: 10.1021/bi00049a032

85. Liu Z, Zhou X, Shapiro SD, Shipley JM, Twining SS, Diaz LA, Senior RM, Werb Z (2000) The Serpin α1-Proteinase Inhibitor Is a Critical Substrate for Gelatinase B/MMP-9 In Vivo. Cell 102:647–655. doi: 10.1016/S0092-8674(00)00087-8

86. Livraghi-Butrico A, Kelly EJ, Klem ER, Dang H, Wolfgang MC, Boucher RC, Randell SH, O'Neal WK (2012) Mucus clearance, MyD88-dependent and MyD88-independent immunity modulate lung susceptibility to spontaneous bacterial infection and inflammation. Mucosal Immunology 5:397–408. doi: 10.1038/mi.2012.17

87. Macdonald SJ., Dowle MD, Harrison LA, Shah P, Johnson MR, Inglis GG., Clarke GD., Smith RA, Humphreys D, Molloy CR, Amour A, Dixon M, Murkitt G, Godward RE, Padfield T, Skarzynski T, Singh OM., Kumar KA, Fleetwood G, Hodgson ST, Hardy GW, Finch H (2001) The discovery of a potent, intracellular, orally bioavailable, long duration inhibitor of human neutrophil elastase—GW311616A a development candidate. Bioorganic & Medicinal Chemistry Letters 11:895–898. doi: 10.1016/S0960-894X(01)00078-6

88. Makam M, Diaz D, Laval J, Gernez Y, Conrad CK, Dunn CE, Davies ZA, Moss RB, Herzenberg LA, Herzenberg LA, Tirouvanziam R (2009) Activation of critical, host-induced, metabolic and stress pathways marks neutrophil entry into cystic fibrosis lungs. Proceedings of the National Academy of Sciences 106:5779–5783. doi: 10.1073/pnas.0813410106

89. Mall M, Grubb BR, Harkema JR, O'Neal WK, Boucher RC (2004) Increased airway epithelial Na+ absorption produces cystic fibrosis-like lung disease in mice. Nature Medicine 10:487–493. doi: 10.1038/nm1028

90. Mall MA (2016) Unplugging Mucus in Cystic Fibrosis and Chronic Obstructive Pulmonary Disease. Annals ATS 13:S177–S185. doi: 10.1513/AnnalsATS.201509-641KV

91. Mall MA, Elborn JS (2014) Cystic Fibrosis. European Respiratory Society

92. Mall MA, Harkema JR, Trojanek JB, Treis D, Livraghi A, Schubert S, Zhou Z, Kreda SM, Tilley SL, Hudson EJ, O'Neal WK, Boucher RC (2008) Development of Chronic Bronchitis and Emphysema in β-Epithelial Na + Channel–Overexpressing Mice. American Journal of Respiratory and Critical Care Medicine 177:730–742. doi: 10.1164/rccm.200708-1233OC

93. Mall MA, Hartl D (2014) CFTR: cystic fibrosis and beyond. European Respiratory Journal 44:1042–1054. doi: 10.1183/09031936.00228013

94. Manicone A, Mcguire J (2008) Matrix metalloproteinases as modulators of inflammation. Seminars in Cell & Developmental Biology 19:34–41. doi: 10.1016/j.semcdb.2007.07.003

95. Mantovani A, Cassatella MA, Costantini C, Jaillon S (2011) Neutrophils in the activation and regulation of innate and adaptive immunity. Nature Reviews Immunology 11:519–531. doi: 10.1038/nri3024

96. Marchant DJ, Bellac CL, Moraes TJ, Wadsworth SJ, Dufour A, Butler GS, Bilawchuk LM, Hendry RG, Robertson AG, Cheung CT, Ng J, Ang L, Luo Z, Heilbron K, Norris MJ, Duan W, Bucyk T, Karpov A, Devel L, Georgiadis D, Hegele RG, Luo H, Granville DJ, Dive V, McManus BM, Overall CM (2014) A new transcriptional role for matrix metalloproteinase-12 in antiviral immunity. Nature Medicine 20:493–502. doi: 10.1038/nm.3508

97. Margaroli C, Garratt LW, Horati H, Dittrich AS, Rosenow T, Montgomery ST, Frey DL, Brown MR, Schultz C, Guglani L, Kicic A, Peng L, Scholte BJ, Mall MA, Janssens HM, Stick SM, Tirouvanziam R (2019) Elastase Exocytosis by Airway Neutrophils Is Associated with Early Lung Damage in Children with Cystic Fibrosis. American Journal of Respiratory and Critical Care Medicine 199:873–881. doi: 10.1164/rccm.201803-0442OC

98. Matsuzaki K, Hiramatsu Y, Homma S, Sato S, Shigeta O, Sakakibara Y (2005) Sivelestat Reduces Inflammatory Mediators and Preserves Neutrophil Deformability During Simulated Extracorporeal Circulation. The Annals of Thoracic Surgery 80:611–617. doi: 10.1016/j.athoracsur.2005.02.038

99. McMillan SJ, Kearley J, Campbell JD, Zhu X-W, Larbi KY, Shipley JM, Senior RM, Nourshargh S, Lloyd CM (2004) Matrix Metalloproteinase-9 Deficiency Results in Enhanced Allergen-Induced Airway Inflammation. The Journal of Immunology 172:2586–2594. doi: 10.4049/jimmunol.172.4.2586

100. Mei J, Liu Y, Dai N, Favara M, Greene T, Jeyaseelan S, Poncz M, Lee JS, Worthen GS (2010) CXCL5 Regulates Chemokine Scavenging and Pulmonary Host Defense to Bacterial Infection. Immunity 33:106–117. doi: 10.1016/j.immuni.2010.07.009

101. Mestas J, Hughes CCW (2004) Of Mice and Not Men: Differences between Mouse and Human Immunology. The Journal of Immunology 172:2731–2738. doi: 10.4049/jimmunol.172.5.2731

102. Montgomery ST, Dittrich AS, Garratt LW, Turkovic L, Frey DL, Stick SM, Mall MA, Kicic A (2018) Interleukin-1 is associated with inflammation and structural lung disease in young children with cystic fibrosis. Journal of Cystic Fibrosis 17:715–722. doi: 10.1016/j.jcf.2018.05.006

103. Montoro DT, Haber AL, Biton M, Vinarsky V, Lin B, Birket SE, Yuan F, Chen S, Leung HM, Villoria J, Rogel N, Burgin G, Tsankov AM, Waghray A, Slyper M, Waldman J, Nguyen L, Dionne D, Rozenblatt-Rosen O, Tata PR, Mou H, Shivaraju M, Bihler H, Mense M, Tearney GJ, Rowe SM, Engelhardt JF, Regev A, Rajagopal J (2018) A revised airway epithelial hierarchy includes CFTR-expressing ionocytes. Nature 560:319–324. doi: 10.1038/s41586-018-0393-7

104. Müller U, Hentschel J, Janhsen WK, Hünniger K, Hipler U-C, Sonnemann J, Pfister W, Böer K, Lehmann T, Mainz JG (2015) Changes of Proteases, Antiproteases, and Pathogens in Cystic Fibrosis Patients' Upper and Lower Airways after IV-Antibiotic Therapy. Mediators of Inflammation 2015:1–16. doi: 10.1155/2015/626530

105. Murray PJ, Wynn TA (2011) Protective and pathogenic functions of macrophage subsets. Nature Reviews Immunology 11:723–737. doi: 10.1038/nri3073

106. Nagase H, Woessner JF (1999) Matrix Metalloproteinases. Journal of Biological Chemistry 274:21491–21494. doi: 10.1074/jbc.274.31.21491

107. Nichols DP, Chmiel JF (2015) Inflammation and its genesis in cystic fibrosis: Inflammation in Cystic Fibrosis. Pediatric Pulmonology 50:S39–S56. doi: 10.1002/ppul.23242

108. Okada S, Kita H, George TJ, Gleich GJ, Leiferman KM (1997) Migration of Eosinophils through Basement Membrane Components *In Vitro*: Role of Matrix Metalloproteinase-9. American Journal of Respiratory Cell and Molecular Biology 17:519–528. doi: 10.1165/ajrcmb.17.4.2877

109. Okada Y, Naka K, Kawamura K, Matsumoto T, Nakanishi I, Fujimoto N, Sato H, Seiki M (1995) Localization of matrix metalloproteinase 9 (92-kilodalton gelatinase/type IV collagenase = gelatinase B) in osteoclasts: implications for bone resorption. Lab Invest 72:311–322

110. O'Kane CM, McKeown SW, Perkins GD, Bassford CR, Gao F, Thickett DR, McAuley DF (2009) Salbutamol up-regulates matrix metalloproteinase-9 in the alveolar space in the acute respiratory distress syndrome: Critical Care Medicine 37:2242–2249. doi: 10.1097/CCM.0b013e3181a5506c

111. Olson TS, Ley K (2002) Chemokines and chemokine receptors in leukocyte trafficking. Am J Physiol Regul Integr Comp Physiol 283. doi: 10.1152/ajpregu.00738.2001

112. O'Sullivan BP, Freedman SD (2009) Cystic fibrosis. The Lancet 373:1891–1904. doi: 10.1016/S0140-6736(09)60327-5

113. Overall CM, Blobel CP (2007) In search of partners: linking extracellular proteases to substrates. Nature Reviews Molecular Cell Biology 8:245–257. doi: 10.1038/nrm2120

114. Oviedo-Orta E, Bermudez-Fajardo A, Karanam S, Benbow U, Newby AC (2008) Comparison of MMP-2 and MMP-9 secretion from T helper 0, 1 and 2 lymphocytes alone and in coculture with macrophages. Immunology 124:42–50. doi: 10.1111/j.1365-2567.2007.02728.x

115. Owen C, Jojas-Quintero J (2016) Matrix metalloproteinases in cystic fibrosis: pathophysiologic and therapeutic perspectives. Metalloproteinases In Medicine Volume 3:49–62. doi: 10.2147/MNM.S96916

116. Owen CA (1995) Cell surface-bound elastase and cathepsin G on human neutrophils: a novel, non-oxidative mechanism by which neutrophils focus and preserve catalytic activity of serine proteinases. The Journal of Cell Biology 131:775–789. doi: 10.1083/jcb.131.3.775

117. Owen CA (2005) Proteinases and Oxidants as Targets in the Treatment of Chronic Obstructive Pulmonary Disease. Proceedings of the American Thoracic Society 2:373–385. doi: 10.1513/pats.200504-029SR

118. Owen CA (2008) Roles for proteinases in the pathogenesis of chronic obstructive pulmonary disease. Int J Chron Obstruct Pulmon Dis 3:253–268

119. Perera NC, Schilling O, Kittel H, Back W, Kremmer E, Jenne DE (2012) NSP4, an elastase-related protease in human neutrophils with arginine specificity. Proceedings of the National Academy of Sciences 109:6229–6234. doi: 10.1073/pnas.1200470109

120. Peroni DG, Boner AL (2000) Atelectasis: mechanisms, diagnosis and management. Paediatric Respiratory Reviews 1:274–278. doi: 10.1053/prrv.2000.0059

121. Pfaffl MW (2001) A new mathematical model for relative quantification in real-time RT–PCR. Nucleic Acids Research 29:e45–e45

122. Pham CTN (2006) Neutrophil serine proteases: specific regulators of inflammation. Nature Reviews Immunology 6:541–550. doi: 10.1038/nri1841

123. Polverino E, Rosales-Mayor E, Dale GE, Dembowsky K, Torres A (2017) The Role of Neutrophil Elastase Inhibitors in Lung Diseases. Chest 152:249–262. doi: 10.1016/j.chest.2017.03.056

124. Prudova A, auf dem Keller U, Butler GS, Overall CM (2010) Multiplex N-terminome Analysis of MMP-2 and MMP-9 Substrate Degradomes by iTRAQ-TAILS Quantitative Proteomics. Molecular & Cellular Proteomics 9:894–911. doi: 10.1074/mcp.M000050-MCP201

125. Puente XS, Sánchez LM, Overall CM, López-Otín C (2003) Human and mouse proteases: a comparative genomic approach. Nature Reviews Genetics 4:544–558. doi: 10.1038/nrg1111

126. Ratjen F (2002) Matrix metalloproteases in BAL fluid of patients with cystic fibrosis and their modulation by treatment with dornase alpha. Thorax 57:930–934. doi: 10.1136/thorax.57.11.930

127. Ratjen F, Bell SC, Rowe SM, Goss CH, Quittner AL, Bush A (2015) Cystic fibrosis. Nature Reviews Disease Primers 15010. doi: 10.1038/nrdp.2015.10

128. Rawlings ND Merops database, https://www.ebi.ac.uk/merops/cgi-bin/pepsum?id=M10.004, Accessed 12.12.2018

129. Reddy MM, Stutts MJ (2013) Status of Fluid and Electrolyte Absorption in Cystic Fibrosis. Cold Spring Harbor Perspectives in Medicine 3:a009555–a009555. doi: 10.1101/cshperspect.a009555

130. Reutershan J, Ley K (2004) Bench-to-bedside review: Acute respiratory distress syndrome – how neutrophils migrate into the lung. Critical Care 8:453. doi: 10.1186/cc2881

131. Roberts H, White P, Dias I, McKaig S, Veeramachaneni R, Thakker N, Grant M, Chapple I (2016) Characterization of neutrophil function in Papillon-Lefèvre syndrome. Journal of Leukocyte Biology 100:433–444. doi: 10.1189/jlb.5A1015-489R

132. Rock JR, Randell SH, Hogan BLM (2010) Airway basal stem cells: a perspective on their roles in epithelial homeostasis and remodeling. Disease Models & Mechanisms 3:545–556. doi: 10.1242/dmm.006031

133. Rommens J, Iannuzzi M, Kerem B, Drumm M, Melmer G, Dean M, Rozmahel R, Cole J, Kennedy D, Hidaka N, et al. (1989) Identification of the cystic fibrosis gene: chromosome walking and jumping. Science 245:1059–1065. doi: 10.1126/science.2772657

134. Saetta M, Shiner RJ, Angus GE, Kim WD, Wang N-S, King M, Ghezzo H, Cosio MG (1985) Destructive Index: A Measurement of Lung Parenchymal Destruction in Smokers. Am Rev Respir Dis 131:764–769. doi: 10.1164/arrd.1985.131.5.764

135. Sagel SD, Kapsner RK, Osberg I (2005) Induced sputum matrix metalloproteinase-9 correlates with lung function and airway inflammation in children with cystic fibrosis. Pediatric Pulmonology 39:224–232. doi: 10.1002/ppul.20165

136. Sagel SD, Wagner BD, Anthony MM, Emmett P, Zemanick ET (2012) Sputum Biomarkers of Inflammation and Lung Function Decline in Children with Cystic Fibrosis. American Journal of Respiratory and Critical Care Medicine 186:857–865. doi: 10.1164/rccm.201203-0507OC

137. Saini Y, Dang H, Livraghi-Butrico A, Kelly EJ, Jones LC, O'Neal WK, Boucher RC (2014) Gene expression in whole lung and pulmonary macrophages reflects the dynamic pathology associated with airway surface dehydration. BMC Genomics 15:726. doi: 10.1186/1471-2164-15-726

138. Sakashita A, Nishimura Y, Nishiuma T, Takenaka K, Kobayashi K, Kotani Y, Yokoyama M (2007) Neutrophil elastase inhibitor (sivelestat) attenuates subsequent ventilator-induced lung injury in mice. European Journal of Pharmacology 571:62–71. doi: 10.1016/j.ejphar.2007.05.053

139. Sandler NG, Mentink-Kane MM, Cheever AW, Wynn TA (2003) Global Gene Expression Profiles During Acute Pathogen-Induced Pulmonary Inflammation Reveal Divergent Roles for Th1 and Th2 Responses in Tissue Repair. The Journal of Immunology 171:3655–3667. doi: 10.4049/jimmunol.171.7.3655

140. Scherle W (1970) A simple method for volumetry of organs in quantitative stereology. Mikroskopie 26:57—60

141. Schönbeck U, Mach F, Libby P (1998) Generation of Biologically Active IL-1β by Matrix Metalloproteinases: A Novel Caspase-1-Independent Pathway of IL-1β Processing. J Immunol 161:3340

142. Sly PD, Gangell CL, Chen L, Ware RS, Ranganathan S, Mott LS, Murray CP, Stick SM (2013) Risk Factors for Bronchiectasis in Children with Cystic Fibrosis. New England Journal of Medicine 368:1963–1970. doi: 10.1056/NEJMoa1301725

143. Snouwaert JN, Brigman KK, Latour AM, Malouf NN, Boucher RC, Smithies O, Koller BH (1992) An Animal Model for Cystic Fibrosis Made by Gene Targeting. Science 257:1083–1088. doi: 10.1126/science.257.5073.1083

144. Sobonya RE, Taussig LM (1986) Quantitative Aspects of Lung Pathology in Cystic Fibrosis. Am Rev Respir Dis 134:290–295. doi: 10.1164/arrd.1986.134.2.290

145. Stevens T, Ekholm K, Granse M, Lindahl M, Kozma V, Jungar C, Ottosson T, Falk-Hakansson H, Churg A, Wright JL, Lal H, Sanfridson A (2011) AZD9668: Pharmacological Characterization of a Novel Oral Inhibitor of Neutrophil Elastase. Journal of Pharmacology and Experimental Therapeutics 339:313–320. doi: 10.1124/jpet.111.182139

146. Tabeling C, Yu H, Wang L, Ranke H, Goldenberg NM, Zabini D, Noe E, Krauszman A, Gutbier B, Yin J, Schaefer M, Arenz C, Hocke AC, Suttorp N, Proia RL, Witzenrath M, Kuebler WM (2015) CFTR and sphingolipids mediate hypoxic pulmonary vasoconstriction. Proceedings of the National Academy of Sciences 112:E1614–E1623. doi: 10.1073/pnas.1421190112

147. Tallant C, Marrero A, Gomis-Rüth FX (2010) Matrix metalloproteinases: Fold and function of their catalytic domains. Biochimica et Biophysica Acta (BBA) - Molecular Cell Research 1803:20–28. doi: 10.1016/j.bbamcr.2009.04.003

148. Tikhonov VE, Lopez-Llorca LV, Salinas J, Jansson H-B (2002) Purification and Characterization of Chitinases from the Nematophagous Fungi Verticillium chlamydosporium and V. suchlasporium. Fungal Genetics and Biology 35:67–78. doi: 10.1006/fgbi.2001.1312

149. Tirouvanziam R, Gernez Y, Conrad CK, Moss RB, Schrijver I, Dunn CE, Davies ZA, Herzenberg LA, Herzenberg LA (2008) Profound functional and signaling changes in viable inflammatory neutrophils homing to cystic fibrosis airways. Proceedings of the National Academy of Sciences 105:4335–4339. doi: 10.1073/pnas.0712386105

150. Trojanek JB, Cobos-Correa A, Diemer S, Kormann M, Schubert SC, Zhou-Suckow Z, Agrawal R, Duerr J, Wagner CJ, Schatterny J, others (2014) Airway Mucus Obstruction Triggers Macrophage Activation and MMP12-dependent Emphysema. American journal of respiratory cell and molecular biology

151. Turner PV, Brabb T, Pekow C, Vasbinder MA (2011) Administration of substances to laboratory animals: routes of administration and factors to consider. J Am Assoc Lab Anim Sci 50:600–613

152. Ugalde AP, Ordóñez GR, Quirós PM, Puente XS, López-Otín C (2010) Metalloproteases and the Degradome. In: Clark IM (ed) Matrix Metalloproteinase Protocols. Humana Press, Totowa, NJ, pp 3–29

153. Vaisar T, Kassim SY, Gomez IG, Green PS, Hargarten S, Gough PJ, Parks WC, Wilson CL, Raines EW, Heinecke JW (2009) MMP-9 Sheds the β_2 Integrin Subunit (CD18) from Macrophages. Molecular & Cellular Proteomics 8:1044–1060. doi: 10.1074/mcp.M800449-MCP200

154. Van den Steen PE, Dubois B, Nelissen I, Rudd PM, Dwek RA, Opdenakker G (2002) Biochemistry and molecular biology of gelatinase B or matrix metalloproteinase-9 (MMP-9). Critical reviews in biochemistry and molecular biology 37:375–536

155. Van Lint P, Libert C (2007) Chemokine and cytokine processing by matrix metalloproteinases and its effect on leukocyte migration and inflammation. Journal of Leukocyte Biology 82:1375–1381. doi: 10.1189/jlb.0607338

156. Vandooren J, Geurts N, Martens E, Van den Steen PE, Opdenakker G (2013) Zymography methods for visualizing hydrolytic enzymes. Nature Methods 10:211–220. doi: 10.1038/nmeth.2371

157. Vandooren J, Van den Steen PE, Opdenakker G (2013) Biochemistry and molecular biology of gelatinase B or matrix metalloproteinase-9 (MMP-9): The next decade. Critical Reviews in Biochemistry and Molecular Biology 48:222–272. doi: 10.3109/10409238.2013.770819

158. Voll RE, Herrmann M, Roth EA, Stach C, Kalden JR, Girkontaite I (1997) Immunosuppressive effects of apoptotic cells. Nature 390:350–351. doi: 10.1038/37022

159. Voynow J, Fischer B, Zheng S (2008) Proteases and cystic fibrosis. The International Journal of Biochemistry & Cell Biology 40:1238–1245. doi: 10.1016/j.biocel.2008.03.003

160. Voynow JA, Gendler SJ, Rose MC (2006) Regulation of Mucin Genes in Chronic Inflammatory Airway Diseases. American Journal of Respiratory Cell and Molecular Biology 34:661–665. doi: 10.1165/rcmb.2006-0035SF

161. Vu TH, Shipley JM, Bergers G, Berger JE, Helms JA, Hanahan D, Shapiro SD, Senior RM, Werb Z (1998) MMP-9/Gelatinase B Is a Key Regulator of Growth Plate Angiogenesis and Apoptosis of Hypertrophic Chondrocytes. Cell 93:411–422. doi: 10.1016/S0092-8674(00)81169-1

162. Wagner CJ, Schultz C, Mall MA (2016) Neutrophil elastase and matrix metalloproteinase 12 in cystic fibrosis lung disease. Molecular and Cellular Pediatrics 3. doi: 10.1186/s40348-016-0053-7

163. Wagner W, Bennett RD, Ackermann M, Ysasi AB, Belle J, Valenzuela CD, Pabst A, Tsuda A, Konerding MA, Mentzer SJ (2015) Elastin Cables Define the Axial Connective Tissue System in the Murine Lung: AXIAL CONNECTIVE TISSUE SYSTEM. The Anatomical Record 298:1960–1968. doi: 10.1002/ar.23259

164. Warnatsch A, Tsourouktsoglou T-D, Branzk N, Wang Q, Reincke S, Herbst S, Gutierrez M, Papayannopoulos V (2017) Reactive Oxygen Species Localization Programs Inflammation to Clear Microbes of Different Size. Immunity 46:421–432. doi: 10.1016/j.immuni.2017.02.013

165. Warner RL, Beltran L, Younkin EM, Lewis CS, Weiss SJ, Varani J, Johnson KJ (2001) Role of Stromelysin 1 and Gelatinase B in Experimental Acute Lung Injury. American Journal of Respiratory Cell and Molecular Biology 24:537–544. doi: 10.1165/ajrcmb.24.5.4160

166. Weathington NM, van Houwelingen AH, Noerager BD, Jackson PL, Kraneveld AD, Galin FS, Folkerts G, Nijkamp FP, Blalock JE (2006) A novel peptide CXCR ligand derived from extracellular matrix degradation during airway inflammation. Nature Medicine 12:317–323. doi: 10.1038/nm1361

167. Weibel ER (2017) Lung morphometry: the link between structure and function. Cell and Tissue Research 367:413–426. doi: 10.1007/s00441-016-2541-4

168. Weitnauer M, Mijošek V, Dalpke AH (2016) Control of local immunity by airway epithelial cells. Mucosal Immunology 9:287–298. doi: 10.1038/mi.2015.126

169. Wielpütz MO, Weinheimer O, Eichinger M, Wiebel M, Biederer J, Kauczor H-U, Heußel CP, Mall MA, Puderbach M (2013) Pulmonary emphysema in cystic fibrosis detected by densitometry on chest multidetector computed tomography. PLoS ONE 8:e73142. doi: 10.1371/journal.pone.0073142

170. Williams SE, Brown TI, Roghanian A, Sallenave J-M (2006) SLPI and elafin: one glove, many fingers. Clinical Science 110:21. doi: 10.1042/CS20050115

171. Wilson TA, Bachofen H (1982) A model for mechanical structure of the alveolar duct. Journal of Applied Physiology 52:1064–1070. doi: 10.1152/jappl.1982.52.4.1064

172. Wittekindt OH (2017) Tight junctions in pulmonary epithelia during lung inflammation. Pflügers Archiv - European Journal of Physiology 469:135–147. doi: 10.1007/s00424-016-1917-3

173. Worlitzsch D, Tarran R, Ulrich M, Schwab U, Cekici A, Meyer KC, Birrer P, Bellon G, Berger J, Weiss T, Botzenhart K, Yankaskas JR, Randell S, Boucher RC, Döring G (2002) Effects of reduced mucus oxygen concentration in airway Pseudomonas infections of cystic fibrosis patients. Journal of Clinical Investigation 109:317–325. doi: 10.1172/JCI13870

174. Young HWJ, Williams OW, Chandra D, Bellinghausen LK, Pérez G, Suárez A, Tuvim MJ, Roy MG, Alexander SN, Moghaddam SJ, Adachi R, Blackburn MR, Dickey BF, Evans CM (2007) Central Role of Muc5ac Expression in Mucous Metaplasia and Its Regulation by Conserved 5′ Elements. American Journal of Respiratory Cell and Molecular Biology 37:273–290. doi: 10.1165/rcmb.2005-0460OC

175. Yu Q, Stamenkovic I (2000) Cell surface-localized matrix metalloproteinase-9 proteolytically activates TGF-β and promotes tumor invasion and angiogenesis. Genes & Development 14:163–176. doi: 10.1101/gad.14.2.163

176. Yu X, Akbarzadeh R, Pieper M, Scholzen T, Gehrig S, Schultz C, Zillikens D, König P, Petersen F (2018) Neutrophil Adhesion Is a Prerequisite for Antibody-Mediated Proteolytic Tissue Damage in Experimental Models of Epidermolysis Bullosa Acquisita. Journal of Investigative Dermatology 138:1990–1998. doi: 10.1016/j.jid.2018.03.1499

177. Yuan S, Hollinger M, Lachowicz-Scroggins ME, Kerr SC, Dunican EM, Daniel BM, Ghosh S, Erzurum SC, Willard B, Hazen SL, Huang X, Carrington SD, Oscarson S, Fahy JV (2015) Oxidation increases mucin polymer cross-links to stiffen airway mucus gels. Science Translational Medicine 7:276ra27-276ra27. doi: 10.1126/scitranslmed.3010525

178. Zheng L, Lam WK, Tipoe GL, Shum IH, Yan C, Leung R, Sun J, Ooi GC, Tsang KW (2002) Overexpression of matrix metalloproteinase-8 and -9 in bronchiectatic airways in vivo. European Respiratory Journal 20:170–176. doi: 10.1183/09031936.02.00282402

179. Zhou-Suckow Z, Duerr J, Hagner M, Agrawal R, Mall MA (2017) Airway mucus, inflammation and remodeling: emerging links in the pathogenesis of chronic lung diseases. Cell and Tissue Research 367:537–550. doi: 10.1007/s00441-016-2562-z

180. (1981) Stereological Methods. Vol. 1. Practical Methods for Biological Morphometry. By Ewald R. Weibel. Journal of Microscopy 121:131–132. doi: 10.1111/j.1365-2818.1981.tb01205.x

Publications from PhD studies

Original articles:

Gehrig S, Duerr J, Weitnauer M, Wagner CJ, Graeber SY, Schatterny J, Hirtz S, Belaaouaj A, Dalpke AH, Schultz C, Mall MA (2014) Lack of Neutrophil Elastase Reduces Inflammation, Mucus Hypersecretion, and Emphysema, but Not Mucus Obstruction, in Mice with Cystic Fibrosis–like Lung Disease. American Journal of Respiratory and Critical Care Medicine 189:1082–1092. doi: 10.1164/rccm.201311-1932OC

Trojanek JB, Cobos-Correa A, Diemer S, Kormann M, Schubert SC, Zhou-Suckow Z, Agrawal R, Duerr J, Wagner CJ, Schatterny J, others (2014) Airway Mucus Obstruction Triggers Macrophage Activation and MMP12-dependent Emphysema. American journal of respiratory cell and molecular biology

Claudius Wagner, Zhe Zhou-Suckow, Jolanthe Schatterny, Simone Schmidt, Carsten Schultz, and Marcus Mall (2019) MMP-9 deficiency does not alter disease severity in mice with cystic fibrosis-like lung disease *(manuscript in preparation)*

Review articles:

Wagner CJ, Schultz C, Mall MA (2016) Neutrophil elastase and matrix metalloproteinase 12 in cystic fibrosis lung disease. Molecular and Cellular Pediatrics 3. doi: 10.1186/s40348-016-0053-7

Abstracts:

Claudius Wagner, Stefanie Gehrig, Jolanthe Schatterny, Zhe Zhou-Suckow, Carsten Schultz, Marcus Mall (2015) Pharmacologic inhibition of neutrophil elastase reduces emphysema in mice with cystic fibrosis-like lung disease, 9th European CF Young Investigator Meeting, February 2015, Paris, France

Wagner C, Schatterny J, Gehrig S, Zhou-Suckow Z, Schultz C, Mall M (2015) Small molecule inhibitor of neutrophil elastase reduces emphysema in mice with cystic fibrosis-like lung disease. Pneumologie 69. doi: 10.1055/s-0035-1556602

Claudius Wagner, Jolanthe Schatterny, Zhe Zhou-Suckow, Stefanie Gehrig, Carsten Schultz, Marcus Mall (2016) Inhibition of neutrophil elastase reduces mucus obstruction in airways of mice with cystic fibrosis-like lung disease, DZL Annual Meeting 2016, Hannover

Matteo Guerra, Claudius Wagner, Marcus Mall, Carsten Schultz (2017) Investigating Neutrophil Serine Protease activity at subcellular resolution, EMBL Heidelberg, 2017

Claudius Wagner, Jolanthe Schatterny, Zhe Zhou-Suckow, Carsten Schultz, Marcus A. Mall (2017) Genetic deletion of MMP-9 does not reduce chronic neutrophilic inflammation and structural lung damage in mice with cystic fibrosis-like lung disease, DZL Annual Meeting 2017, München

Matteo Guerra, Claudius Wagner, Marcus Mall, Carsten Schultz (2018) Investigating Neutrophil Serine Protease activity at subcellular resolution, DZL Annual Meeting 2018, Bad Nauheim

Claudius Wagner, Jolanthe Schatterny, Zhe Zhou-Suckow, Carsten Schultz, Marcus A. Mall (2019) Deletion of matrix metalloproteinase-9 does not attenuate cystic fibrosis-like lung disease in mice, DZL Annual Meeting 2019, Mannheim

Oral presentations:

The role of neutrophil elastase in the βENaC-Tg mouse as a model for chronic obstructive lung disease, 2nd COST summer school, June 2014, Groningen, Netherlands

Pharmacologic inhibition of neutrophil elastase reduces emphysema in mice with cystic fibrosis-like lung disease, 9th European CF Young Investigator Meeting, February 2015, Paris, France

Role of matrix metalloproteinase-9 in CF lung disease and preclinical studies with protease inhibitor sivelestat, TLRC Research Seminar, February 2019, Heidelberg

Acknowledgements

I want to thank everybody who contributed to the successful completion of my PhD thesis.

A special thanks to Prof. Dr. Marcus Mall for his excellent supervision and extensive support throughout my time as PhD student - and for sharing his profound scientific experience, for giving me the opportunity to work in a great environment and for mentoring this thesis.

A big thank you to Prof. Dr. Stefan Wölfl for helpful ideas and input, for his valuable advices, for encouragements and his friendly support.

Thanks to Prof. Dr. Carsten Schultz for shaping this thesis and important advices as part of the thesis advisory committee.

I thank Jolanthe Schatterny for expert experimental support, for her huge help in treatment studies and the positive spirit, even during ambitious endpoints. I thank Simone Butz for proofreading this thesis, for competent help and technical support. Thanks to Stephanie Hirtz, Heike Scheuermann and Angela Frank for help in technical questions and supportive discussions - also about non-scientific topics.

I thank Dr. Raman Agrawal for helpful advices, hints and philosophical insights. A great thanks to Dr. Zhe Zhou-Suckow and Dr. Matthias Hagner for proofreading this thesis. A collective thank you to Dominik Leitz, Ayça Seyhan Agircan, Pamela Millar-Büchner, Matteo Guerra, Dario Frey, Dr. Verena Rickert-Zacharias, Dr. Sandra Christochowitz and Dr. Matthias Hagner as fellow doctoral students and for creating a stimulating working environment.

Finally, I thank my parents Elfi and Dr. Hans Wagner for their endless support, the aid-packages and for their great care throughout my studies. Thanks to Julian and Dorthe Wagner, to Elly and Anton for joyful distractions and activities outside the lab.